EUR Research Information Portal

Quantitative 3-D echocardiography of the heart and the coronary vessels

Publication status and date:
Published: 16/12/1998

Document Version
Publisher's PDF, also known as Version of record

Citation for the published version (APA):
Bruining, N. (1998). *Quantitative 3-D echocardiography of the heart and the coronary vessels*. [Doctoral Thesis, Erasmus University Rotterdam]. Erasmus Universiteit Rotterdam (EUR).

Link to publication on the EUR Research Information Portal

Terms and Conditions of Use
Except as permitted by the applicable copyright law, you may not reproduce or make this material available to any third party without the prior written permission from the copyright holder(s). Copyright law allows the following uses of this material without prior permission:

- you may download, save and print a copy of this material for your personal use only;
- you may share the EUR portal link to this material.

In case the material is published with an open access license (e.g. a Creative Commons (CC) license), other uses may be allowed. Please check the terms and conditions of the specific license.

Take-down policy
If you believe that this material infringes your copyright and/or any other intellectual property rights, you may request its removal by contacting us at the following email address: openaccess.library@eur.nl. Please provide us with all the relevant information, including the reasons why you believe any of your rights have been infringed. In case of a legitimate complaint, we will make the material inaccessible and/or remove it from the website.

Erasmus University Rotterdam
Making Minds Matter

Quantitative 3-D Echocardiography of The Heart and The Coronary Vessels

ISBN: 90-9012092-0

Cover Illustrations:

Cover photo (made by Jan Tuin©): view of Rotterdam from the 'Euromast'. The bridge in the middle, the Erasmus bridge (called 'The Swan'), crossing the maze, is linking Rotterdam-south (at the right) with Rotterdam-North.

Photo at the back: The academic hospital Rotterdam Dijkzigt (gray building) together with the Thoraxcenter (long, white foreground building) and the medical faculty (tall white building) forming the Erasmus Medical Centre Rotterdam.

Inserted photos: A Virtual Heart model (devloped by GMD, Bonn, Germany; left side), a three-dimensional reconstruction of the heart in a 4-chamber projection (middle) and an endoscopic three-dimensional intracoronary ultrasound reconstruction, showing an implanted SciMed Radius™ stent (right).

Quantitative 3-D Echocardiography of The Heart and The Coronary Vessels

Kwantitatieve 3-D Echocardiografie van Het Hart en De Kransslagvaten

PROEFSCHRIFT

ter verkrijging van de graad van doctor
aan de Erasmus Universiteit Rotterdam
op gezag van de rector magnificus
Prof. dr P.W.C. Akkermans M.A.
en volgens het besluit van het College voor Promoties

De openbare verdediging zal plaatsvinden op
woensdag 16 December 1998 om 13.45 uur

door

Nico Bruining

geboren te Rotterdam

PROMOTIECOMMISSIE

PROMOTOR:	Prof. dr J.R.T.C. Roelandt
OVERIGE LEDEN:	Prof. dr P.W. Serruys
	Prof. dr Ir N. Bom
	Prof. dr C. Borst
CO-PROMOTOR:	Dr N. van der Putten



Financial support by the Netherlands Heart Foundation (NHS) for the publication of this thesis is gratefully acknowledged.

"Associate with the noblest people you can find; read the best books; live with the mighty. But learn to be happy alone. Rely upon your own energies, and so do not wait for, or depend on other people."

Professor Thomas Davidson.

Aan mijn ouders

CONTENTS

Chapter 1	Introduction and overview of thesis	1
	Part I: Three-dimensional reconstruction of the heart and the coronary vessels	
Chapter 2	Precordial multiplane echocardiography for dynamic anyplane, paraplane and three-dimensional imaging of the heart. *The Thoraxcentre Journal, 1994; 6:4-13.*	9
Chapter 3	Dynamic Three-Dimensional Reconstruction of ICUS Images Based on an ECG-Gated Pull-Back Device. *Computers In Cardiology, IEEE Computer Society Press, Los Alamitos, 1995; 633-36.*	21
Chapter 4	Dynamic Imaging of Coronary Stent Structures: An ECG-gated Three-dimensional Intracoronary Ultrasound Study In Humans. *Ultrasound in Medicine and Biology, 1998; 24: 631-37.*	27
Chapter 5	Ultrasound Appearances of Coronary Stents as Obtained by Three-dimensional Intracoronary Ultrasound Imaging In-Vitro. *Journal of Invasive Cardiology, 1998; 6: 332-38.*	37
Chapter 6	Virtual reality: a Teaching and Training Tool or just a Computer Game? *The Thoraxcentre Journal, 1998; 10: 7-10.*	47
	Part II: Quantitative analysis of coronary vessel dimensions	
Chapter 7	ECG-Gated ICUS Image Acquisition Combined with a Semi-Automated Contour Detection Provides Accurate Analysis of Vessel Dimensions. *Computers In Cardiology, IEEE Computer Society Press, Los Alamitos, 1996; 53-56.*	53

Chapter 8	ECG-Gated versus Nongated Three-Dimensional Intracoronary Ultrasound Analysis: Implications for Volumetric Measurements. *Catheterization and Cardiovascular Diagnosis, 1998; 43: 254-60.*	59
Chapter 9	ECG-Gated Three-dimensional Intravascular Ultrasound. Feasibility and Reproducibility of the Automated Analysis of Coronary Lumen and Atherosclerotic Plaque Dimensions in Humans. *Circulation, 1997; 96: 2944-52.*	69
Chapter 10	Electrocardiogram-Gated Intravascular Ultrasound Image Acquisition after Coronary Stent Deployment Facilitates On-Line Three-Dimensional Reconstruction and Automated Lumen Quantification. *JACC, 1997; 30: 436-43.*	81
Chapter 11a	Summary, discussion and conclusions	91
Chapter 11b	Samenvatting, discussie en conclusies	101
Dankwoord		111
Publications		117
Curriculum vitae		123

CHAPTER 1

Introduction and overview of thesis

The recognition of the existence of ultrasound is credited to L. Spallanzani (1729-1799). In recent years, ultrasound has been used as an imaging modality in medicine. I. Edler and C.H. Hertz produced the first ultrasound images of the heart in 1953. In the 1960's great progress was made in the clinical application of ultrasound when real-time two-dimensional ultrasound scanners were developed. In 1968, J. Somer constructed the first electronic phased-array scanner and this technology is still the most widely used in ultrasound equipment. In 1974 F.E. Barber and colleagues produced a duplex scanner which integrated imaging with pulsed-wave Doppler measurements. C. Kasai and colleagues constructed in 1982 the color-coded Doppler flow imaging system based on autocorrelation detection, providing a noninvasive "angiogram" simulation of normal and abnormal blood flow on a "beat-to-beat" basis. Transesophageal echocardiography became available to clinicians in 1985 due to the developments of J. Soquet who invented the mono- and biplane electronic phased-array probe[1]. Echocardiography has become one of the most commonly used diagnostic imaging techniques in cardiology.

The development of commercial 3-D echocardiographic equipment began in the early 1990's. In 1993 a technique allowing acquisition of tomographic parallel sliced data set of echocardiographic images of the heart with a lobster tail TEE probe, was developed by the German based company "TomTec GmbH". The TEE probe had an imaging element which could be controlled by computer applying a stepping motor. They also developed an interface to the patient to record the respiration and R-R intervals. This allowed the acquisition of ultrasound images ECG-triggered and gated, which reduced motion artifacts caused by beat-to-beat and respiratory variations in cardiac dimensions and position. After the acquisition of a tomographic data set, the images were post-processed and with application of software interpolation algorithms, gaps in the data set could be filled. This post-processed data set could then be used to reconstruct 3-D volume rendered images of the heart. 3-D ultrasound provides cardiac images which more closely mimic actual anatomy than 2-D cross-sectional images, and may thus be easier to interpret.

Potential cardiovascular applications for 3-D include:

- Assessment of ventricular function, volume and mass. These parameters are particularly relevant for the assessment of ischemic heart disease and cardiomyopathies, in which 2-D methods based on geometric assumptions are subject to error from distorted geometry and regional dysfunction.
- Evaluation of complex surfaces, such as the atrial septum, valve leaflets, prosthe-

tic heart valves, papillary muscles and ventricle aneurysms.

- Definition of complex congenital heart defects.
- 3-D color-coded Doppler which can improve understanding of the spatial distribution of blood flow.
- Surgical planning. The 3-D imaging provides the ability to display a structure in varied planes and offers the surgeon unique and useful views of cardiac anatomy.
- 3-D reconstruction of intravascular ultrasonic images.

More recent transthoracic and transesophageal rotoplane devices have been developed which make the acquisition simpler and less invasive[2-4]. Today, M-mode, two-dimensional, three-dimensional, pulsed-wave, continuous-wave and color-coded Doppler flow modalities have been combined in the one diagnostic console and provides a very comprehensive cardiac diagnostic facility providing integrated structural, functional and hemodynamic information.

In 1972 the development of catheters for intravascular and intracardiac application began[5]. Since the mid 1980's intracoronary ultrasound (ICUS) catheters have become commonly used research tools providing cardiac interventionalists with high-resolution cross-sectional images of the vessel wall which cannot be obtained with contrast angiography, this modality only displaying silhouette views of the vessel lumen. ICUS imaging permits visualization of lesion morphology and can provide accurate measurements of vessel cross-sectional dimensions. At this stage, ICUS is still a research tool and its full clinical potential remains to be realized. There is however increasing evidence from large prospective studies that ultrasound guided coronary interventions have the advantage of improvements in immediate lumen enlargement[6-9], reduced procedure-related complications[10] and long-term restenosis[11,12].

In 1994 we adapted the technique which had been used for tomographic acquisition of echocardiographic images of cardiac chambers and walls, to the imaging of coronary arteries. At first, these coronary tomographic ICUS data sets were used to produce 3-D reconstructions. Subsequently a volumetric analysis software package for vessels was adapted for quantitative analysis of the image data.

OVERVIEW OF THE THESIS

Part I: Three-dimensional reconstruction of the heart and the coronary vessels

In chapter 2, a technique is described of acquiring ECG-triggered and gated tomographic echocardiographic data sets, to perform dynamic any-plane, para-plane and three-dimensional (3-D) imaging of the heart. This technique was a breakthrough in the clinical application of 3-D echocardiography.

Chapter 3 describes a technique of performing dynamic three-dimensional reconstruction of ICUS images based on an ECG-gated pullback device. This technique was an extension of the technique described in chapter 2 and was developed at the Thoraxcenter, Rotterdam.

In chapter 4, 3-D reconstructions of implanted intracoronary stents in humans are examined. In this study two types of stent designs are compared, a wire-mesh design (Wallstent™) and a coil-type stent (Cordis coronary stent). The designs of stents could be of importance for the success of an attempt at 3-D reconstruction.

Chapter 5 describes the ultrasound appearances of coronary stents. Every stent has its own ultrasound "fingerprint". Knowledge of the ultrasound appearance of a stent in-vitro is useful in assessing the stent in-vivo, and helps recognition of image artifacts. Further information is gathered as to ICUS catheter image resolution. 3-D reconstruction of the stents was performed using a so-called "endoscopic" view or "black-and-white" angioscopy simulation, a novel development which may become clinically useful.

In chapter 6, current and future developments of 3-D echocardiography are discussed. "Virtual Reality" techniques could be useful for training and teaching purposes.

Part II: Quantitative analysis of coronary vessel dimensions

Chapter 7 describes how quantitative analysis of ICUS 3-D reconstructions can provide accurate measurements of vessel dimensions. This technique is of great clinical interest since ICUS measurements can be used in the evaluation of interventional techniques.

In chapter 8, a study comparing ECG-gated and non-gated three-dimensional intracoronary ultrasound analyses is reported. The main objective was to investigate the effect of different methods of image acquisition volumetric measurements.

Chapter 9 describes the feasibility and reproducibility of ECG-gated three-dimensional ultrasound acquisition in combination with a volumetric analysis software package.

Finally, chapter 10 describes how the developed technique can be used on-line for coronary stent placement in the catheterization laboratory.

References

1. Roelandt JRTC. Seeing the invisible - a short history of cardiac ultrasound -. The Thoraxcentre J, 1994; 6:31-33.
2. Roelandt JR, ten Cate FJ, Vletter WB, Taams MA. Ultrasonic dynamic three-dimensional visualization of the heart with a multiplane transesophageal imaging transducer. J Am Soc Echocardiogr 1994; 7:217-29.
3. Roelandt J, Salustri A, Vletter W, Nosir Y, Bruining N. Precordial multiplane echocardiography for dynamic anyplane, paraplane and three-dimensional imaging of the heart. The Thoraxcentre J 1994; 6:4-13.
4. Roelandt J, Ten Cate FJ, Bruining N, Salustri A, Vletter WB, Mumm B, van der Putten N. Transesophageal rotoplane echo-CT A novel approach to dynamic three-dimensional echocardiography. The Thoraxcentre J 1994; 6:4-8.
5. Bom N, Lancee CT, van Egmond FC. An ultrasonic intracardiac scanner. Ultrasonics 1972; 10:72-6.
6. Zellner C, Sweeney JP, Ko E, Sudhir K, Chou TM. Use of intravascular ultrasound in evaluating repeated balloon rupture during coronary stenting. Cathet Cardiovasc Diagn 1997; 40:52-4.
7. Kovach JA, Mintz GS, Pichard AD, Kent KM, Popma JJ, Satler LF, Leon MB. Sequential intravascular ultrasound characterization of the mechanisms of rotational atherectomy and adjunct balloon angioplasty. J Am Coll Cardiol 1993; 22:1024-32.
8. Mintz GS, Kovach JA, Javier SP, Pichard AD, Kent KM, Popma JJ, Salter LF, Leon MB. Mechanisms of lumen enlargement after excimer laser coronary angioplasty. An intravascular ultrasound study. Circulation 1995; 92:3408-14.
9. Umans VA, Baptista J, di Mario C, von Birgelen C, Quaedvlieg P, de Feyter PJ, Serruys PW. Angiographic, ultrasonic, and angioscopic assessment of the coronary artery wall and lumen area configuration after directional atherectomy: the mechanism revisited. Am Heart J 1995; 130:217-27.
10. Haase KK, Athanasiadis A, Mahrholdt H, Treusch A, Wullen B, Jaramillo C, Baumbach A, Voelker W, Meisner C, Karsch KR. Acute and one year follow-up results after vessel size adapted PTCA using intracoronary ultrasound [see comments]. Eur Heart J 1998; 19:263-72.
11. Stone GW. Rotational atherectomy for treatment of in-stent restenosis: role of intracoronary ultrasound guidance. Cathet Cardiovasc Diagn 1996; Suppl:73-7.
12. Di Mario C, Gil R, Camenzind E, Ozaki Y, von Birgelen C, Umans V, de Jaegere P, de Feyter PJ, Roelandt JR, Serruys PW. Quantitative assessment with intracoronary ultrasound of the mechanisms

of restenosis after percutaneous transluminal coronary angioplasty and directional coronary atherectomy. Am J Cardiol 1995; 75:772-7.

CHAPTER 2

Precordial multiplane echocardiography for dynamic anyplane, paraplane and three-dimensional imaging of the heart

J. Roelandt, A. Salustri, W. Vletter, Y. Nosir and N. Bruining

The Thoraxcentre Journal, 1994; 6:4-13.

Precordial multiplane echocardiography for dynamic anyplane, paraplane and three-dimensional imaging of the heart

J. ROELANDT, A. SALUSTRI, W. VLETTER, Y. NOSIR, N. BRUINING
WITH THE TECHNICAL ASSISTANCE OF L. BEKKERING, K.K. DJOA AND R. FROWIJN

From the division of Cardiology, Thoraxcentre, University Hospital Rotterdam -Dijkzigt and Erasmus University Rotterdam, The Netherlands

Abstract

We constructed a hand-held transducer assembly to which any commercially available transducer can be adapted for performing precordial multiplane echocardiography. The transducer rotation around its center axis is computer controlled via a step motor and permits image acquisition in predetermined angular steps for three-dimensional image reconstruction (*three-dimensional echocardiography*). From the collected volume data set, cardiac cross-sections which are physically impossible to obtain from precordial or transesophageal acoustic windows can be computed in any desired plane (*anyplane echocardiography*). Electronic parallel slicing through the volume data set allows the generation of equidistant cross-sections at selected intervals in any direction (*paraplane echocardiography*).
These new computer generated imaging capabilities will change the practice of echocardiography in the future by making it a less operator-dependent technique with minimal performance variability. Clearly, the range of clinical questions that can be answered will be further expanded by these developments.

Introduction

In two decades, cardiac ultrasound has become the most widely disseminated diagnostic imaging method in clinical cardiology. The method allows one to noninvasively look into the heart by providing serial tomographic views recorded from limited precordial and transesophageal acoustic windows. However, most of our diagnostic decision making is based on a mental reconstruction of these tomographic views into their three-dimensional geometry. Clearly, this is a difficult process requiring skill and experience. Thus, the availability of objective and more intelligible three-dimensional images would greatly facilitate the diagnosis of unknown and complex pathology and improve diagnostic accuracy in general. This also applies to other tomographic techniques such as computer tomography and magnetic resonance imaging.
The most practical approach to three-dimensional echocardiography is the acquisition of a consecutive series of tomographic views using standard available ultrasound equipment together with accurate spatial and temporal information and subsequent "off-line" reconstruction.

Recently, computer technology became available allowing both precordial and transesophageal controlled image acquisition using parallel,[1-3] fan-like[4-6] and rotational scanning methods.[7-9] Data processing algorithms for volume rendered reconstruction with grey scale tissue imaging represented another major breakthrough.[10]

Our experience with three-dimensional reconstruction using transesophageal rotational acquisition with a commercially available multiplane imaging probe has been described.[7,8] In this approach, a computer-based steering logic which considers both heart cycle variation and the respiration phase controls a step motor which rotates the imaging plane in predetermined steps via the external control knob of the multiplane probe.

However, the rotational approach can also be used at a single pivot point over a small acoustic window. We have constructed a transducer assembly which can accommodate any commercially available transducer for precordial rotational image acquisition.[9] The transducer is centered in the inner cylindrical housing of a double walled cylindrical rotation mechanism and can be rotated around its center axis via a step-motor under control of the same steering logic as is used for transesophageal image acquisition. With this transducer assembly, controlled precordial multiplane echocardiography can be performed similar to multiplane transesophageal echocardiography. This approach is not only the basis for routine three-dimensional echocardiography but also for a more standardized semi-automated examination procedure.
In this paper we report our experience with this prototype transducer assembly demonstrating the feasibility of precordial three-dimensional echocardiography in adult patients.

The precordial transducer assembly and ultrasound system

The inner components of the transducer assembly for precordial image acquisition consist of a cylindrical housing with a cog-wheel to which any standard precordial imaging transducer can be adapted.
This cylindrical housing with the contained transducer fits into a cylindrical holder and can be rotated with a step-motor via a wheel-work interface (figure 1). The step-motor is commanded by a steering-logic for controlled image acquisition



Figure 1.
The upper panel shows the hand-held transducer assembly used for precordial image acquisition containing a Vingmed 3.5 MHz sector scanning transducer. The stepmotor is mounted on the cylindrical holder and rotates via a wheel-work interface, the transducer inside the holder. A cable which transmits the pulses from the computer algorithm to steer the step-motor for controlled acquisition is attached to the connector mounted next to the step-motor. There is a micro-switch to control the start at 0 degrees and the end at 178 degrees of the image acquisition. By adapting the size and shape of the inner housing any commercially available precordial transducer can be used. The hand-held transducer assembly containing a Toshiba 3.5 MHz phased-array transducer is shown in the lower panel.

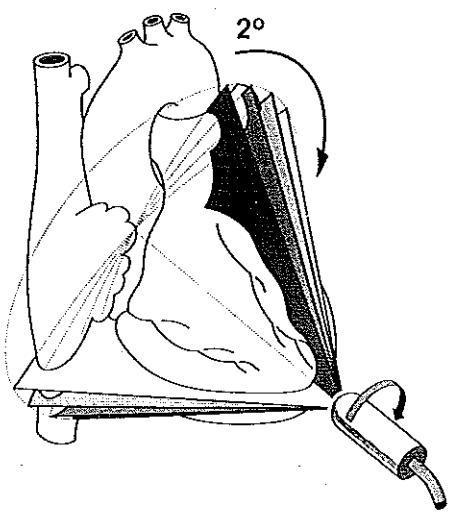

Figure 2.
This diagram explains the principle of acquisition of sequential cross-sectional images at 2 degrees steps from the apical transducer position.

(Echo-scan, TomTec GmbH, Munich, Germany). The transducer assembly is hand held and can be placed either over the parasternal, apical or subcostal window (figure 2). The probe can be aimed in any direction to find the center axis of the sector images encompassing the region or structure of interest. During acquisition, the probe is kept stationary while the transducer is rotated through 180^0 degrees around this center axis in predetermined steps by means of the step-motor. The sampled cardiac cross-sections encompass a conical image volume with the transducer positioned at its apex. The video output of the echocardiographic imaging system is interfaced with the TomTec Echo-scan system for three-dimensional reconstruction.

Precordial image acquisition

The step-motor in the transducer assembly is commanded by a software-based steering logic which controls the image acquisition in a given plane by an algorithm considering both heart cycle variation by ECG-gating and respiratory cycle phase by impedance measurement. These parameters are recorded prior to the actual image acquisition for a certain time period to select the average cardiac cycle and respiratory phase pattern. Based on this information, the step-motor is commanded by the steering logic to acquire cross-sections of cardiac cycles that fall within a selected range of cycle length

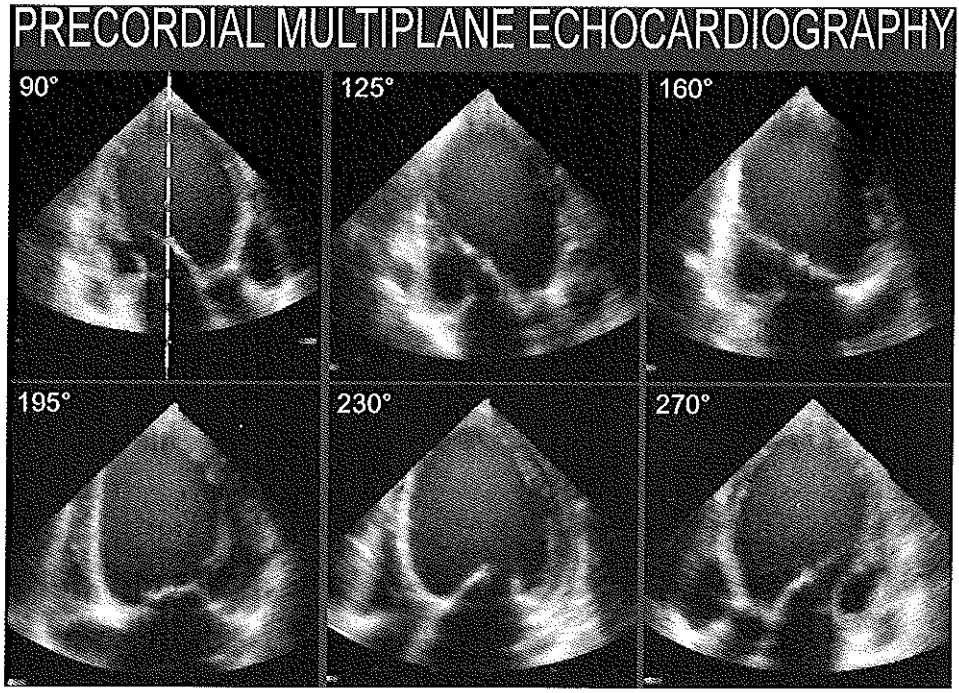

Figure 3.
Apical (precordial) multiplane echocardiography of a patient with a dilated left ventricle. Under computer control, the imaging plane is rotated over 180° starting with a left ventricular long-axis plane and with steps of 35°. The axis of rotation is indicated in panel A. All images are recorded in the same phase of the respiratory cycle. Images A and F are mirror images. The images can be recorded on videotape or optical disc for further analysis. Increments of 2° during acquisition allow the completion of a rotational dataset for three-dimensional reconstruction.

and respiratory phase. This permits optimal temporal and spatial registration of the precordial images. After a cardiac cycle is selected by the steering logic, the cardiac images are sampled at 40 msec intervals (25 frames/sec), digitized and stored in the computer memory. Then, the step-motor is activated and rotates the transducer 2 degrees to the next scanning plane, where the same steering logic is followed. To fill the conical data volume, 90 sequential cross-sections from 0-178 degrees must be obtained each during a complete cardiac cycle.

The transducer assembly can also be used for routine precordial multiplane echocardiography (figure 3) or semi-automated echocardiographic image acquisition for left ventricular function studies or stress-echocardiography. Respiration gated recording of cardiac cycles in a given plane avoids the influence and random error caused by extracardiac motion effects.

Data processing

The recorded images are formatted in the correct sequence according to their ECG phase in volumetric data sets (256*256*256* pixel/each 8 bit). To convert the rotated images into an isotropic cubic data set, a geometric transformation is necessary. To fill the gaps in the far fields, a "trilinear cylindric interpolation" is used. The size of the gaps is dependent on the distance from the rotation axis and the angle increment between two acquired images. An oversampling is done near the rotation axis and an undersampling in the outer region. This phenomenon can be compared to a regular two-dimensional sector image. In such an image, the near field is over- and the far field is undersampled as well. To reduce motion artifacts which can be created by patient movement, respiratory artifacts or probe movement, a dedicated image processing filter is used (ROSA filter: Reduction Of Spatial Artifacts).

Anyplane echocardiography

Any desired cross-section of the heart or of a selected structure which is difficult or physically impossible to obtain from standard precordial or transesophageal acoustic windows can be computed from the data set and displayed in motion with zoom facility in cine-loop format at 25 frames/sec (figure 4).

Paraplane echocardiography

Parallel slicing through the data set is possible and allows the generation of equidistant cross-sections at selected intervals in any plane through a region or structure of interest

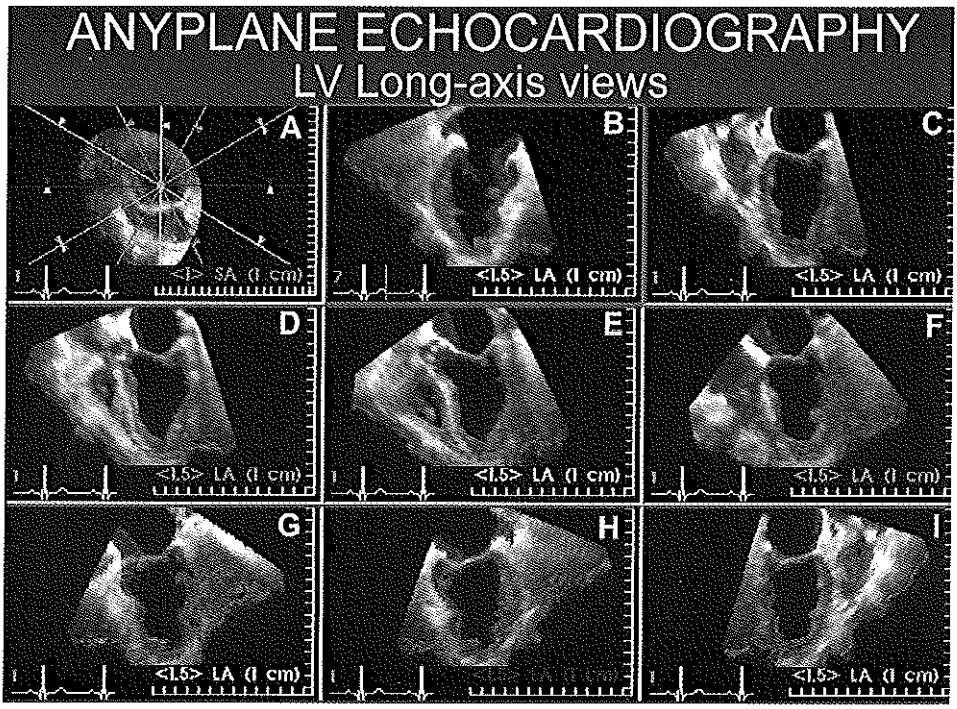

Figure 4.
Anyplane echocardiography. From the three-dimensional data set up to 8 cut planes can be selected and reconstructed by computer. In this example left ventricular (LV) long-axis views are generated (panels B-I) and their orientation is shown in panel A. A comprehensive standardized analysis of the shape, size and wall motion of the left ventricle is possible.

(figure 5). These computed cross-sections can be displayed in cine-loop format at 25 frames/sec.

Three dimensional reconstruction

To distinguish between a structure of interest and the background image, a greylevel threshold is used. This difficult process is known as image segmentation. A "hard" decision is somewhat relaxed by using a "fuzzy segmentation", where a probability is assigned to each greylevel, to decide whether it belongs to a structure or the background. A more or less subjective decision is always necessary (i.e. to adjust for the Time Gain Compensation used during acquisition of the original two-dimensional images).
Since ultrasound images are noisy, algorithms for edge enhancement and noise reduction must be applied. The performance characteristics of these algorithms will have an effect on the overall quality of the three-dimensional image. Furthermore, the definition of a threshold to recognize the interface between cardiac structures and the blood pool during the segmentation procedure is based on visual inspection. This introduces a subjective factor similar to the optimization of two-dimensional echocardiograms during standard examination procedures.
Different rendering algorithms are used and mixed with different weighting factors to create a three-dimensional shaded display.[11] These algorithms are: a) distance shading; b) transparent adaptive greylevel gradient shading; c) texture shading and d) maximum intensity projection.
The tissue display of the three-dimensional reconstructions has a close resemblance to the actual anatomy of the heart. This effect can be further enhanced by creating rotational sequences on the output screen.

Clinical procedure

Echocardiographic studies are performed with the transducer system in the parasternal or apical positions while the patient is comfortable lying in the 45-degree left recumbent position. The operator has to find the center axis around which the imaging plane is rotated to encompass the structure(s) or region of interest. Since the spatial coordinate system changes with transducer movement, motion of the transducer must be avoided. We found that after a learning period an experienced operator is able to keep the transducer stationary during the acquisition period. Inadvertent patient movement during the image acquisition can be largely prevented by thoroughly explaining the procedure before the study. The examination, including the calibration procedures, selection of the optimal gain settings and conical volume with a few test runs and the actual image acquisition, requires approximately 8-10 minutes in patients with sinus rhythm. In order to secure

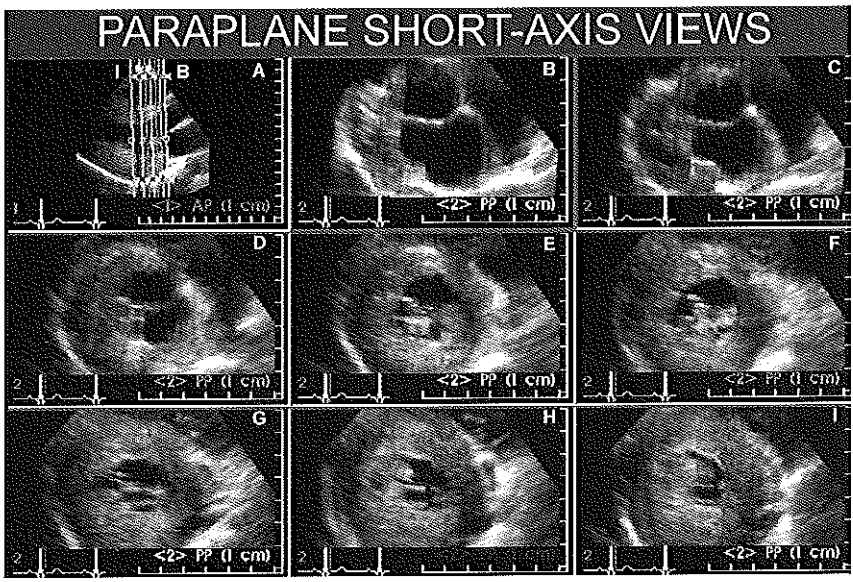

Figure 5.
Paraplane echocardiography using the three-dimensional data set of a patient with hypertrophic cardiomyopathy. The parasternal long-axis view is shown in panel A and the lines indicate the computer generated parallel short axis views of the left ventricle from B to I.

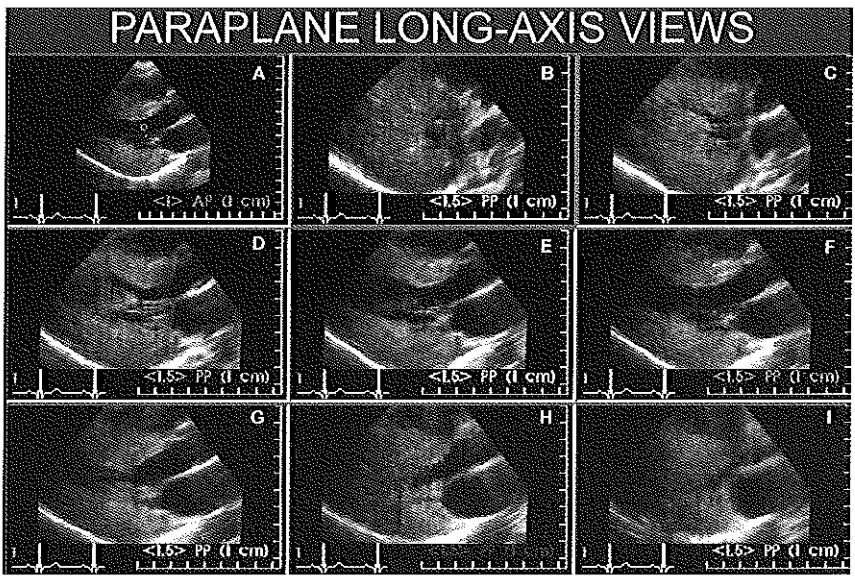

Figure 6.
The same patient as in figure 5. The left ventricle is now sliced in planes parallel to the long axis view from interventricular septum to the lateral wall. Panel E corresponds to the standard parasternal long-axis view.

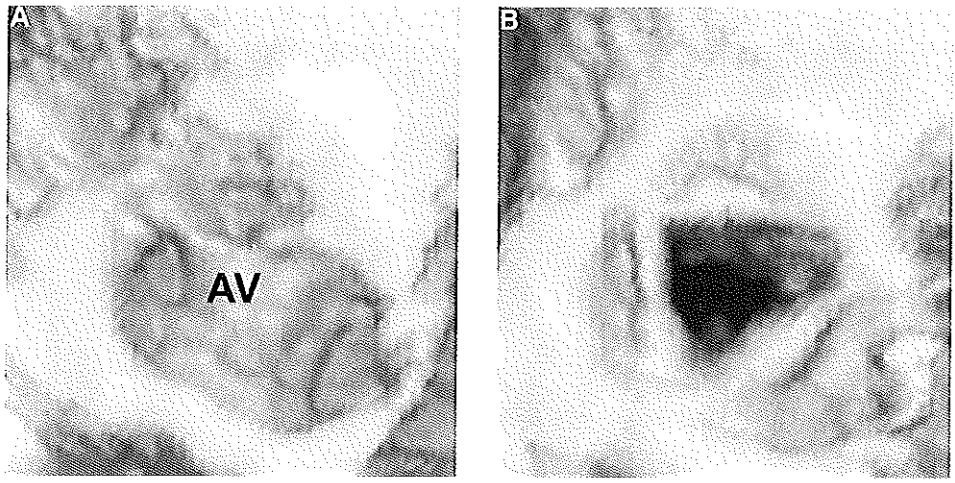

Figure 7.
Three-dimensional reconstruction with volume rendered display of the aortic valve (AV). Electronic aortotomy is performed and the valve is visualized from above in the closed position during diastole (A) and open position during systole (B).

optimal image quality of individual regions of interest, different image acquisition sequences from different windows are performed. Calibration and storage of the data in the computer memory between acquisition sequences requires approximately 3 minutes.

Off-line three-dimensional reconstruction of an area of interest requires 30-60 minutes depending how difficult it is to select the optimal cut planes to visualize a given structure in its three-dimensional perspective as there may be significant anatomical variability between patients. Guidelines to identify approximate cutting planes in various disease categories have been proposed.[12]

Results and illustrative patient studies

Our experience includes 97 patients (mean age 32 ± 9 years) selected on the basis of good precordial image quality and sinus rhythm with a variety of cardiac disorders including myocardial disease (26), valvular heart disease (26), congenital heart disease (35) and normal subjects (10). In these patients, a total of 176 acquisition sequences, 78 with the transducer in the parasternal and 98 in the apical position, were performed.
Adequate dynamic volume rendered display was possible in 77% of the patients. Three-dimensional image quality was considered adequate when there was complete visualization

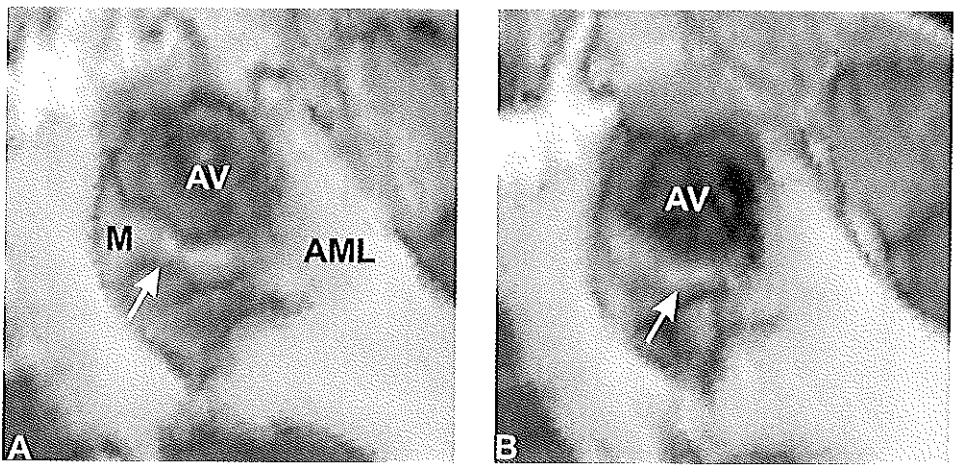

Figure 8
Three-dimensional volume rendered display of a subaortic membrane (M) seen from within the left ventricle. Note the aortic valve (AV) closed in diastole (A) and open in systole (B). AML: anterior mitral leaflet.

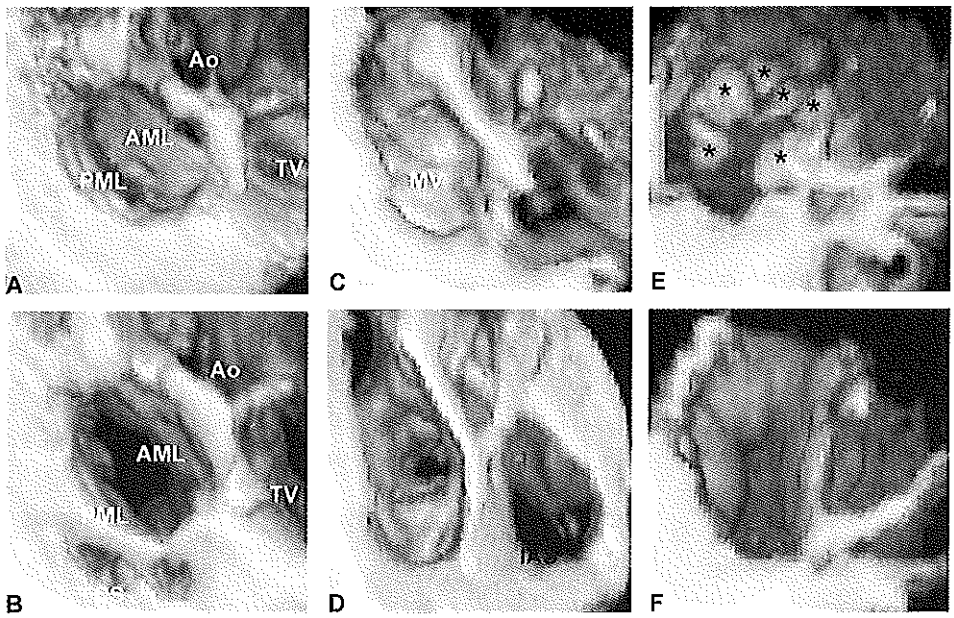

Figure 9.
Examples of volume rendered three-dimensional reconstructions of normal, stenotic and prolapsing mitral valves. Electronic atriotomy is performed and the mitral valve leaflets are seen from an atrial viewpoint. Panel A shows a normal mitral valve in the closed position during systole and panel B in the open position during diastole (B). A stenotic mitral valve is shown closed in panel C and in the open position during diastole in panel D. Note the small stenotic orifice. The prolapsing scallops of both mitral leaflets are seen in panel E (see asterisks). Panel F shows the mitral valve open in diastole.
Ao: aorta; AML and PML: anterior and posterior mitral valve leaflets; CS: coronary sinus; IAS: interatrial septum; MV: mitral valve; TV: tricuspid valve.

in depth of the structures of interest. Inadequate reconstructions may result from incomplete acquisition, poor image quality or inadequate gain settings during acquisition of the original data so that structures could not be detected by threshold changes during the volume rendered procedure. Dynamic anyplane and paraplane echocardiography were always possible and allowed the display of cut planes unobtainable from precordial windows of selected structures. Three-dimensional reconstructions showing the aortic valve from the ascending aorta allow a direct qualitative evaluation (figure 7). The left ventricular outflow can be visualized from a ventricular viewpoint and the nature of subaortic pathology is directly visualized (figure 8). Imaging of the normal and pathologic mitral valve is possible from both atrial and ventricular viewpoints. Excellent delineation of the leaflets and qualitative analysis of the pathology is possible (figures 9 and 10). Direct visualization of the ventricular septal defect and its structural relationships in a patient with tetralogy of Fallot is shown in figure 11. In these conditions the pathomorphology was better appreciated from the three-dimensional than from the standard two-dimensional images. The potential of electronic anyplane and paraplane echocardiography for both qualitative and quantitative analysis of specific cardiac pathologies is illustrated in figures 4-6, 12 and 13.

Figure 10. Three-dimensional reconstructions of a stenotic mitral valve viewed from within the left ventricle in the closed position during systole (A) and open during diastole (B).
Figure 11. Three-dimensional reconstruction following a long-axis cut plane of the left ventricle in diastole of a patient with tetralogy of Fallot. The ventricular septal defect (arrow) and the overriding aorta are visualized.

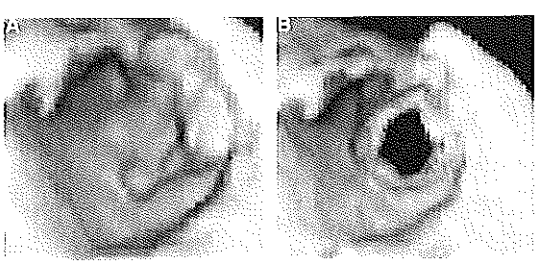

Figure 10.

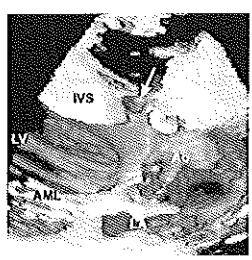

Figure 11.

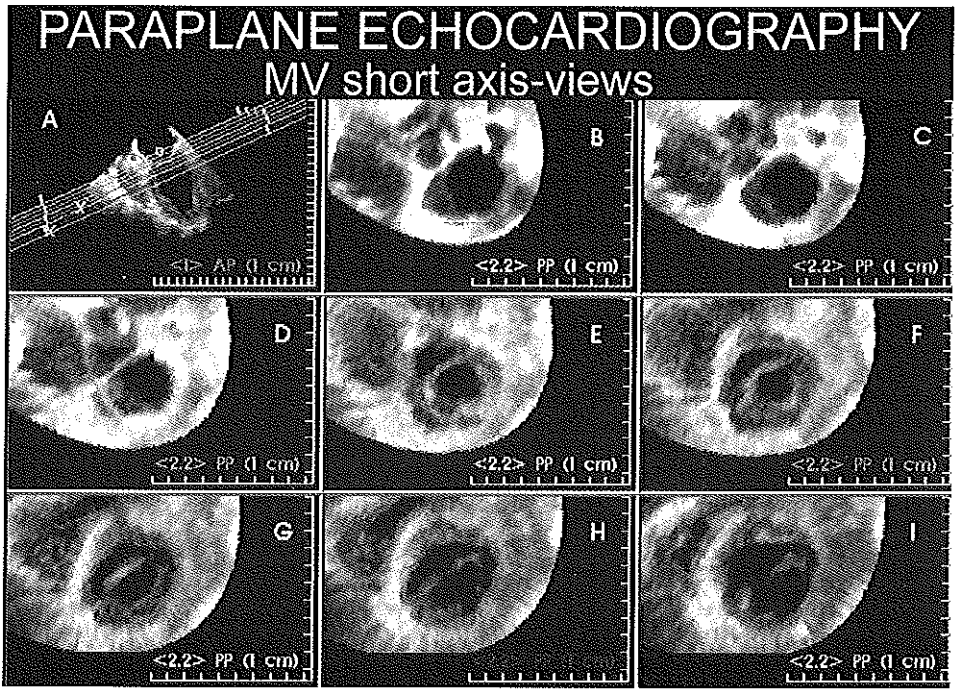

Figure 12.
Paraplane echocardiography in a patient with mitral stenosis.
From the original three-dimensional data set (panel A), 8 parallel cut planes in the optimal orientation (anyplane capability) through the mitral valve are generated and the corresponding two-dimensional images are represented in panels B to I. This allows a slicing of the structure in a way similar to computed tomography or magnetic resonance imaging. The smallest orifice area is represented in panel F. This approach allows accurate planimetry of the mitral valve orifice.

Discussion

Three-dimensional reconstruction of the heart has been an important research goal ever since the introduction of two-dimensional echocardiography. Several directions have been followed. Scanning in "real-time" of a pyramidal volume encompassing the whole heart is the most exciting development but progress is slow and clinical application remote.[13] Most approaches towards three-dimensional echocardiography are "off-line" and are based on the sequential acquisition of multiple cross-sectional images together with their spatial position and orientation using either external or internal coordinate reference systems. Mechanical articulated arm[14] and acoustical spark gap[15,16] location systems allow the continuous registration of the transducer position and the imaging plane with respect to an external reference point and have been used for precordial image acquisition. In most of these studies, static wire-frame or surface rendered displays have been generated. These displays do not contain the important grey scale information about tissue.[17]
Parallel, fan-like and rotational scanning methods are based on internal coordinate reference systems and have recently been successfully applied for precordial[12,18,19,20] acquisition in infants and small children. However, it appears that small acoustic windows make rotational scanning the most effective precordial acquisition approach in children and certainly in adults since the basic images are obtained from a small and fixed pivot point.

The possibility of generating three-dimensional reconstructions from standard precordial two-dimensional images will undoubtedly stimulate interest in and expand the clinical application of three-dimensional echocardiography since information similar to that obtained from other tomographic imaging techniques including radionuclide, computed tomography and magnetic resonance can be obtained with the additional advantages of better temporal resolution, portability, bedside application and relatively low cost. Three-dimensional echocardiography is still in its infancy and interest in this technique is growing. From our experience we feel that three-dimensional reconstruction will facilitate the assessment of structures and pathology of unknown or complex geometry such as the right ventricle, aneurysmatic ventricles in coronary artery disease and complex congenital heart disease.[22,23] Topographic maps of elusive structures such as the mitral valve can be created helping to better understand its pathology.[24] The surgeon can now have a preview of what he will find during surgery (electronic cardiotomy) but with additional information on function. This will be of particular help in valve and congenital defect repair.
The acquisition time is at present short enough to consider three-dimensional imaging as part of a standard echocardio-

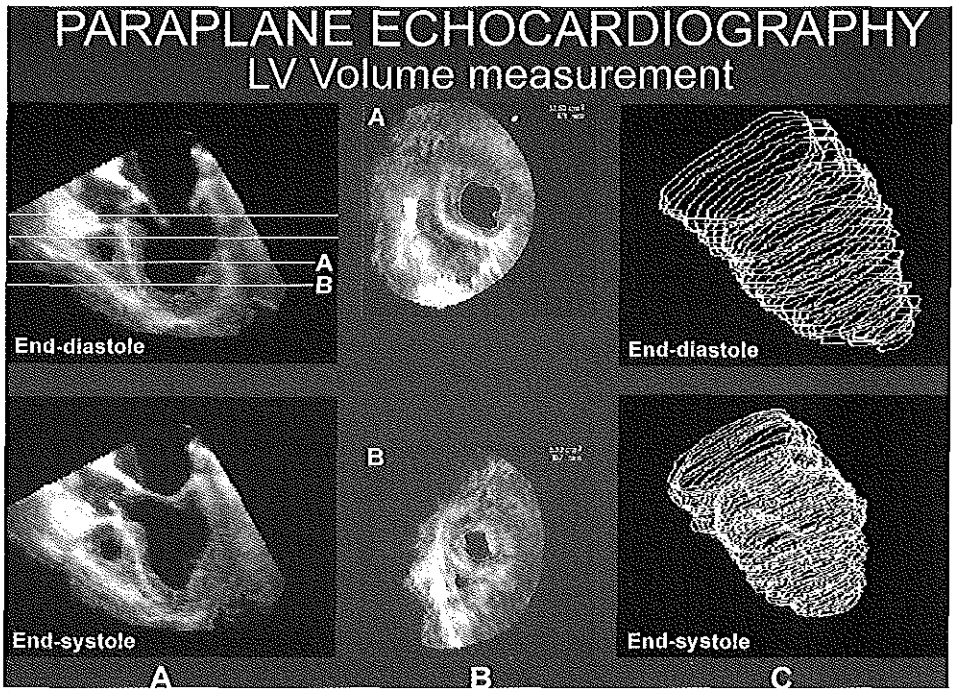

Figure 13.
The principle of left ventricular volume measurement using a three-dimensional data set. An end-diastolic long-axis view is selected as a reference view (panel A) and the left ventricle is sliced at equidistant intervals to generate a series of short axis views (paraplane capabilities). The surface area of each cross-section is measured by planimetry and the volume of each slice calculated. Adding up the volumes of all slices provides an accurate volume measurement of the left ventricle (Simpson's rule). This is performed for both end-diastolic and end-systolic data sets. The figure shows an end-diastolic long-axis view on which the two lines A and B correspond to the short-axis views shown in the middle panels A and B. Panel C shows reconstructions of the left ventricle using the planimetered contours of short axis views obtained at 3 mm intervals.

graphic examination whenever is felt that it would provide incremental information for clinical decision-making.

However, at this stage of its development the long reconstruction time and the need for a dedicated operator remain major limitations of its routine use. Although we have demonstrated the feasibility of precordial acquisition using rotational scanning, it should be emphasized that this study included only patients in sinus rhythm with good image quality. It thus remains an investigational tool with respect to clinical practicality and the independent additional information it provides in different clinical conditions and scenarios.

Perhaps the greatest advantage of acquiring a three-dimensional data-set is that now cross-sectional images can be computed in any desired plane independent from orientations dictated by the available acoustic windows and that parallel slicing of selected structures can be performed electronically. These capabilities allow the selection of cut planes for optimal visualization of a cardiac structure and accurate quantitative measurement. By using a series of computer generated equidistant parallel cross-sections accurate measurement of specific structures can be made such as orifice areas of normal or pathologic valves (figure 12). Accurate volume calculation of the right or left ventricle is possible and the need for making geometric assumptions is eliminated (figure 13). Clearly, new complex parameters to define global and regional left ventricular function will become available in the future.[25]

The semi-automated and controlled registration of multiplane precordial with the hand-held transducer assembly will allow an easier and more standardized examination procedure for routine echocardiography in the future.[20] For example, the exact relationship between the apical views can be accurately documented rather than assuming an orthogonal relationship. Respiration gated cardiac cycles can be recorded during stress echocardiography thus avoiding random variability resulting from extracardiac motion in both interpretation and quantitative analysis.[25] Automatic endocardial border detection can be integrated to calculate left ventricular volumes on-line from a limited number of cross-sections. The echocardiographic examination will become less operator-dependent and more objective. Most of the performance variability will thus be avoided.

Conclusion

We are entering an exciting new era in the development of cardiac ultrasound, which may ultimately have a greater impact on clinical cardiology than two-dimensional echocardiography. With further developments in computer technology both the image quality and display facilities will improve and the reconstruction time rapidly decrease. The semi-automated standardized examination procedure with the transducer assembly necessary for three-dimensional image acquisition will change the practice of echocardiography in the future by making the procedure less operator dependent. The computer generation of anyplane and paraplane images will further expand the range of clinical diagnostic problems that can be solved.

Acknowledgement:
we gratefully acknowledge the secretarial help of Mrs. W. Korpershoek.

References

1. Wollschläger H, Zeiher AM, Klein HP, Geibel A, Wollschläger S. Transesophageal echo computer tomography (echo-CT): a new method for perspective views of the beating heart. Circulation 1990;82(suppl 3):III-670 [abstract].
2. Pandian NG, Nanda NC, Schwartz SL, Fan P, Cao QL, Sanyal R, Hsu TL, Mumm B, Wollschläger B, Weintraub A. Three-dimensional and four-dimensional transesophageal echocardiographic imaging of the heart and aorta in humans using a computer tomographic imaging probe. Echocardiography 1992;9:677-87.
3. Vogel M, Lösch S. Dynamic three-dimensional echocardiography with a computed tomography imaging probe: initial clinical experience with transthoracic application in infants and children with congenital heart defects. Br Heart J 1994;71:462-7.
4. Martin RW, Basbeln G, Zimmer R, Sutherland J. An endoscopic micro-manipulator for multiplanar transesophageal imaging. Ultrasound Med Biol 1986;12:965-75.
5. Kuroda T, Kinter TM, Seward JB, Yanagi H, Greenleaf JF. Accuracy of three-dimensional volume measurement using biplane transesophageal echocardiographic probe: in vitro experiment. J Am Soc Echocardiogr 1991;4:475-84.
6. Belohlavek M, Foley DA, Gerber TC, Kinter TM, Greenleaf JF, Seward JB. Three- and four-dimensional cardiovascular ultrasound imaging: a new era for echocardiography. Mayo Clin Proc 1993;68:211-40.
7. Roelandt J, Cate FJ ten, Bruining N, Salustri A, Vletter WB, Mumm B, Putten N van der. Transesophageal rotoplane echo-CT. A novel approach to dynamic three-dimensional echocardiography. Thoraxcentre J 1994;6/1:4-8.
8. Roelandt JRTC, Cate FJ ten, Vletter WB, Taams MA. Ultrasonic dynamic three-dimensional visualization of the heart with a multiplane transesophageal imaging transducer. J Am Soc Echocardiogr 1994;7:217-29.
9. Roelandt J, Salustri A, Bruining N. Precordial and transesophageal dynamic three-dimensional echocardiography with rotatable (multiplane) transducer systems. Ultrasound Med Biol 1994;20:S32 [abstract].
10. Levy M. Display of surfaces from volume data. IEEE Comput Graphics Applications 1988;8:29-37.
11. Hoehne KH et al. Three-dimensional imaging in medicine. NATA ASI Series, Vol F60, Springer Verlag New York, Heidelberg, Berlin 1990.
12. Pandian N, Roelandt J, Nanda NC, et al. Dynamic three-dimensional echocardiography: methods and clinical potential. Echocardiography 1994;11:237-59.
13. Sheikh KH, Smith SW, Von Ramm O, Kisslo J. Real-time, three-dimensional echocardiography: feasibility and initial use. Echocardiography 1991;8:119-25.
14. Geiser EA, Ariet M, Conetta DA, Lupkiewicz SM, Christie LG Jr, Conti CR. Dynamic three-dimensional echocardiographic reconstruction of the intact human left ventricle: technique and initial observations in patients. Am Heart J 1982;103:1056-65.
15. Moritz WE, Shreve PL. A microprocessor-based spatial-locating system for use with diagnostic ultrasound. Proc IEEE 1976;64:966-74.
16. Levine RA, Handschumacher MD, Sanfilippo AJ, Hagege AA, Harrigan P, Marshall JE, Weyman AE. Three-dimensional echocardiographic reconstruction of the mitral valve, with implications for the diagnosis of mitral valve prolapse. Circulation 1989;80:589-98.
17. Siu SC, Rivera M, Guerrero L, Handschumacher MD, Lethor JP, Weyman AE, Levine RA, Picard MH. Three-dimensional echocardiography. In vivo validation for left ventricular volume and function. Circulation 1993;88:1715-23.
18. Vogel M, Pandian N, Marx G, Fulton D, Azevedo J, Cao QL, Buhlmeyer K. Transthoracic real-time three-dimensional echocardiography in 100 pediatric and adult patients with heart disease: clinical utility of unique new views unavailable in 2-dimensional echocardiography [abstract]. Circulation 1993;88:1868.
19. Fulton DR, Marx GR, Pandian NG, Romero BA, Mumm B, Krauss M, Wollschläger H, Ludomirski A, Cao QL. Dynamic three-dimensional echocardiographic imaging of congenital heart defects in infants and children by computer-controlled tomographic parallel slicing using a single integrated ultrasound instrument. Echocardiography 1994;11:155-64.
20. Pandian NG, Cao QL, Caldeira M, et al. Application of semi-automated multiplane imaging transducer to transthoracic echocardiography makes transthoracic examination easier and faster, and yields new imaging planes - a new direction in transthoracic echocardiography [abstract]. J Am Coll Cardiol 1993;1:346A
21. Ludomirsky A, Silberbach M, Kenny A, Shiota T, Rice MJ, Klas B, Kranzowicz B, Klein P, Derman R, Saha DJ. Superiority of rotational scan reconstruction strategies for transthoracic 3-dimensional real-time echocardiography studies in pediatric patients with CHD [abstract]. Circulation 1994;89;169A.
22. Levine RA, Weyman AE, Handschumacher MD. Three-dimensional echo-cardiography: techniques and applications. Am J Cardiol 1992;69(20):121H-30H.
23. Linker DT, Moritz WE, Pearlman AS. A new three-dimensional echocardiographic method of right ventricular volume measurement: in vitro validation. J Am Coll Cardiol 1986;8:101-6.
24. Flachskampf FA, Handschumacher M, Vandervoort PM, Hanrath P, Weyman AE, Levine RA, et al. Dynamic three-dimensional reconstruction of the mitral annulus using a multiplane transesophageal echo-transducer [abstract]. Circulation 1991;84(Suppl 2):II-686.
25. Handschumacher MD, Lethor JP, Siu SC, Mele D, Rivera JM, Picard MH, Weyman AE, Levine RA. A new integrated system for three-dimensional echocardiographic reconstruction: development and validation for ventricular volume with application in human subjects. J Am Coll Cardiol;1993:21:743-53.
26. Assmann PE, Slager CJ, Borden G van der, Sutherland GR, Roelandt J. Reference systems in echocardiographic quantitative wall motion analysis with registration of respiration. J Am Soc Echocardiogr 1991;4:224-34.

Address to correspondence:
J.R.T.C. Roelandt, M.D.
Erasmus University Rotterdam
Thoraxcentre, Bd 408
P.O. Box 1738
3000 DR ROTTERDAM
The Netherlands
Tel: (0)10 – 463.5312
Fax: (0)10 – 436.3096

CHAPTER 3

Dynamic Three-dimensional Reconstruction of ICUS Images Based on an ECG-Gated Pull-Back Device

N. Bruining, C. von Birgelen, C. Di Mario, F. Prati, W. Li, W. den Hoed, M. Patijn, P.J. de Feyter, P.W. Serruys and J.R.T.C. Roelandt

Computers In Cardiology, IEEE Computer Society Press, Los Alamitos, 1995; 633-6

As part presented at the ESC, August 22, 1995, Amsterdam, Netherlands

As part presented at IEEE Engineering in Medicine and Biology Society, November 2, 1996, Amsterdam, Netherlands.

Dynamic Three-dimensional Reconstruction of ICUS Images Based on an ECG-Gated Pull-Back Device

N. Bruining, C. von Birgelen, C. Di Mario, F. Prati, W. Li, W. Den Hoed, M. Patijn, P.J. de Feyter, P.W. Serruys, J.R.T.C. Roelandt

Erasmus University/University Hospital Rotterdam Dijkzigt, Thoraxcenter, Rotterdam, The Netherlands

Abstract

At present most systems used for three-dimensional reconstruction (3-D) of two-dimensional intracoronary ultrasound (ICUS) images are based on an image acquisition with a pull-back device which withdraws the catheter with a constant speed, not taking account of cardiac motion and coronary dynamics/pulsation. Cyclic changes of the vessel dimensions and the movement of the catheter inside the vessel result in artifacts and inaccuracies of quantitative measurements. This phenomenon limits accuracy and resolution when an attempt of 3-D reconstruction is performed, since images obtained in different phases of the cardiac cycle are compiled.

To overcome these limitations we developed a custom-designed pull-back device driven by a stepping motor, which is controlled by a steering logic ensuring an ECG-gated image acquisition.

1. Introduction

Intracoronary ultrasound (ICUS) provides high- resolution cross-sectional imaging of the vessel wall which is increasingly used during diagnostic cardiac catheterization and as a guiding tool during interventional procedures. However, it is hard to get a three-dimensional (3-D) concept of the spatial vascular structure based on a series of two-dimensional parallel slices of ICUS images. The 3-D reconstruction of ICUS images allows to overcome this limitation, but at present most 3-D systems are based on an image acquisition with a pull-back device which withdraws the ICUS catheter at an uniform speed, not taking account of the cardiac motion and coronary dynamics/pulsation. Artifacts and inaccurate measurements of the 3-D reconstruction may result from the systolic-diastolic changes of the vascular dimensions and the cyclic movement of the catheter [1].

This problem can be solved by the use of a pull-back device driven by an accurate stepping motor which is controlled by a steering logic of a 3-D acquisition station, ensuring an ECG-gated acquisition of the ICUS images.

1.1. Background

In recent years several methods have been developed to acquire tomographic ICUS data sets and perform 3-D reconstructions:

- Manual pull-back.
- Manual pull-back with the ICUS catheter shaft placed in a displacement sensing device [2].
- Motorised pull-back by a uniform velocity motor, applying a speed of 1 - 0.5mm/sec [3].
- Motorised pull-back by an uniform velocity motor and use of an ECG-labelling device so that only one phase during the R-R interval is acquired at a continuous speed of 0.2mm/sec ("Pseudo-Gating") [4].
- Motorised ECG-gated pull-back using a stepping motor.

In this manuscript the ICUS acquisition by the latter, permitting a dynamic 3-D reconstruction of the coronary segment is described.

2. ICUS Acquisition Setup

A scheme of the set-up of the 3-D reconstruction system in the catheterization laboratory is shown in figure 1.

The ultrasound examination has been performed using a 2.9F MicroView 30 MHz mechanical rotating element catheter (CVIS, Sunnyvale, CA, USA) and the echo unit Insight III. The 3-D acquisition and reconstruction station receives a video signal input from the ICUS machine and is connected to the patient to monitor the ECG and respiration (impedance method).

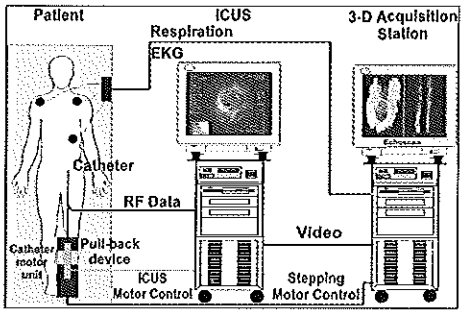

Figure 1 Cathlab setup

The acquisition station is also connected to a custom-designed pull-back device, developed at the Thoraxcenter, to be controlled by a steering logic of the acquisition station (TomTec, Munich, Germany), considering heart rate variability and (optionally) the respiration [5].

2.1. Pull-back Device

The pullback device consists of a front-plate and a back-end, containing the stepping motor, were in- between a table is pulled on a spindle driven by the stepping motor. The pullback device is displayed in figure 2.

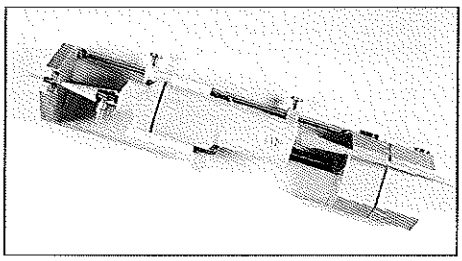

Figure 3 Pullback device

The handgrip to which the catheter is connected contains the motor unit driving the rotation of the imaging cable. It can be clamped onto the table of the pullback device. To move the table 1mm the motor needs to receive 220 stepping pulses. Thus, theoretically it is possible to pull the catheter with a minimum step resolution of 1/220mm (0.0045mm = 4.5μm), but the software has currently a lower limit of 0.1mm longitudinal step intervals.

The catheter configuration (external echo-transparent sheath with an independent imaging cable inside) guarantees that pulling a defined distance at the proximal end of the catheter results in an equivalent movement of the tip of the catheter. The stepping pulses are generated by the steering logic in the acquisition station where the scan distance, the longitudinal step resolution, the ECG, and the respiration intervals can be set.

2.2. Image Acquisition

The acquisition station digitises images with 40 ms intervals to a maximum of 25 frames for one heart cycle. It starts with the digitisation after detecting the peak of the R-wave and the first vertical synchronisation of the video signal of the echo unit (see figure 3).

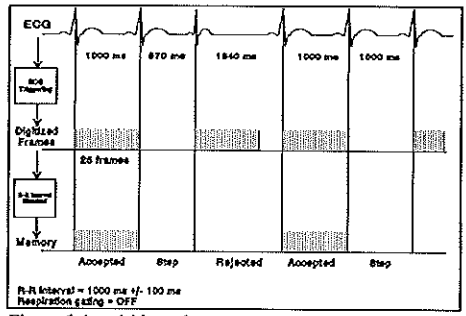

Figure 1 Acquisition scheme

It is also possible to delay the start of the image acquisition with X * 5 ms intervals to a maximum delay of 400 ms. This is useful if one desires to acquire only one phase instead of 25 phases for one R-R interval.

At first the station monitors the ECG and respiration for two minutes and produces two histograms of the measurements. The software determines the upper and lower limits of the duration of the cardiac cycle and the depth of inspiration/expiration, but the operator can also define the range. The ECG and/or respiration gating can be switched on/off by the operator. After the ICUS images of one heart cycle are acquired the software retrospectively checks if the R-R interval and respiration depth meet the predetermined ranges, before the digitised frames are stored. Otherwise, the cycle is rejected, removed from the computer memory, and a new sequence at the same transducer position is acquired. After a valid acquisition of one cycle the stepping motor receives pulses until the next position on the longitudinal axis is reached. The process is repeated until the end of the scan distance is reached. Now the operator must calibrate the echo images for on- and off-line quantitative measurements, and the acquired images can be stored.

The mean acquisition time to obtain one data set was 3±2 minutes, applying longitudinal intervals of 0.1mm, image resolution of 256*256 pixels with 8 bits per pixel, 6 phases per R-R cycle, and an average scan length of 3cm.

3. Image Processing

During the post-processing phase the images are formatted in the correct sequence according to their ECG phase in volumetric data sets (256*256*256 pixels/each 8 bits). A grey level range is used to separate and subtract the blood pool and background from the coronary wall structures in each cross-section, followed by the application of several algorithms to reduce noise, enhance edges, and reduce spatial artifacts (ROSA filter). Volume rendering techniques are then applied for dynamic three-dimensional reconstruction.

3.1. Image Display

The 3-D reconstruction of each volumetric data set is used to produce a dynamic reconstruction display of the coronary vessel (maximum: 25 data sets/cardiac cycle). The tissue display of these reconstructions has a close resemblance to the actual pathology of the coronary wall. Distance shading, grey level gradient shading, and texture mapping algorithms are applied to produce a surface shaded 3-D display of the coronary wall anatomy. Any desired cross-section of the coronary vessel can be computed and displayed in motion with zoom facility in cine-loop format (dynamic anyplane intracoronary ultrasound). However the most favoured display mode is a longitudinal cut-plane, projected with a slight angle. The system has multiple screen formats for operator-defined dynamic anyplane and 3-D displays.

A "maximum mode display" allows creating a "transparent" echographic view of the coronary vessel. In this representation an operator defined maximal grey value along each ray through the data volume is displayed so that only bright structures in the volume are represented. This display mode can be useful to visualise implanted stents in coronary vessels. The software also allows producing a reconstruction with the same perspective as an angioscopy catheter (endoscopic view). Furthermore, it is possible to remove objects from the data set by manually drawing the contours of an object and then removing it (masking). The catheter artifact (blindspot) and/or the blood pool can thus accurately be removed from the data set. Undesired signal information can be suppressed by filtering, permitting to display only signals derived from calcified plaques or implanted stents.

3.2. Three-dimensional Reconstruction

An example of an ECG-gated pullback reconstruction is displayed in figure 4.

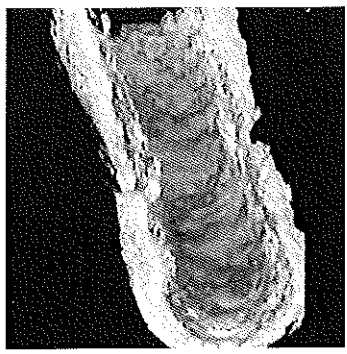

Figure 4 Calcified coronary vessel

It can be appreciated that the coronary vessel wall is calcified. The typical saw artifact of non ECG-gated reconstructions is not present here.

The proposed approach may also show tiny details as metal stent struts, shown in figure 5.

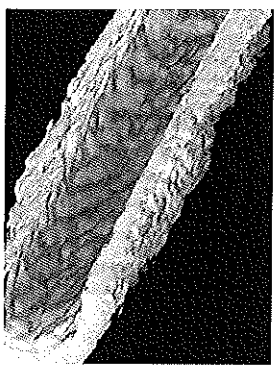

Figure 5 Implanted Wall-stent™

The figure displays a longitudinal view of a coronary artery after implantation of a metal mesh stent. The following parameters were applied:

Scan distance	: 2cm
Longitudinal step size	: 0.1mm
Viewing angle	: 145°
Phase	: systolic
Render mode	: gradient

The struts of the stent at the left side of the coronary vessel in the 3-D reconstruction are clearly visible. This is possible because this type of stent has a predominantly longitudinal orientation of its struts. At present the resolution of the ICUS catheters (150μm by 250μm) does not allow to acquire data sets of stents with a transverse strut orientation (coil stents). These stents cannot be sufficiently visualised in a reconstruction. The echo resolution makes it also difficult to routinely reconstruct the struts of stents with predominantly longitudinal strut architecture. Echo-catheters with higher resolution and application of smaller longitudinal step intervals (<0.1mm) may improve the results in the future.

3.3. Off-line Analysis

Besides achieving high quality data sets for producing 3-D reconstructions, the approach also provides excellent data sets for off-line analysis. At the Thoraxcenter an in-house produced semi-automated contour detection program for cross-sectional and volumetric quantification of 3-D ICUS data sets is used [6,7].

4. Limitations

The proposed technique has some limitations:

- No realistic curvature of the vessel but an artificially straightened reconstruction is shown.
- The resolution of the ICUS transducers determines the upper resolution limit of 3-D reconstructions.
- The acquisition time is longer compared with uniform velocity pullbacks.

5. Conclusion

The feasibility of ECG-gated pullbacks for producing dynamic 3-D reconstructions could be demonstrated. High-quality reconstructions were obtained, not showing cyclic saw-shaped artifacts as seen by non-gated approaches.

The data sets can also be used to perform a volumetric and cross-sectional quantification by a custom-designed contour detection system for off-line analysis.

References

[1] Roelandt JRTC, Di Mario C, Pandian NG, Li W, Keane D, Slager CJ, de Feyter PJ, Serruys PW. Three-dimensional reconstruction of intracoronary ultrasound images: rationale, approaches, problems, and directions. Circulation 1994; 90:1044-1055.

[2] van Egmond FC, Li W, Gussenhoven EJ, Lancée CT. Catheter Displacement Sensing Device. Thoraxcentre J 1994; 6:9-12.

[3] Di Mario C, von Birgelen C, Prati F, Soni B, Li W, Bruining N, de Jaegere PJ, de Feyter PJ, Serruys PW. Three-dimensional reconstruction of intracoronary ultrasound: clinical of research tool? Br Heart J 1995; 73 (suppl. 2):26-32

[4] von Birgelen C, Di Mario C, Prati F, Bruining N, Li W, de Feyter PJ, Roelandt JRTC. Intracoronary ultrasound: Three-dimensional reconstruction techniques. In: de Feyter PJ, Di Mario C, Serruys PW, eds. Quantitative coronary imaging. Rotterdam: Barjesteh, Meeuwse & Co. 1995: 181-197.

[6] Li W, von Birgelen C, Di Mario C, Boersma E, Gussenhoven EJ, van der Putten N, Bom N. Semi-Automatic Contour Detection for Volumetric Quantification of Intracoronary Ultrasound. In: Computers In Cardiology 1994. Los Alamitos : IEEE Computer Society Press, 1994:277-280.

[7] von Birgelen C, Di Mario C, Li W, Camenzind E, Ozaki Y, de Feyter PJ, Bom N, Roelandt JRTC. Volumetric quantification in intracoronary ultrasound: validation of a new automatic contour detection method with integrated user interaction. Circulation 1994; 90: I-550.

Address for correspondence.

Bruining N.
Thoraxcenter, University Hospital Rotterdam Dijkzigt
Room BD 308b
Dr. Molewaterplein 40
3015 GD Rotterdam
The Netherlands
Tel.:(31)104635334
Fax.:(31)104634444
Email: Bruining@thch.azr.nl

CHAPTER 4

Dynamic Imaging of Coronary Stent Structures: An ECG-gated Three-dimensional Intracoronary Ultrasound Study In Humans

N. Bruining, C. von Birgelen, P.J. de Feyter, J. Ligthart, P.W. Serruys

and J.R.T.C. Roelandt

Ultrasound in Medicine and Biology, 1998; 24: 631-37

As part presented at the AHA, November 13, 1995, Anaheim, USA

As part presented at the ASM, August 4, 1996, Brisbane, Australia

DYNAMIC IMAGING OF CORONARY STENT STRUCTURES: AN ECG-GATED THREE-DIMENSIONAL INTRACORONARY ULTRASOUND STUDY IN HUMANS

NICO BRUINING, CLEMENS VON BIRGELEN, PIM J. DE FEYTER, JURGEN LIGTHART, PATRICK W. SERRUYS and JOS R. T. C. ROELANDT

Thoraxcenter, Department of Cardiology, and Erasmus University, Rotterdam, The Netherlands

(*Received* 17 *October* 1997; in final form 2 *March* 1998)

Abstract—Three-dimensional (3D) intracoronary ultrasound (ICUS) systems allow dynamic 3D reconstruction of coronary segments after stent deployment, but motion artifacts are frequently present. The use of an electrocardiographic-gated ICUS image acquisition workstation and a dedicated pullback device may overcome this problem. In the present study, we evaluated the potential of dynamic 3D reconstruction of intracoronary stents in 51 patients. Two different types of stent designs were investigated: (1) the Wallstent (mesh type; $n = 36$) and (2) the Cordis Coronary stent (coil type; $n = 15$). There was a tendency for imaging of the mesh stent type to be better than imaging of coil type stents ($p = 0.06$). Differences in the orientation of the stent struts (mesh:longitudinal; coil:transversal) most likely explain this difference. These *in vivo* observations were tested and confirmed in *in vitro* experiments. In conclusion, dynamic 3D ICUS reconstruction of the entire stent architecture *in vivo* was feasible for stents of mesh type, while stents of coil type were incompletely visualized.
© 1998 World Federation for Ultrasound in Medicine & Biology.

Key Words: **Intracoronary ultrasound, Stents, Image processing, Computer-assisted methods, Coronary vessels, Ultrasonography.**

INTRODUCTION

Intracoronary ultrasound (ICUS) allows detailed cross-sectional imaging of coronary arteries *in vivo* (Fitzgerald et al. 1992; Mintz et al. 1995) and direct visualization of metallic stent struts (Deaner et al. 1992; Dussaillant et al. 1995; Goldberg et al. 1994; von Birgelen et al. 1996). Stent expansion and apposition to the coronary wall can be studied *in vivo*, providing information not obtainable with other imaging techniques. Recently, three-dimensional (3D) ICUS systems have become available with software allowing automated boundary analysis (Deaner et al. 1992; Dussaillant et al. 1995; Goldberg et al. 1994; von Birgelen et al. 1996). These use a sequence of planar ICUS images acquired at uniform speed during motorized pullback of the imaging catheter (Bruining et al. 1995; Mintz et al. 1993; Prati et al. 1996; Rosenfield et al. 1991). Systolic-diastolic variations in vessel dimensions and the cyclic movement of the ICUS catheter relative to the vessel wall ("catheter fluttering") may result in significant image artifacts in the 3D reconstructed views, and fine details of the stent structures can be obscured (Bruining et al. 1995, 1996; Mintz et al. 1993; Prati et al. 1996; Rosenfield et al. 1991; von Birgelen et al. 1997a, 1997b). The use of an electrocardiographic (ECG)-gated pullback device (stepping motor) may overcome this problem. The aim of the present study was to evaluate the ECG-gated dynamic 3D ICUS reconstruction in the *in vivo* assessment of coronary stents and test the findings in an *in vitro* model.

Address correspondence to: Dr. Jos R.T.C. Roelandt, Thoraxcentre, Erasmus University, P.O. Box 1738, 3000 DR Rotterdam, The Netherlands. E-mail: Roelandt@card.azr.nl

METHODS

Study population

We studied 51 patients (43 men; age: 51 ± 28 y) with ICUS. All were in sinus rhythm. Patients were examined directly after implantation of Wallstents™ (Schneider Europe AG, Bülach, Switzerland; $n = 36$) and Cordis™ Coronary balloon-expandable coiled stents (Cordis, Johnson & Johnson Company, Warren NJ, USA; $n = 15$) or during 6-month follow-up studies. The stented segments were located in the right coronary ar-

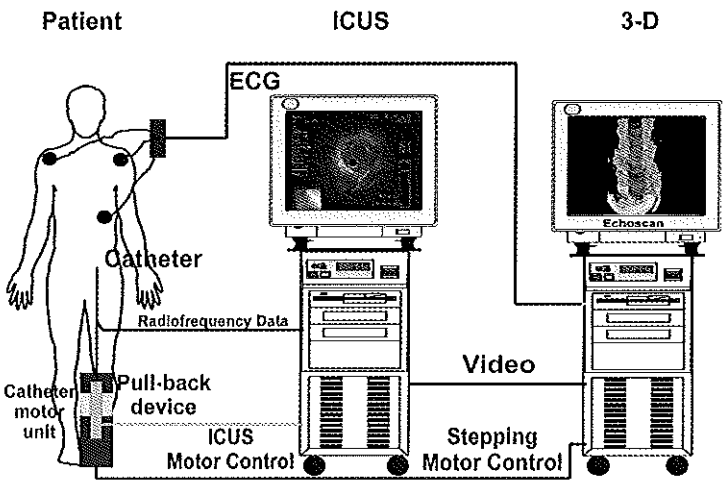

Fig. 1. Equipment set up in the catheterization laboratory. Besides the basic intracoronary ultrasound (ICUS) system, a three-dimensional (3D) image acquisition workstation (EchoScan, TomTec) was used (displayed on the righthand side). The 3D reconstruction system received the video output of the ICUS system and the patient's electrocardiographic (ECG) signal to control the stepping motor.

tery (RCA, $n = 22$), left anterior descending coronary artery (LAD, $n = 24$) and left circumflex coronary artery (LCX, $n = 5$). The study was approved by the Local Council on Human Research. All patients signed a written informed consent form, which had been approved by the Local Medical Ethics Committee. There were no procedural or postprocedural in-hospital complications.

Interventional procedure and intracoronary ultrasound imagining

Patients received 250-mg aspirin and 10,000-U heparin intravenously. If the duration of the entire interventional procedure exceeded 1 h, the activated clotting time was measured, and intravenous heparin was administered in order to maintain an activated clotting time of >300 s. Intracoronary ultrasound imaging was performed after intracoronary injection of 0.2-mg nitroglycerine, and imaging was started at least 10 mm distal to the stented segment. The mechanical ICUS systems Insight III, ClearView (CardioVascular Imaging Systems Inc., [CVIS] Sunnyvale, CA, USA), and Sonos (Hewlett-Packard, Andover, MA, USA) were used with 2.9-F sheath-based ICUS imaging catheters (MicroView, CVIS) that incorporated a 30-MHz beveled single-element transducer rotating at 1800 rpm. These catheters are equipped with a 15-cm-long sonolucent distal sheath, which has a lumen that alternatively houses the guidewire during catheter introduction, or the transducer during imaging after the guidewire has been retracted. The sheath prevents direct contact of the imaging core with the stent or the vessel wall. A custom-designed ECG-gated pullback device and a 3D ultrasound workstation (EchoScan, TomTec GmbH, Munich, Germany) were used to acquire and process the ICUS images (Bruining et al. 1995; von Birgelen et al. 1997b).

In vitro study

A Cordis Coronary stent and a Wallstent were expanded in a water bath and images were acquired between two synthetic blocks with two 2.9-F drilled holes, with a straightened 2.9-F sheath-based ICUS catheter (UltraCross, CVIS). The ICUS catheter was pulled back using the motorized pullback device used in the *in vivo* study. Steering and digitization of the images were performed by the 3D workstation (EchoScan, TomTec GmbH).

ECG-gated intracoronary ultrasound image acquisition

The custom-designed ECG-gated pullback device (Bruining et al. 1995) used a stepping motor to move the transducer stepwise through the stationary imaging sheath. The pullback device was controlled by the 3D ultrasound workstation. The workstation received video

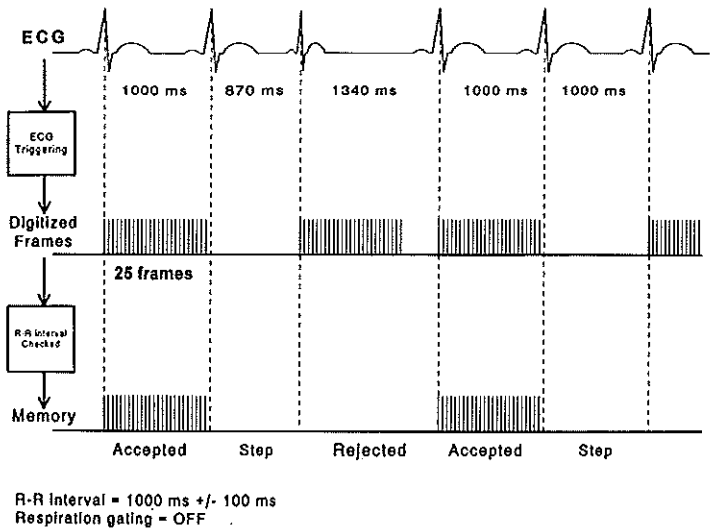

Fig. 2. Diagram showing the image acquisition schematics. The peak of the R wave triggered the gated image acquisition. After acquisition of each cardiac cycle, the software checked if the R-R interval met the preset range. If this was the case, the images were transferred to the computer main memory, and the stepping motor received pulses to move the catheter axial by 0.2 mm. Otherwise, the images were removed from the memory of the frame grabber, and a new cardiac cycle was acquired with the catheter remaining at the same site.

input from the ICUS machine and an ECG signal from the patient (Fig. 1). Prior to the acquisition run, it measured the range of RR intervals, defining the upper and lower limits of the RR intervals.

The workstation began acquiring images after detecting the peak of the R wave at a speed of 25 images/s (one image each 40 ms), stopping after 1000 ms or after detecting the peak of the R wave of the next cardiac cycle. After acquiring one cardiac cycle, the workstation stored the images (six images to represent one heart cycle, which preserves computer memory for storage capacity) in the computer main memory if the acquired beat fell in the preset range, and the catheter was then moved by a 0.2-mm axial increment (0.2 mm was chosen to prevent the necessity for software interpolation between two cross-sectional images for missing imaging data). If the acquired beat fell outside the preset range, the catheter was left at the same site and a new cardiac cycle was acquired. This process was repeated until the end of the scan distance was reached (Fig. 2). After acquiring the coronary segment of interest, the operator calibrated the ICUS images for on- and off-line quantitative analyses.

Three-dimensional image processing

In accordance with their ECG phase, all images were formatted in volumetric data sets (256 * 256 * 256 pixels/each 8 bits). During postprocessing, several algorithms were applied to the images to reduce noise, enhance edges and reduce spatial artifacts (ROSA filter). A gray-level threshold range was used to separate and subtract the blood pool and background from the arterial wall structures and stents on each cross-sectional ICUS image (*i.e.*, segmentation). To permit reliable segmentation, it was sometimes necessary manually to remove artifacts, such as sheath artifacts, from the image data set. Care was taken not to remove any data that corresponded with vessel wall structures or stents. Figure 3 shows a coronary segment, reconstructed after segmentation at different gray-level thresholds.

Volume rendering techniques were used to obtain dynamic 3D reconstructions of the coronary segments studied. Rendering is a processing step, producing a spatial (3D) appearance on a planar computer monitor or hardcopy printout. The coronary segment was sliced in two halves from which the bottom or the top part was used for 3D reconstruction. The reconstructed segment

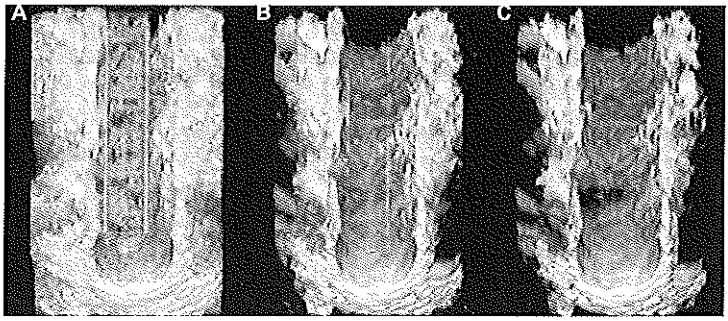

Fig. 3. Three-dimensional reconstructions created with different levels of the gray-level threshold algorithm. (A) A threshold was chosen so that no tissue was removed. This resulted in the blind spot of the catheter and the near-field artifact blocking the view of the vessel wall. (B) A gray-level threshold was chosen so as significantly to reduce the blind spot (the area of the image, in the middle, where is no vessel image information) and the near-field artifact of the catheter, but this produced loss of some tissue and plaque. (C) The threshold was chosen so that the near-field artifact was cleared, but this was associated with significant tissue loss.

was angled to create depth perception (Fig. 3). "Endoscopic" views (Fig. 5c, 5f and 6c), mimicking views from a "black-and-white" low-resolution angioscopic catheter, could also be produced.

The two best rendering modes for stents were as follows. (1) Gradient shading. In this rendering technique, an illumination model is used. "Light" emitted from the viewer's perspective is "reflected" from surface undulations of the reconstructed object. This type of rendering provides very realistic and detailed views, but is susceptible to artifacts in the voxel data (Fig. 4A) (*e.g.*, noisy images). (2) Maximum mode. Along numerous

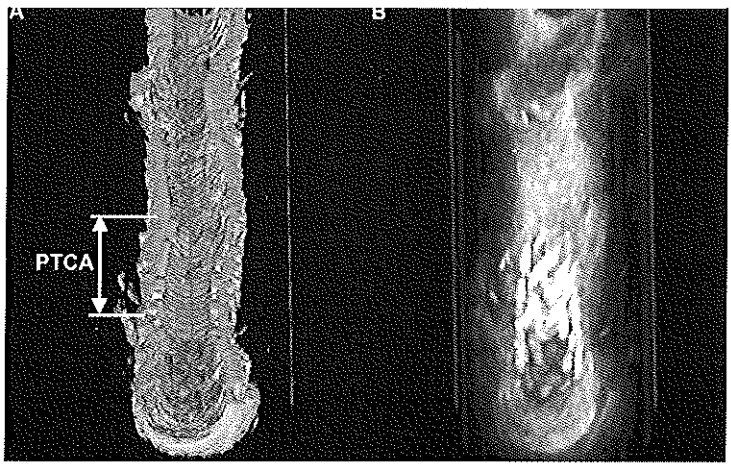

Fig. 4. (A) The gradient shading and (B) maximum rendering mode of a non-ECG-gated pullback study (causing a ribbon effect of the vessel surface) of a SciMed Radius stent. In (A) the site of angioplasty in the coronary vessel can be identified because the segment is smoother than other visible parts. However, no stent struts can be identified. In (B), applying the maximum rendering mode, struts of a stent can be appreciated.

Table 1. Three-dimensional stent visualization quality

	Crossflex	Wallstent
Excellent	1 (8%)	9 (21%)
Good	2 (15%)	13 (32%)
Moderate	8 (61%)	8 (34%)
Poor	2 (16%)	4 (13%)

Chi-square test between the groups showed a value of $p = 0.06$.

rays through the voxel set, only the maximal gray value is displayed, with the threshold of this gray value being operator defined. As a result, only bright structures such as calcified tissue or metallic stent struts are displayed. The maximum mode display allows a "transparent" ICUS view of the coronary segment (Fig. 4B) and emphasizes implanted stent structures.

The gradient shading rendering mode was used when the stent was not covered with tissue, as is usually the case directly after implantation. If the stent was covered by tissue, maximum mode rendering was used to visualize the stent struts.

Data analysis and statistics

Two independent and experienced ICUS operators rated the quality of the 3D reconstruction and visualization of the stents, on a scale of excellent to poor. The Chi-square test was used to compare the qualitative results of the different stent types. $p < 0.05$ was considered statistically significant.

RESULTS

Image acquisition of the stented coronary segments was performed within 3 ± 2 min (six images/cardiac cycle, 250 heart cycles needed), using a longitudinal step resolution of 0.2 mm and an average scan length of 5 cm. Processing of the 3D rendered reconstruction took at least 1 h.

In vivo intracoronary ultrasound study

Dynamic 3D reconstruction could be performed in all cases. All 3D reconstructions were rated for quality of imaging and the visibility of stent struts (Table 1). The imaging of mesh stents was much better than that of coil stents ($p = 0.06$). There was a good agreement between the two observers.

In vitro intracoronary ultrasound study

The *in vivo* findings were confirmed *in vitro*: 3D visualization of the entire Wallstent architecture could be successfully performed (Fig. 5C), but the reconstruction of the Cordis Coronary stent failed to display the full stent architecture (Fig. 5F).

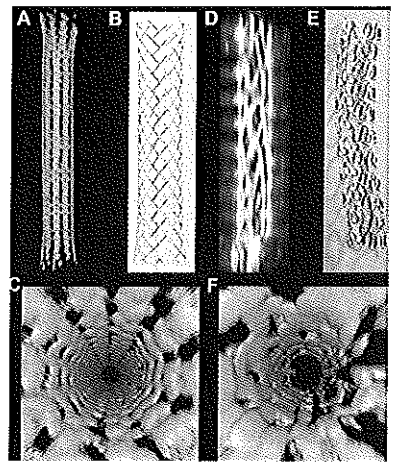

Fig. 5. *In vitro* intracoronary ultrasound images of (A) and (C) The Wallstent (D) and (F) The Crossflex stent. The three-dimensional (3D) reconstructions of the Wallstent (A) and (B) show a continuous framework of the stent architecture with a blurring effect at the crossings of the stent wires. The 3D reconstructions of the Crossflex stent (D) and (F) show the struts, but the complete stent architecture is discontinuous and is not completely visualized.

DISCUSSION

Three-dimensional reconstruction of human coronary arteries using ICUS and sequential tomographic

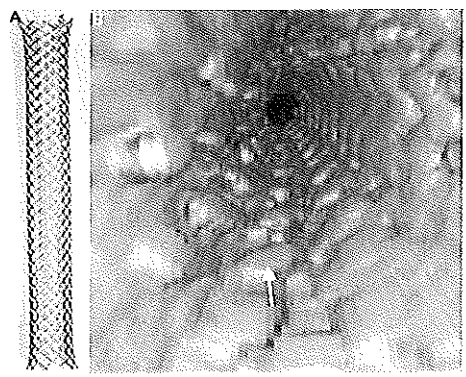

Fig. 6. (A) An expanded Wallstent showing that the architecture of the struts is predominantly longitudinal. (B) A gradient rendered three-dimensional reconstruction of a Wallstent implanted in the right coronary artery of a 57-y-old male is shown. A strut is indicated by the arrow.

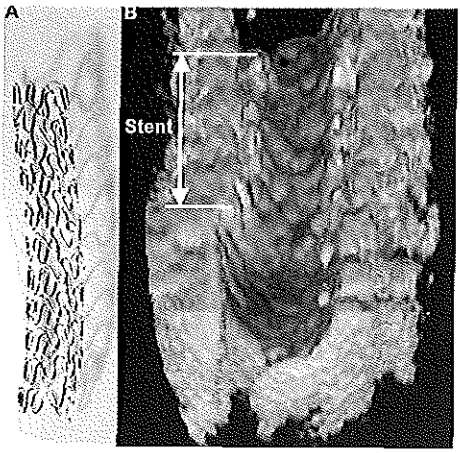

Fig. 7. (A) The predominantly transversal architecture of the struts of the Cordis Coronary stent can be seen. (B) In the three-dimensional rendered image, the stent implantation site is suggested by the elevation of the surface of the lumen. However, no single strut can be identified.

images has been achieved (Bruining et al. 1995; Coy et al. 1992; Mintz et al. 1993; Roelandt et al. 1994; Rosenfield et al. 1991; von Birgelen et al. 1995). Most frequently, a motorized uniform-speed pullback is used for data acquisition. More recently, an ECG-controlled pullback of the ultrasound transducer was introduced, providing significant advantages for quantitative analysis (Bruining et al. 1995) and 3D reconstruction. Cyclic changes of vessel dimensions (Bruining et al. 1996) and displacement of the ultrasound transducer in the lumen produces sawblade-shaped artifacts in longitudinally reconstructed views. By applying an ECG-triggered gated image acquisition, the images compiled in the tomographic image sets were acquired at the same moment of the cardiac cycle, resulting in smoother contours of the coronary lumen and vessel wall in reconstructed longitudinal views (Bruining et al. 1995; Coy et al. 1992; Mintz et al. 1993; Roelandt et al. 1994; Rosenfield et al. 1991; von Birgelen et al. 1995). Furthermore, applying this way of ICUS image acquisition, dynamic 3D reconstructions can be computed showing vessel dynamics.

Three-dimensional reconstruction of stents

The 3D reconstruction of stents struts *in vivo* remains difficult, and image artifacts of individual stent struts may result from differences in: (1) stent architecture, (2) strut thickness, (3) strut density (number of struts per mm^2), (4) catheter position relative to the vessel, (5) ICUS image resolution (Benkeser et al. 1993), and (6) cyclic movement. The cobalt-alloy round-wire struts with platinum core (thickness: 0.08–0.10 mm) of the Wallstent are predominantly oriented in a longitudinal direction, permitting detailed visualization of the stent architecture *in vivo* (Fig. 6), whereas the architec-

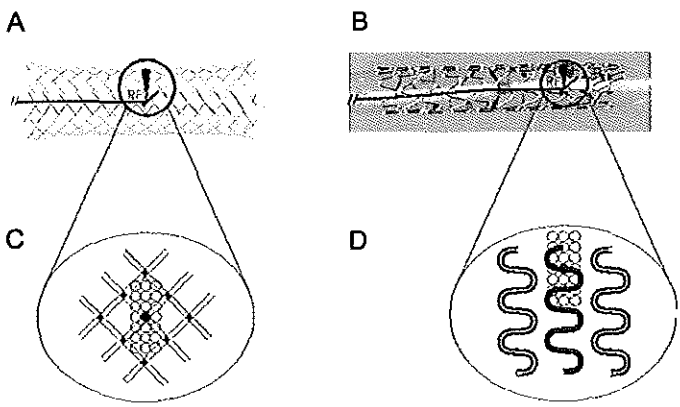

Fig. 8. (A) Intracoronary ultrasound (ICUS) catheter sampling of The Wallstent and (B) the Crossflex stent. Ellipses indicating the projection of the ultrasound beam against the stent struts. The rows of ellipses indicate two consecutive axial positions of the ICUS catheter during a stepped pullback procedure. The density of struts, longitudinal architecture of the stent, resolution (axial and lateral) of the ICUS catheter used and the software smoothing and interpolation algorithms resulted in a higher number of voxels (three-dimensional [3D] pixels) containing struts of the Wallstent, leading to a 3D reconstruction in which the stent architecture could be appreciated.

ture of the Cordis Coronary stent, consisting of predominantly transversely oriented round tantalum wires (thickness: 0.127 mm), was not completely visualized in 3D reconstructed views (Fig. 7). In these stents the resolution of the ICUS catheters used, the method of image acquisition (axial displacement of the ICUS catheter) and the software smoothing and interpolation algorithms (configured to smooth and interpolate axial gaps in the imaging data and thus ineffective on lateral imaging data) result in a low quantity of strut "samples" for computing a 3D reconstruction (Fig. 8). The *in vivo* observations were confirmed by the results of the *in vitro* study.

Limitations and potential sources of error

(1) The basic image quality and the resolution of the current ICUS transducers were important limiting factors in the overall quality of 3D ICUS reconstructions. With the limited resolution and the software smoothing and interpolation, thin transversely oriented strut wires were not able to be visualized. (2) The 3D reconstructed views were artificially straightened and do not reproduce vascular curvatures (Thrush et al. 1997). Coronary segments, however, are relatively straight after stent implantation. Conceptually, approaches that combine data obtained from angiography and ICUS can provide information on real spatial vessel geometry, but these sophisticated techniques are still laborious and currently in need of refinement and further research (von Birgelen et al. 1997a, 1997b). (3) Our experience suggests that ECG-gated image acquisition was feasible in >90% of patients referred for coronary intervention, but may be difficult in patients with irregular heart rhythms and even impossible in the presence of atrial fibrillation, unless cardiac pacing is performed. (4) ECG-gated image acquisition requires more time than uniform-speed pullbacks.

CONCLUSION

Dynamic three-dimensional reconstruction of the entire stent architecture from *in vivo* images was feasible for stents with a mesh structure, whereas the struts of stents with a coil type could only be partially reconstructed. These *in vivo* observations were supported by *in vitro* experiments.

Acknowledgement—Dr. von Birgelen is the recipient of a fellowship from the German Research Society, DFG, Bonn, Germany.

REFERENCES

Benkeser PJ, Churchwell AL, Lee C, et al. Resolution limitations in intravascular ultrasound imaging. J Am Soc Echocardiogr 1993;6: 158–165.

Bruining N, von Birgelen C, Di Mario C, et al. Dynamic three-dimensional reconstruction of ICUS images based on an ecg-gated pull-back device. In: Computers in cardiology. Vienna: IEEE Computer Society Press, 1995:633–636.

Bruining N, von Birgelen C, Mallus MT, et al. ECG-gated ICUS image acquisition combined with a semi-automated contour detection provides accurate analysis of vessel dimensions. In: Computers in cardiology. Indianapolis: IEEE Computer Society Press, 1996:53–56.

Coy KM, Park JC, Fishbein MC, et al. In vitro validation of three-dimensional intravascular ultrasound for the evaluation of arterial injury after balloon angioplasty. J Am Coll Cardiol 1992;20:692–700.

Deaner AN, Cubukcu AA, Rees MR. Assessment of coronary stent by intravascular ultrasound. Int J Cardiol 1992;36:124–126.

Dussaillant GR, Mintz GS, Pichard AD, et al. Small stent size and intimal hyperplasia contribute to restenosis: A volumetric intravascular ultrasound analysis. J Am Coll Cardiol 1995;26:720–724.

Fitzgerald PJ, St. Goar FG, Connolly AJ, et al. Intravascular ultrasound imaging of coronary arteries. Is three layers the norm? Circulation 1992;86:154–158.

Goldberg SL, Colombo A, Nakamura S, et al. Benefit of intracoronary ultrasound in the deployment of Palmaz-Schatz stents. J Am Coll Cardiol 1994;24:996–1003.

Mintz GS, Painter JA, Pichard AD, et al. Atherosclerosis in angiographically "normal" coronary artery reference segments: An intravascular ultrasound study with clinical correlations. J Am Coll Cardiol 1995;25:1479–1485.

Mintz GS, Pichard AD, Satler LF, et al. Three-dimensional intravascular ultrasonography: Reconstruction of endovascular stents in vitro and in vivo. J Clin Ultrasound 1993;21:609–615.

Prati F, Di Mario C, Gil R, et al. Usefulness of on-line three-dimensional reconstruction of intracoronary ultrasound for guidance of stent deployment. Am J Cardiol 1996;77:455–461.

Roelandt JR, Di Mario C, Pandian NG, et al. Three-dimensional reconstruction of intracoronary ultrasound images. Rationale, approaches, problems, and directions. Circulation 1994;90:1044–1055.

Rosenfield K, Losordo DW, Ramaswamy K, et al. Three-dimensional reconstruction of human coronary and peripheral arteries from images recorded during two-dimensional intravascular ultrasound examination. Circulation 1991;84:1938–1956.

Thrush AB, Bonnet DE, Elliot MR. An evaluation of the potential and limitations of three-dimensional reconstructions from intracoronary ultrasound images. Ultrasound Med Biol 1997;23:437–445.

von Birgelen C, Erbel R, Di Mario C, et al. Three-dimensional reconstruction of coronary arteries with intravascular ultrasound. Herz 1995;20:277–289.

von Birgelen C, Gil R, Ruygrok P, et al. Optimized expansion of the Wallstent compared with the Palmaz-Schatz stent: On-line observations with two- and three-dimensional intracoronary ultrasound after angiographic guidance. Am Heart J 1996;131:1067–1075.

von Birgelen C, Mintz GS, Nicosia A, et al. Electrocardiogram-gated intravascular ultrasound image acquisition after coronary stent deployment facilitates on-line three-dimensional reconstruction and automated lumen quantification. J Am Coll Cardiol 1997a;30:436–443.

von Birgelen C, de Vrey EA, Mintz GS, et al. ECG-gated three-dimensional intravascular ultrasound: Feasibility and reproducibility of an automated analysis of coronary lumen and atherosclerotic plaque dimensions in humans. Circulation 1997b;96:2944–2952.

CHAPTER 5

Ultrasound Appearances of Coronary Stents as Obtained by Three-dimensional Intracoronary Ultrasound Imaging In-Vitro

N. Bruining, C. von Birgelen, P.J. de Feyter, J.R.T.C. Roelandt and P.W. Serruys

Journal of Invasive Cardiology, 1998; 6: 332-338
Partly published In: Handbook of coronary stents, second edition. Martin Dunitz, 1998; 289-316

Ultrasound Appearances of Coronary Stents as Obtained by Three-Dimensional Intracoronary Ultrasound Imaging *In Vitro*

Nico Bruining, BSc, Clemens von Birgelen, MD, Pim J. de Feyter, MD, PhD, Jos R.T.C. Roelandt, MD, PhD, Patrick W. Serruys, MD, PhD

ABSTRACT: Intracoronary ultrasound (ICUS) is an imaging technique which can provide a cross-sectional image of coronary arteries and implanted stents. Different stents may have individual ICUS imaging characteristics. To investigate the imaging characteristics and three-dimensional (3-D) reconstruction of different coronary stent designs, we examined 26 different stents using ICUS *in vitro*. All stents could be well visualized with planar ICUS. In 18 stents, 3-D imaging succeeded in reconstructing the spatial stent architecture. This was not possible in the other 8 stents, most probably because of predominantly transversally-orientated strut architecture, the small size of the strut wire width, the limited ICUS lateral catheter resolution, and the smoothing and interpolation algorithms applied for 3-D reconstruction. ICUS *in vitro* provides a means of identifying coronary stent structures which may be applicable *in vivo*. Three-D reconstruction of the entire stent architecture *in vitro* can be achieved in stents with mesh or slotted tube design, while stents with coil design and thin strut wires can only be partially reconstructed.

J INVAS CARDIOL 1998;10:332–338

Key words: intravascular ultrasound, stents, image processing, three-dimensional reconstruction

Endovascular stenting is commonly used in conjunction with balloon angioplasty for the management of atherosclerotic coronary artery disease.[1-5] Intracoronary Ultrasound (ICUS) is superior to angiography in assessing the adequacy of stent deployment.[6-8] ICUS is frequently helpful in improving the results of stenting procedures. Conventional ICUS provides only cross-sectional images. Three-D reconstruction of the spatial information gathered during ultrasound catheter pullback allows easier interpretation of the images. Improvements in the computer software and hardware used for 3-D reconstruction, the ICUS catheter and scanner technology permit highly accurate 3-D reconstruction of stent morphology.

The variety of stents available for clinical use is increasing. Each stent has individual ICUS imaging characteristics. The aim of this *in vitro* study was to assess the ICUS appearances of different stent designs. We performed *in vitro* ICUS studies of 26 commercially available stents, and examined their ICUS appearance in 2-D longitudinally reconstructed views, 3-D longitudinal views and 3-D endoscopic views.[9-13]

From the Thoraxcenter, Department of Cardiology, Erasmus Medical Center, Rotterdam and Erasmus University, Rotterdam, The Netherlands.

Dr. von Birgelen is the recipient of a fellowship of the German Research Society (DFG, Bonn, Germany).

Address reprint requests to: N. Bruining, AZR Dijkzigt/Thoraxcentre, Erasmus University, Room BD308b, Dr. Molewaterplein 40, 3015 GD Rotterdam, The Netherlands. E-mail: Bruining@thch.azr.nl

Table 1. Manufacturer details of the used stents, the letters of the first column identifies the stents in Figures 2 and 3.

Figure 2&3	Stent	Manufacturer	Complete 3-D image
A	ACS new	Guidant/Advanced Cardiovascular Systems, Santa Clara, CA, USA	No
B	ACT-One	Progressive Angioplasty Systems Inc, Menlo Park, CA, USA	Yes
C	Angiostent	AngioDynamics, Glen Falls, NY, USA	No
D	AVE MICRO II	Arterial Vascular Engineering, Inc. Santa Rosa, CA, USA	Yes
E	BARD XT	Bard Ireland Ltd, Galway, Ireland	No
F	BeStent	Medtronic Instent, Minneapolis, MN, USA	Yes
G	Crossflex	Cordis, a Johnson& Johnson Company, Warren, NJ, USA	No
H	Crown	Johnson & Johnson Interventional Systems	Yes
I	Divysio A	BiodYviso	Yes
J	Divysio B	BiodYviso	Yes
K	Freedom	Global Therapeutics Inc, Broomfield, CO, USA	Yes
L	Gianturco-Roubin II	Cook, Inc., Bloomington, IN, USA	Yes
M	Cardiocoil	Medtronic Instent, Minneapolis, MN, USA	No
N	IRIS	Uni-Cath Inc., Saddlebrook, NJ, USA	Yes
O	Balloon eXpandable (BX)	IsoStent Inc., Belmont, CA, USA	Yes
P	Jostent M Bifurcation	JOMED International, AB Helsingborg, Sweden	Yes
Q	Navius	Navius Corporation, San Diego, CA, USA	Yes
R	NIR 7 & 9 Cell	Medinol, Ltd., Tel Aviv, Israel	Yes
S	Palmaz-Schatz (new design)	Cordis, Johnson&Johnson Interventional Systems, Warren, NJ, USA	Yes
T	Palmaz-Schatz (old design)	Cordis, Johnson&Johnson Interventional Systems, Warren, NJ, USA	Yes
U	Pura Vario	Devon Medical, Hamburg, Germany	No
V	Radius	SciMED Life systems, Maple Grove, Minnesota, USA	Yes
W	Tensum	Biotronik, Berlin, Germany	Yes
X	Wallstent	Schneider Europe AG, Bülach, Switzerland	Yes
Y	Wiktor I	Medtronic Interventional Vascular-EUROPE, Kerkrade, The Netherlands	No

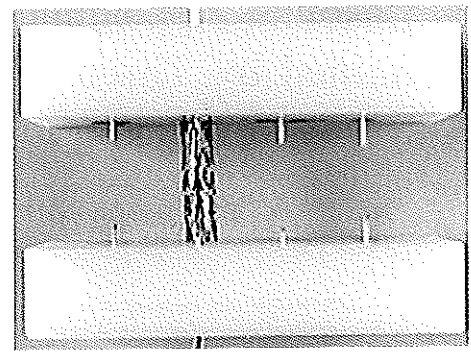

Figure 1. *The stents were positioned by two small pins between two blocks through which the ICUS catheter was led via tiny holes. The holes in the blocks were made so that the ICUS catheter was positioned on the center of the long axis of the stents.*

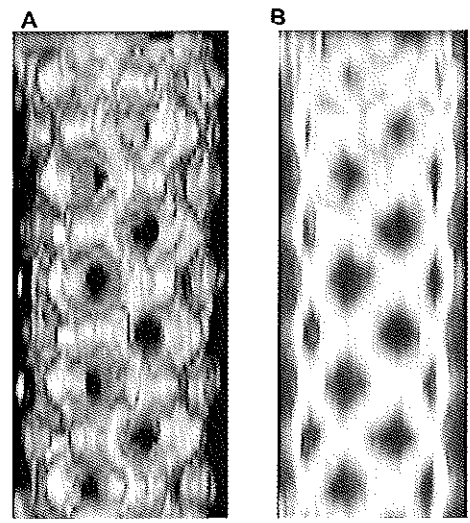

Figure 2. *The gradient shading, panel A, and maximum, panel B, rendering mode.*

MATERIALS AND METHODS

Stent population, imaging procedure and equipment set-up. Details of the stents are presented in Table 1. Stents with diameter sizes from 2–4 mm and lengths from 1–5 cm were used. All stents were suspended in a water bath at a temperature of 20°C. The ICUS catheter [UltraCross, CardioVascular Imaging Systems Inc. (CVIS), Sunnyvale, California] was straightened and centered in the longitudinal axis of the stent (Figure 1). The gain settings of the ICUS

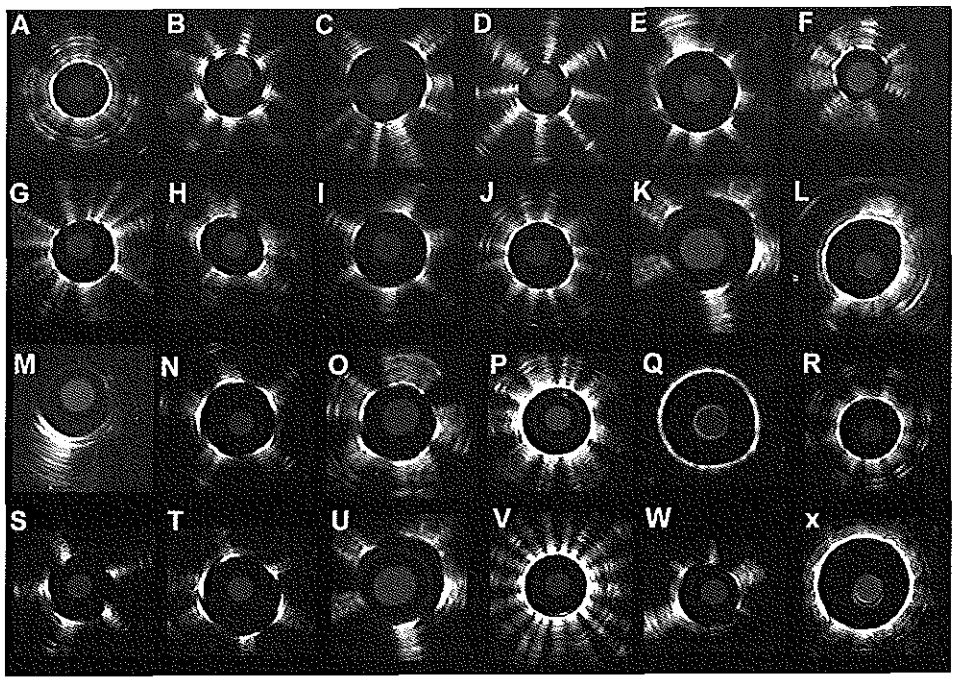

Figure 3. *Composition of the 2-D ICUS appearances of all the different stents examined. Details of the stents can be found in Table 1.*

scanner (Clearview, CVIS) were optimized for data acquisition from the individual stents and in particular were increased to accentuate the stent struts. The catheter incorporates a 30 MHz beveled single element transducer rotating at 1,800 rpm. These catheters have a 2.9 Fr, 15 cm long sonolucent distal sheath with a lumen which alternatively houses the guide wire during catheter introduction or the transducer during imaging after the guide wire has been retracted. This design prevents direct contact of the imaging core with the vessel wall when used *in vivo*, and facilitates *in vitro* straightening of the catheter. A custom designed pullback device and a 3-D ultrasound workstation (EchoScan, TomTec GmbH, Munich, Germany) were used to acquire the ICUS images.[9,14]

Image acquisition. The images were acquired during a computer controlled pullback sequence. The step between 2 adjacent acquisition-imaging sites on the transducer pullback path was 0.2 mm. The video images generated by the ICUS scanner were digitized and stored in computer memory by the 3-D workstation.

Image processing and 3-D reconstruction. After acquisition the images were formatted in volumetric data sets (256*256*256 pixels, 8 bits each). During post-processing, several algorithms were applied to reduce noise, enhance edges, and reduce spatial (axial) artifacts (ROSA filter) without user interaction. Volume rendering techniques were used to obtain 3-D reconstructed views of the stents. Rendering is a processing step, producing a spatial (3-D) appearance on a computer monitor or printout. The operator specified an observing point from where he wanted to have a view of the stent. The stent structure was then rotated around its long axis to have a view from all sides (90 different positions of the stent were calculated). The stents were also reconstructed in an "endoscopic" view. An "observation" location was selected just beyond the stent in its long axis, with the "blindspot" of the ICUS catheter located in the middle of the stent lumen. After the first reconstruction, the "observation" point was moved 0.5 mm and a new 3-D reconstruction was computed. This process was repeated until the whole of the stent had been imaged. When these 3-D reconstructions are shown in rapid sequence (12.5 images/second) on the computer display, the animation mimics the same images that a black and white angioscopy catheter being moved into the stent would display. A user interactive gray level threshold range,

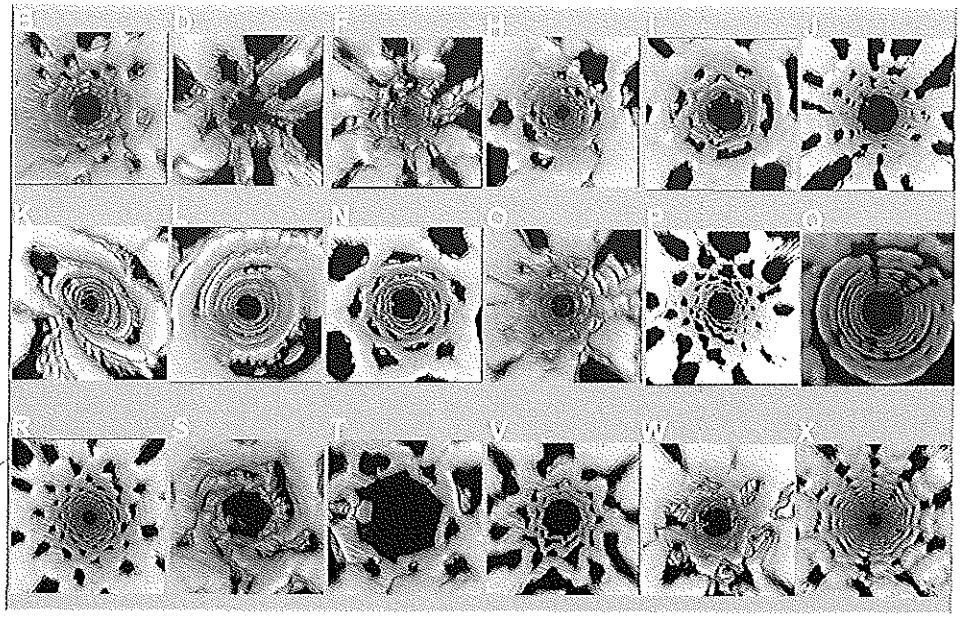

Figure 4. *Composition of all the successful 3-D reconstructed endoscopic views, the stents are listed in Table 1.*

or segmentation, was used to separate and subtract the stent from background.

Different rendering modes were available and the 2 best suited for 3-D reconstruction of stents were applied.

Gradient shading. In this rendering technique, a realistic illumination model is used. The 'light' source is assumed to be mounted on the head of the observer. 'Light' emitted from this source, is 'reflected' from the surface undulations of the reconstructed object. This type of rendering provides very realistic and detailed views, but is susceptible to artifacts in the voxel data (Figure 2A).

Maximum mode. Along numerous rays through the voxel set, only the maximal grey values are displayed with the threshold of this grey value being operator-defined. As a result, only highly reflective structures such as metallic stent struts are displayed or calcified (Figure 2B).

RESULTS

All stents could be well visualized with ICUS (Figure 3). The mean acquisition time to acquire the tomographic 3-D image set for each stent was < 1 minute. The time to perform a dynamic longitudinal 3-D reconstruction was 2 hours per stent. The time to produce dynamic endoscopic 3-D reconstructions was 5 hours for 30 images, because of the more complex nature of these computations.

Saggital views of all stents could be computed. The strut architecture of 18 stents could be well visualized in the 3-D longitudinal reconstructions (Table 1). Endoscopic 3-D reconstruction of the same 18 stents was possible (Figure 4). It was not possible to compute a 3-D reconstruction in which the stent architecture could be appreciated in the other 8 stents. In the 18 successful 3-D reconstructions, details such as diamond shaped gaps, central articulations and flaring of the stent ends could be appreciated. From Table 1, 3 stents were randomly selected to be shown in detail in Figures 5–7.

DISCUSSION

In vitro ICUS investigations and 3-D reconstruction of stents have previously been performed.[10,13] This is the first study to highlight differences and similarities between a large range of stents. The direct comparison between the stent and its 3-D reconstruction provides an excellent standard against which to gauge ICUS imaging systems and 3-D reconstruction software. The initial expectation of the investigators was to find similar ICUS images between the different stents. Despite

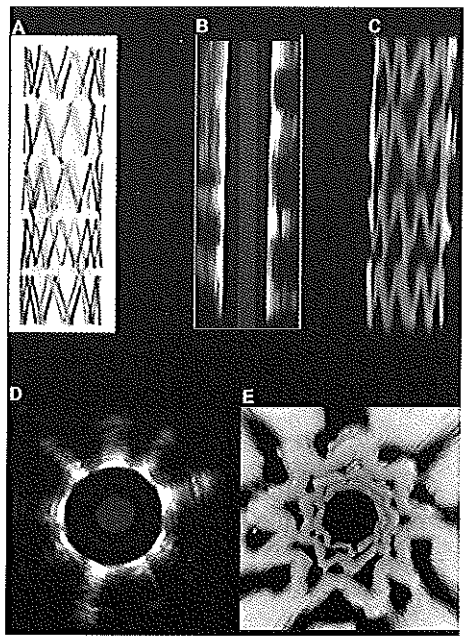

Figure 5. *ICUS representations of the Scimed Radius stent (photo of the stent in panel A). In panel B, a computed 2-D longitudinal view is presented. Panel C shows a longitudinal 3-D reconstruction cut into half. In panel D, the "normal" 2-D ICUS appearance of the stent is given and finally, panel E shows the endoscopic 3-D view of this stent.*

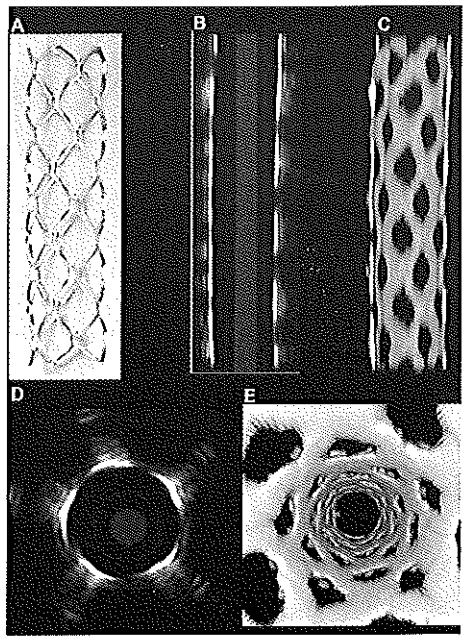

Figure 6. *ICUS representations of the IRIS stent (photo of the stent in panel A). In panel B, a computed 2-D longitudinal view is presented. Panel C shows a longitudinal 3-D reconstruction cut into half. In panel D, the "normal" 2-D ICUS appearance of the stent is given and finally, panel E shows the endoscopic 3-D view of this stent.*

similarity in stent architectures and the limited resolution of ICUS imaging, all stents had their own specific ICUS image characteristics. The *in vitro* setting in which the ICUS studies were performed greatly contributed to the excellent imaging results.

Three-D reconstruction of stents. Three-D reconstruction of the complete stent architecture remains a difficult task. There were several factors which caused artifacts or prevented 3-D reconstruction of individual stent struts. These included: (1) A predominantly longitudinally-oriented stent architecture; (2) thin width of strut wires; (3) low strut density (number of struts per mm²). Moreover, the basic ICUS image resolution of the current ICUS technology remains limited.[15] Stents with thick strut wires and predominantly longitudinally-oriented strut construction were best suited for 3-D reconstruction. 3-D visualization of the stent struts was not possible in stents with predominantly transversally orientated strut architectures such as the Wiktor stent (Figure 7). The main reason for this was data undersampling due to the lack of digitized cross-sectional ICUS images in the region of the struts (Figure 8B). In mesh and/or slotted tube stent designs (Figure 8A) a sufficient amount of data from the stent struts were able to be sampled to produce 3-D reconstructions, and the architecture of the stent could be well appreciated.

Limitations and potential sources of error. The present optimized *in vitro* study of the stents avoids problems *in vivo* studies will encounter. Eccentric catheter position within a deployed stent, tortuosity of the coronary artery, stents covered with endothelium or protruding atherosclerotic plaque, and catheter motion during the cardiac cycle can prevent satisfactory 3-D reconstruction and limit assessment of the stent. Nevertheless, *in vivo* examinations performed with an ECG-gated pullback of the ICUS catheter directly after implantation have shown promising results for the assessment of coronary stents (Figure 9). However, one of the most important factors for success of 3-D reconstruction of a stent *in vivo* is the "quality" of the planar ICUS images. The backscatter information of the blood should not be as bright as possibly found soft

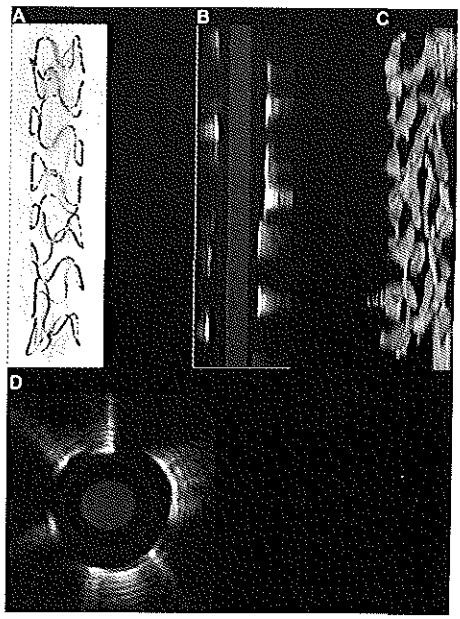

Figure 7. *ICUS representations of the Wiktor stent (photo of the stent in panel A). In panel B, a computed 2-D longitudinal view is presented. Panel C shows a longitudinal 3-D reconstruction cut into half. In panel D, the "normal" 2-D ICUS appearance of the stent is given. This stent design was not suitable for an attempt of 3-D reconstruction in which the architecture of the stent could be appreciated.*

tissue in the investigated segment (*ie.* a lumen as black as possible on the monitor of the ICUS machine). Due to the used threshold algorithm, bright backscatter images of the blood can block the view to the struts. Furthermore, a near-field artifact, sometimes present by mechanical ICUS catheters (reflection of the outer sheath), could limit the success for reconstruction. Large amounts of calcifications with the same brightness as the stent struts could further limit appreciation of the stent structure in 3-D.

Unfortunately, it is difficult, maybe even impossible, to set up an *in vitro* situation in which all the described limiting factors can be simulated. Probably only "real" cases can show us if this approach for 3-D reconstruction works in practice (Figure 9). Another current limit to the use of this method in a clinical setting is the long computational time needed. Taking into account that the 3-D reconstructions were performed on a normal PC, a considerable reduction of this time could be gained when specialized computing systems for 3-D are used. However, these systems are still expensive.

CONCLUSION

ICUS examination of stents *in vitro* provided characteristic ICUS images of all 26 stents examined allowing detailed visualization of coronary stent structures. A 3-D reconstruction of the stent architecture *in vitro* was achieved in stents with mesh or slotted tube design, whereas stents with coil design or thin strut wires could only be partially reconstructed.

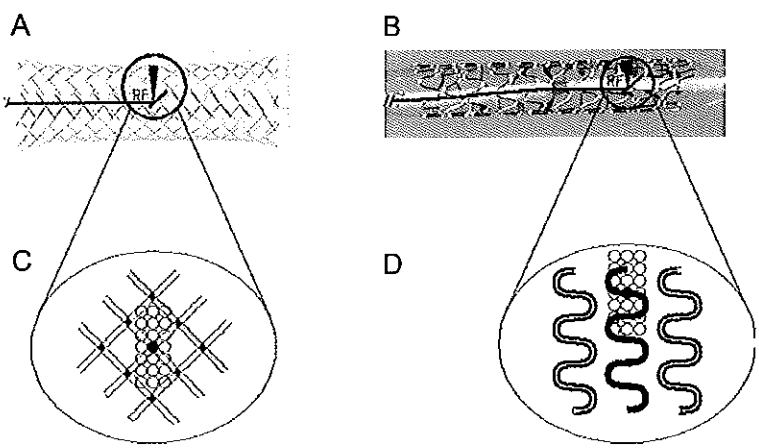

Figure 8. *In panel A, ICUS catheter sampling of the Wallstent, and in panel B the Crossflex stent is shown. In the "schematic" top panel figures (C and D), ellipses indicating the projection of the ultrasound beam against the stent struts are drawn. The rows of ellipses indicate two consecutive axial positions of the ICUS catheter during a stepped pullback procedure. The density of struts, longitudinal architecture of the stent, resolution (axial and lateral) of the ICUS catheter used, and the software smoothing and interpolation algorithms resulted in a higher number of voxels (3-D pixels) containing struts of the Wallstent leading to a 3-D reconstruction in which the stent architecture could be appreciated.*

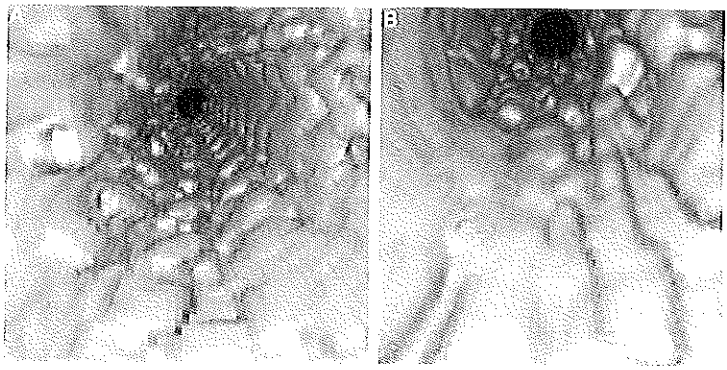

Figure 9. *In panel A, an implanted Wallstent can be appreciated. In panel B an implanted Radius stent is presented.*

REFERENCES

1. von Birgelen C, Gil R, Ruygrok P, et al. Optimized expansion of the Wallstent compared with the Palmaz-Schatz stent: On-line observations with two- and three-dimensional intracoronary ultrasound after angiographic guidance. *Am Heart J* 1996;131:1067–1075.
2. Mintz GS, Pichard AD, Kovach JA, et al. Impact of preintervention intravascular ultrasound imaging on transcatheter treatment strategies in coronary artery disease. *Am J Cardiol* 1994;73:423–430.
3. Ge J, Erbel R, Gerber T, et al. Intravascular ultrasound imaging of angiographically normal coronary arteries: A prospective study *in-vivo*. *Br Heart J* 1994;71:572–578.
4. Kimura BJ, Bhargava V, DeMaria AN. Value and limitations of intravascular ultrasound imaging in characterizing coronary atherosclerotic plaque. *Am Heart J* 1995;130:386–396.
5. Colombo A, Hall P, Nakamura S, et al. Intracoronary stenting without anticoagulation accomplished with intravascular ultrasound guidance. *Circulation* 1995;91:1676–1688.
6. Thrush AB, Bonnet DE, Elliot MR, et al. An evaluation of the potential and limitations of three-dimensional reconstructions from intravascular ultrasound images. *Ultrasound in Med & Biol* 1997;23:437–445.
7. Goldberg SL, Colombo A, Nakamura S, et al. Benefit of intracoronary ultrasound in the deployment of Palmaz-Schatz stents. *J Am Coll Cardiol* 1994;24:996–1003.
8. Prati F, De Mario C, Gil R, et al. Usefulness of on-line three-dimensional reconstruction of intracoronary ultrasound for guidance of stent deployment. *Am J Cardiol* 1996;77:455–461.
9. Bruining N, von Birgelen C, Di Mario C, et al. Dynamic three-dimensional reconstruction of ICUS images based on ecg-gated pull-back device. *Computers in Cardiology*. Vienna: IEEE Computer Society Press, 1995: pp. 633–636.
10. von Birgelen C, de Vrey IE, Mintz GS, et al. ECG-gated three-dimensional intravascular ultrasound: Feasibility and reproducibility of an automated analysis of coronary lumen and atherosclerotic plaque dimensions in humans. *Circulation* 1997;96:2944–2952.
11. Roelandt JR, di Mario C, Pandian NG, et al. Three-dimensional reconstruction of intracoronary ultrasound images: Rationale, approaches, problems, and directions. *Circulation* 1994;90:1044–1055.
12. Rosenfield K, Losordo DW, Ramaswamy K, et al. Three-dimensional reconstruction of human coronary and peripheral arteries from images recorded during two-dimensional intravascular ultrasound examination. *Circulation* 1991;84:1938–1956.
13. Mintz GS, Pichard AD, Satler LF, et al. Three-dimensional intravascular ultrasonography: Reconstruction of endovascular stents *in vitro* and *in vivo*. *J Clin Ultrasound* 1993;21:609–615.
14. von Birgelen C, Mintz GS, Nicosia A, et al. Electrocardiogram-gated intravascular ultrasound image acquisition after coronary stent deployment facilitates on-line three-dimensional reconstruction and automated lumen quantification. *J Am Coll Cardiol* 1997;30:436–443.
15. Benkeser PJ, Churchwell AL, Lee C, et al. Resolution limitations in intravascular ultrasound imaging. *J Am Soc Echocardiogr* 1993;6:158–165.

CHAPTER 6

Virtual Reality: a Teaching and Training tool or just a Computer Game?

N. Bruining, J.R.T.C. Roelandt, M. Janssen, G. Grunst, T. Berlage, J. Waldinger and Bernhard Mumm

The Thoraxcentre Journal, 1998; 10: 7-10

As part presented at Computers In Cardiology, September 9, 1997, Lund, Sweden

Virtual reality: a teaching and training tool or just a computer game?

NICO BRUINING[1], JOS R.T.C. ROELANDT[1], M. JANSSEN[1], GERNOTH GRUNST[2], THOMAS BERLAGE[2], JOHANNES WALDINGER[3] AND BERNHARD MUMM[3]

[1]Thoraxcentre, Department of Cardiology, Erasmus Medical Centre Rotterdam and Erasmus University, Rotterdam, The Netherlands, [2]GMD, Bonn, Germany, [3]TomTec GmbH, Munich, Germany

Introduction

The heart is a complex structure and assessment of its pathomorphology and function can be facilitated by three-dimensional (3-D) presentation of imaging data[1]. Sophisticated cardiac imaging techniques such as cross-sectional echocardiography[2-4], color-coded flow[5] and Doppler tissue imaging[6,7], ultrafast cine computer tomography[8] and magnetic resonance imaging[9,10] provide two-dimensional (2-D) images of the heart. If a sequence of 2-D images can be combined in a data set, a 3-D presentation of the heart can be generated[11-17]. At present, however, these 3-D reconstructions are presented in 2-D format. These reconstructions can still pose interpretation difficulties, principally for the observer in understanding the origins and orientations of the views[18]. Virtual dynamic techniques, known as Virtual Reality (VR), can assist with the interpretation of 3-D presentations of the heart[19, 20].
Virtual Reality (VR) is now being introduced into practice for evaluation as a teaching aid[19, 21-23], diagnostic modality, and to assist the surgeon in planning procedures[24].

Virtual Reality Systems

Computer graphics is a fascinating subject as it provides a mechanism to build and view 3-D objects without any physical materials. The objects may be teapots, cars, buildings, human bodies or human organs – in fact there are no limits to what can be simulated within a computer's memory. Computer animation introduces the dimension of time into this virtual world and allows us to manipulate these objects



Figure 1. Cryosection through Visible Human Male - thorax including heart, lungs, spinal column, major vessels, musculature, left ventricle (from Thorax data subset). (Reprinted with permission, National Library of Medicine and National Institutes of Health, Bethesda, Maryland, USA.)



Figure 2. 3-D reconstruction of the heart based on anatomical sections of a cadaver specimen. (Reprinted with permission, Conley DM and Rosse C, Digital Anatomist program, Dept. Biological structure, University of Washington, Seattle, USA.)

and create the illusion of animated movement[25]. A VR model is build by translating an object into geometric data. Whatever the source of the data, whether it involves cutting the model into pieces, scanning it with a laser, measuring it with a ruler, reading from drawings, it must be available before the modeling process can begin. Commercial computer animation systems provide an interactive environment where the user can construct 3-D models using various software tools. VR technology is used in training and simulation systems for military personnel and pilots[25].
Although computer animation has found an excellent niche in advertising, film special effects and television credits, it is also used for visualizing a wide variety of 3-D databases (by example a tomograhic data set) and numerical data sets. Projects such as the 'Visible Human™' in which anatomical

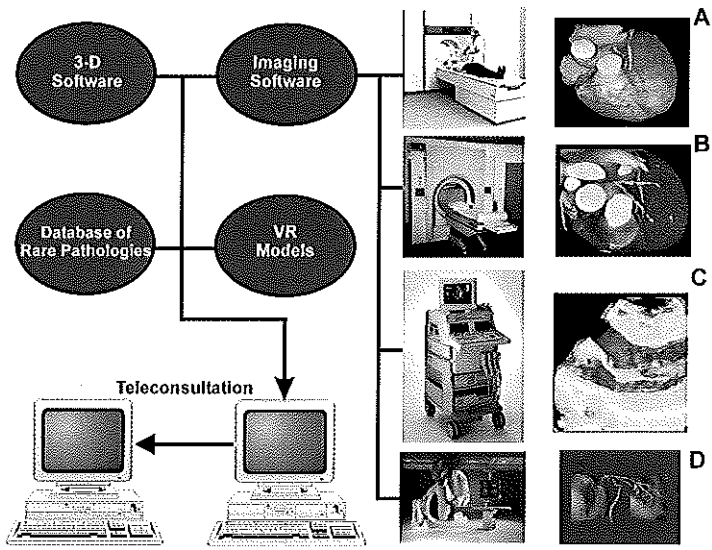

Figure 3. Different cardiac imaging modalities. A MRI (a), an EBT (b) (images courtesy of Van Ooijen P, DDHK), an echocardiographic scanner (c) and an angiogroom (d), are presented. The obtained images can be viewed through imaging software on a separate workstation. The viewing of the images can be extended to 3-D with specialized software. VR-models and databases of rare pathologies can be stored for medical training and teaching. (3-D coronary angiogram reconstruction, reprinted with permission from thesis of Wahle A, PhD, Technical University of Berlin, 1996, pag. 125.)

structures are displayed as VR models are of interest to the medical profession[26-29] (Figures 1 and 2).

VR is already used in medical disciplines[1, 24, 28, 30]. Full appreciation of bone structures such as the skull and pelvis after a complex fracture is greatly enhanced by VR presentation of the X-ray data.

The complex anatomy, pathology and dynamic changes make it difficult and time-consuming to build VR models of the heart[14]. Furthermore, the computer power necessary to simulate and display such dynamic models was until recently only possible with expensive 'high-end' computer systems. New developments in hardware, software and computer graphics have made this VR technology accessible to 'low-end' computer systems increasing the availability to potential users.

Cardiac imaging systems

Tomographic images of the heart are nowadays acquired with non-invasive or minimally invasive techniques and there have been recent major improvements in image resolution, digital storage and the electronic transfer of images, facilitating conversion of data to 3-D format (Figure 3).

Due to the limitations of displaying 3-D data on 2-D screens or printouts, the 3-D images are 'rendered'[18], a technique, which produces an image simulating an actual 3-D view when displayed on a computer monitor. Despite this process, interpretation of the 3-D image remains difficult (Figure 4).

3-D Cardiac Ultrasound

3-D echocardiography[3, 11-17] has been used in clinical practice for over 4 years. 3-D ultrasound provides cardiac images, which more closely mimic actual anatomy than 2-D cross-sectional images, and may thus be easier to interpret.

Potential cardiovascular applications for 3-D include:

- Assessment of ventricular function, volume and mass. These parameters are particularly relevant for the assessment of ischemic heart disease and cardiomyopathies, in which 2-D methods based on geometric assumptions are subject to error from distorted geometry and regional dysfunction.
- Evaluation of complex surfaces, such as the atrial septum, valve leaflets, prosthetic heart valves, papillary muscles and ventricle aneurysms.
- Definition of complex congenital heart defects.
- 3-D color flow Doppler which will improve understanding of the spatial distribution of blood flow.
- Surgical planning. The 3-D imaging provides the ability to display a structure in varied planes and offers the surgeon unique and useful views of cardiac anatomy.

However, when a 3-D rendered image is shown, the spatial information is most often lost. VR models are useful in maintaining this spatial information. This is important, since the 2-D image has limited dimensions and the whole heart is not captured into the data set. Furthermore, it is sometimes desirable to view some structures from nearby (zooming). The interpretation of the spatial relations of the magnified

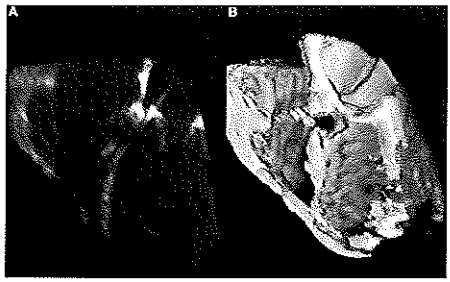

Figure 4. In panel A, a 2-D cross-section out of a tomographic data set is presented. In panel B, a 3-D reconstruction of the 4-chamber view is presented.

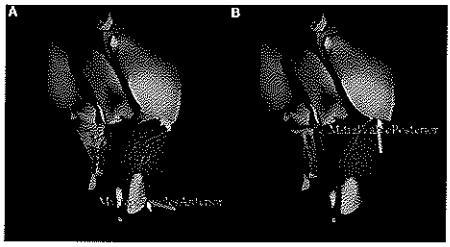

Figure 5. In panel A, a VR model of a 4-chamber long-axis view in diastole is presented. The 3-D cursor is located at the anterior mitral valve leaflet papillary muscle. In panel B the same projection is presented in systole. The small green and red balls in the model represent calibration points with which the model can be linked to a 'real' 3-D image data set of the heart.

area to the rest of the heart is then lost.

When the VR model is then coupled to real echo data, e.g. during examination of a patient, an interactive scenario becomes possible in which the operator can select a standardized echocardiographic view, which are defined in the VR model. This view is then also visible into the real echo data from which a 3-D reconstruction of the desired standard view can be computed. Standardization of clinical relevant views has been proposed[31], but a systematic approach of 3-D echocardiographic views is currently not available, which gives room for confusing. Identifying landmarks in the real echo data (Figure 5) can perform the coupling of the VR model with real echo data.

Cardi-Assist

Cardi-Assist[19] is a European project in cardiology in which VR has a crucial role. The Cardi-Assist project aims at providing remote support for the diagnosis of cardiac abnormalities, with echocardiography and transmission of data using telecommunication being pivotal. The managing consortium brings together industrial, medical, and scientific partners:

1. GMD, the German national research center for information technology.
2. Vingmed Sound, ultrasound manufacturer, Norway.
3. TomTec GmbH, manufacturer of workstation software for 3-D acquisition and 3-D reconstruction, Germany.
4. University of Trondheim, SINTEF/IDT, Norway.
5. University Bonn, Kinderklinik, Germany.
6. University Lisbon, Portugal.
7. Thoraxcentre, Erasmus University Rotterdam, The Netherlands.

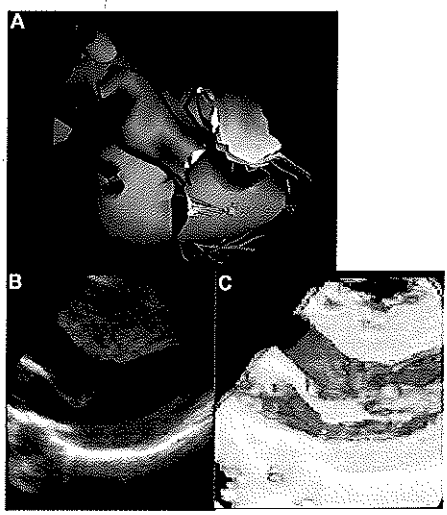

Figure 6. In panel A, the VR model is altered so that it closely resembles the 2-D echocardiographic image presented in panel B. In panel C, a 3-D reconstruction from this patient is presented.

The study aims to advance the use of 3-D imaging in echocardiography and improve its usefulness for cardiac surgery planning. To achieve this, the present approach is to combine two project work fields:

- the improvement of actual 3-D ultrasound images, and
- the integration of these images in interactive 3-D graphics and incorporate the use of animation.

Animation is used in a software program with the acronym TiDAS[19] (Toolkit for the interactive Design of Animation and Simulation), which is being developed as part of Cardi-Assist. 'Basic building blocks' are assembled to produce the animation, with the operator specifying the abnormalities present according to the following parameters:

1. VSD/ASD
   - Position, size and shape of the defect.
   - Length and spatial orientation of the jet through the defect.
   - Temporal direction of the jet - whether left-right or right-left with respect to the ECG.
   - Volume of the jet.

2. Aneurysm
   - Location and size of the affected region.
   - Degree of abnormal aneurysmatic motion.

3. Hypertrophy (Figure 6)
   - Degree of hypertrophy.
   - Global or local occurrence.

4. LV dynamics
   - Location of affected area of the myocardium.
   - Degree of wall motion abnormality.

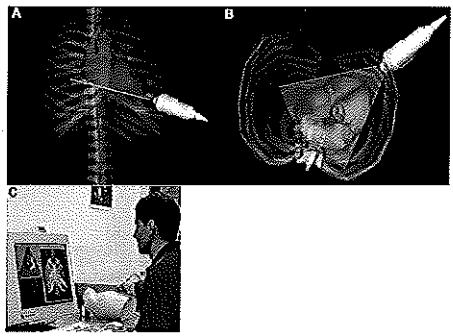

Figure 7. In panel A, the VR model is placed into a VR thorax. A VR echocardiogram probe is modeled with representation of an ultrasound field. The operator holds a dummy echo probe on a dummy thorax. A magnetic field and a sensor attached to the dummy probe, register motion of the transducer. The operator can now perform a virtual echocardiographic examination on the dummy patient, rotating the model probe to view how the ultrasound field is cross-sectioning the heart. The model can be linked to 'real' echocardiographic image data, making the examinations even more realistic.

Ultrasound training and teaching

Parts of the Cardi-Assist project will be used to develop a teaching station for sonographers and cardiologists (Figure 7). Experts have mental models of the heart structure and function that guide their interpretation of ultrasound images, while novices are completely lacking these mental models. A 3-D presentation of the heart supports in the learning process of these models. Experts employ standard procedures to verify a diagnosis. These procedures can be included into an interactive scenario as multimedia tutorials and can be made available during the examination. Based on a partial diagnosis for a patient, a diagnostic guidance system could preselect the most probable paths to follow and could advise on missing verification steps. Databases of cardiac diseases, which are documented in the form of 3-D ultrasound images and illustrated by interactive 3-D graphics and animation furthermore, provide a most valuable form of medical training.

Future training systems will include the facility known as 'force-feedback'[32]. Tactile information can interact with a 3-D model animation. The physical interface device can be anything from a joystick to a transthoracic or transesophageal echocardiogram probe. The physical interface and the force-feedback properties of the different human tissues provide the most challenging part to the development of interactive training and teaching systems.

Conclusion

Cardiac ultrasound imaging is continuously improving as a clinical investigation tool. 3-D imaging has now been available for several years but has still limitations; not in the least difficulties in interpretation. Virtual Reality is entering into the clinical theatre and this development could herald a revolution for medical training, examinations, diagnosis and treatment of disease states.

References

1. Mahoney DP. The art and science of medical visualization. Computer Graphics World, 1996;25-32.
2. Wells PN. Milestones in cardiac ultrasound: echoes from the past. History of cardiac ultrasound. Int J Card Imaging 1993;9:3-9.
3. Salustri A, Becker AE, van Herwerden L, Vletter WB, Ten Cate FJ, Roelandt JR. Three-dimensional echocardiography of normal and pathologic mitral valve: a comparison with two-dimensional transesophageal echocardiography. J Am Coll Cardiol 1996;27:1502-10.
4. Henry WL, Griffith JM, Michaelis LL, McIntosh CL, Morrow AG, Epstein SE. Measurement of mitral orifice area in patients with mitral valve disease by real-time, two-dimensional echocardiography. Circulation 1975;51:827-31.
5. Johnston KW, deMorais D, Kassam M, Brown PM. Cerebrovascular assessment using a Doppler carotid scanner and real-time frequency analysis. J Clin Ultrasound 1981;9:443-9.
6. Miyatake K, Yamagishi M, Tanaka N, Uematsu M, Yamazaki N, Mine Y, Sano A, Hirama M. New method for evaluating left ventricular wall motion by color-coded tissue Doppler imaging: in vitro and in vivo studies. J Am Coll Cardiol 1995;25:717-24.
7. Rambaldi R, Poldermans D, Vletter WB, ten Cate FJ, Roelandt JR, Fioretti PM. Doppler tissue imaging in the new era of digital echocardiography. G Ital Cardiol 1997;27:827-39.
8. Bateman TM, Sethna DH, Whiting JS, Chaux A, Berman DS, Forrester JS. Comprehensive noninvasive evaluation of left atrial myxomas using cardiac cine-computed tomography. J Am Coll Cardiol 1987;9:1150-3.
9. Goldman MR, Pohost GM, Ingwall JS, Fossel ET. Nuclear magnetic resonance imaging: potential cardiac applications. Am J Cardiol 1980;46:1278-83.
10. Roelandt JR, ten Cate FJ, Vletter WB, Taams MA. Ultrasonic dynamic three-dimensional visualization of the heart with a multiplane transesophageal imaging transducer. J Am Soc Echocardiogr 1994;7:217-29.
11. Salustri A, Roelandt JR. Ultrasonic three-dimensional reconstruction of the heart. Ultrasound Med Biol 1995;21:281-93.
12. Salustri A, Spitaels S, McGhie J, Vletter W, Roelandt JR. Transthoracic three-dimensional echocardiography in adult patients with congenital heart disease. J Am Coll Cardiol 1995;26:759-67.
13. Salustri A, Roelandt J. Three dimensional reconstruction of the heart with rotational acquisition: methods and clinical applications. Br Heart J 1995;73:10-5.
14. Salustri A, Roelandt J. Images in cardiovascular medicine. Left atrial myxoma visualized by transesophageal retoplane echocardiographic computed tomography. Circulation 1995;91:2290.
15. Salustri A, Kofflard MJ, Roelandt JR, Nosir Y, Trocino G, Keane D, Vletter WB, Cate FJ. Assessment of left ventricular outflow in hypertrophic cardiomyopathy using anyplane and paraplane analysis of three-dimensional echocardiography. Am J Cardiol 1996;78:462-8.
16. Roelandt J, Ten Cate FJ, Bruining N, Salustri A, Vletter WB, Mumm B, van der Putten N. Transesophageal retoplane echo-CT. A novel approach to dynamic three-dimensional echocardiography. The Thoraxcentre J 1994;6:4-8.
17. Roelandt J, Salustri A, Vletter W, Nosir Y, Bruining N. Precordial multiplane echocardiography for dynamic anyplane, paraplane and three-dimensional imaging of the heart. The Thoraxcentre J 1994;6:4-13.
18. Mahoney DP. Visualizing volumes. Computer Graphics World, 1997;42-48.
19. Berlage T, Grunst G, Akhar HJ, Mumm B, Angelsen B, Komorowski J, Redel DA, Pinto F, Bruining N, Roelandt JRTC. CardiAssist: Developing a Support Platform for 3D Ultrasound. The Thoraxcentre J 1996;8:5-8.
20. Fröhlich B, Grunst G, Krüger W, Wesche G. The responsive workbench: a virtual working environment for physicians. Comput Biol Med 1995;25:301-8.
21. Mahoney DP. Simulating medical emergencies. Computer Graphics World, 1997;95-96.
22. Takeuchi A, Nara Y, Ikeda N, Mijahara H, Mitobe H. Computer-assisted instruction of arrhythmia for MS-windows. Medinfo 1995;8:1230.
23. Wood AK, Dadd MJ, Lublin JR. Students' learning of clinical sonography: use of computer-assisted instruction and practical class. Acad Radiol 1996;3:683-7.
24. Thomfart WF, Freysinger W, Gunkel AR, Truppe MJ. 3D image-guided surgery on the example of the 5,300-year-old Innsbruck Iceman. Acta Otolaryngol (Stockh) 1997;117:131-4.
25. Vince J. 3-D Computer Animation. Suffolk: Addison-Wesley, 1992;1-5.
26. Ackerman MJ, Spitzer VM, Scherzinger AL, Whitlock DG. The Visible Human data set: an image resource for anatomical visualization. Medinfo 1995;8:1195-8.
27. Spitzer V, Ackerman MJ, Scherzinger AL, Whitlock D. The visible human male: a technical report. J Am Med Inform Assoc 1996;3:118-30.
28. Toh MY, Falk RB, Main JS. Interactive brain atlas with the Visible Human Project data: development methods and techniques. Radiographics 1996;16:1201-6.
29. Cooley DM. Computer-Generated Three-Dimensional reconstruction of the mediastinum correlated with sectional and radiological anatomy. Clin Anatomy 1992;5:185-202.
30. Lo LJ, Marsh JL, Vannier MW, Patel VV. Craniofacial computer-assisted surgical planning and simulation. Clin Plast Surg 1994;21:501-16.
31. Pandian NG, Roelandt JRTC, Nanda NC, Sugeng L, Cao QL, Azevedo J, Schwartz SL, Vannan MA, Ludomirski A., Marx G, Vogel M. Dynamic three-dimensional echocardiography: methods and clinical potential. Echocardiography 1994;237-259.
32. Mahoney DP. The power on touch. Computer Graphics World, 1997;4148.

CHAPTER 7

ECG-Gated ICUS Image Acquisition Combined with a Semi-Automated Contour Detection Provides Accurate Analysis of Vessel Dimensions

N. Bruining, C. von Birgelen, M.T. Mallus, P.J. de Feyter, E. de Vrey, W. Li, F. Prati, P.W. Serruys and J.R.T.C. Roelandt

Computers In Cardiology, IEEE Computer Society Press, Los Alamitos, 1996; 53-6

As part presented at the AHA, November 19, 1996, New Orleans, USA

ECG-Gated ICUS Image Acquisition Combined with a Semi-Automated Contour Detection Provides Accurate Analysis of Vessel Dimensions.

N. Bruining, C. von Birgelen, M.T. Mallus, P.J. de Feyter, E. de Vrey,
W. Li, F. Prati, P.W. Serruys, J.R.T.C. Roelandt

Erasmus University/University Hospital Rotterdam Dijkzigt, Thoraxcenter,
Rotterdam, The Netherlands

Abstract

At present most systems used for three-dimensional (3-D) reconstruction's of two-dimensional Intracoronary ultrasound (ICUS) images are based on an image acquisition with a pullback device which withdraws the catheter with a constant speed, not taking account of cardiac motion and coronary dynamics/pulsation. Cyclic changes of the vessel dimensions and the movement of the catheter inside the vessel result in artifacts and inaccuracies of quantitative analysis. Furthermore, most systems in use for this kind of analysis applications store the ICUS image data on videotape for off-line analysis, which results in quality loss.

To overcome these limitations and to achieve a rapid on-line analysis without quality loss resulting from unnecessary A/D-conversions, ECG-gated acquisition and direct digitisation of ICUS images was performed on-line.

1. Introduction

Intracoronary ultrasound (ICUS) provides high-resolution cross-sectional imaging of the vessel wall which is increasingly used during diagnostic cardiac catheterization and as a guiding tool during interventional procedures. However, it is hard to mentally conceptualise a tomographic data set of 2-D parallel sliced ICUS images into a 3-D structure. Furthermore single measurements often performed manually, by example proximal, within and distal of the stenoses provides limited accurate analysis results. At present most 3-D and analysis systems commercially available are based on an image acquisition with a pullback device which withdraws the ICUS catheter at an uniform speed, not taking account of the cardiac motion and coronary dynamics/pulsation. Artifacts and inaccurate measurements of the tomographic data set may result from the systolic-diastolic changes of the vascular dimensions and the cyclic movement of the catheter [1]. A secondary problem is that most systems store the ICUS image data on videotape for off-line analysis, which results in severe quality loss [2].

Automated ECG-gated ICUS image acquisition combined with 3-D rendering and Semi-automated contour detection software allows overcoming these limitations.

1.1. Background

In recent years several methods have been developed to acquire tomographic ICUS image data sets and to perform 3-D reconstruction's and 3-D vessel analysis:

- Manual pullback.
- Manual pullback with the ICUS catheter shaft placed in a displacement-sensing device.
- Motorised pullback by a uniform velocity motor, applying a speed of 1 - 0.2 mm/sec [3].
- Motorised pullback by an uniform velocity motor and use of an ECG-labelling device so that only one phase during the R-R interval is acquired at a continuous speed of 0.2 mm/sec ("Pseudo-Gating") [4].
- Motorised ECG-gated pullback using a stepping motor.

The technique described in this paper is based on analysis on ICUS image data sets, which are acquired with a motorised ECG-gated pullback device.

2. ICUS Acquisition Set-up

A scheme of the set-up of the 3-D reconstruction system in the catheterization laboratory is shown in figure 1. The ultrasound examinations have been performed using a 2.9F MicroView 30 MHz mechanical rotating element catheter (CVIS, Sunnyvale, CA, USA) and the echo units Insight III and HP Sonos (Hewllet-Packard, Andover, MA, USA).

The catheter configuration (external echo-transparent sheath with an independent imaging cable inside)

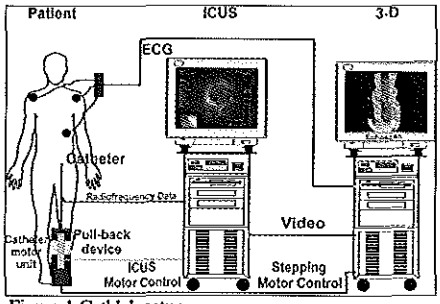

Figure 1 Cathlab setup

guarantees that pulling a defined distance at the proximal end of the catheter results in an equivalent movement of the tip of the catheter.

The image acquisition and reconstruction station (EchoScan, TomTec, Munich, Germany) receives a video signal input from the ICUS machine and is connected to the patient to monitor the ECG and respiration (impedance method). The acquisition station is also connected to a custom-designed pullback device (Thoraxcenter, Rotterdam, The Netherlands) to be controlled by the steering logic of the acquisition station, considering heart rate variability and (optionally) the respiration [5].

2.1. Image Acquisition

The acquisition station digitises the ICUS images (frames) with 40 ms intervals to a maximum of 25 images for one heart cycle. It starts with the digitisation after detecting the peak of the R-wave and it acquires the first new available ICUS image on the echo unit (see figure 2).

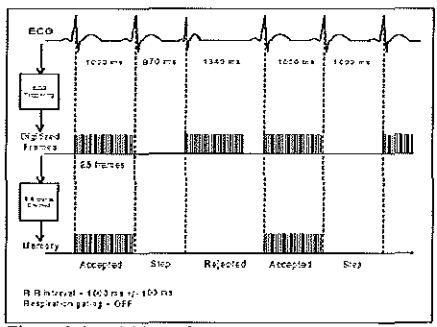

Figure 2 Acquisition scheme

At first the station monitors the ECG and respiration for two minutes and produces two scatter diagrams of the measurements. The software determines the upper and lower limits of the duration of the cardiac cycle and the depth of inspiration/expiration, after which the operator can fine-tune these intervals.

After the ICUS images of one heart cycle are acquired the software retrospectively checks if the R-R interval and respiration depth meet the predetermined ranges (see figure 2), before the digitised images are stored. Otherwise, the cycle is rejected, removed from the computer memory, and a new sequence at the same transducer position is acquired. After a valid acquisition of one heart cycle the stepping motor receives pulses until the next position on the longitudinal axis is reached. The process is repeated until the end of the longitudinal scan distance is detected. Now the operator must calibrate the echo images for on- and off-line quantitative measurements, and the acquired images can be stored on hard- and/or M.O.-disk.

The mean acquisition time to obtain one data set was 3 ± 2 minutes, applying longitudinal intervals of 0.1 to 0.25 mm, an image resolution of 256*256 pixels using 8 bits per pixel, 6 images per R-R cycle, and an average scan length of 4 cm.

3. Image Processing

To save time and to speed up the acquisition process the images are stored consecutively in one single data structure. The analysis software used is able to access the images needed for analysis directly from this stack of unprocessed images with respect to their place in the R-R interval.

The same data sets are also being used for three-dimensional reconstruction's. However, it is necessary to separate the images and to position them to their correct place in the R-R interval for this purpose. During this post-processing phase the images are formatted in volumetric data sets (256*256*256 pixels/each 8 bits), as can been seen in figure 3. During this process the images are being filtered and the vessel contours are smoothened.

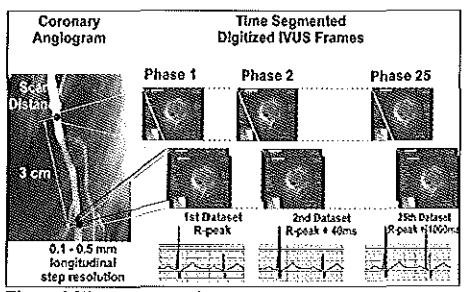

Figure 3 Time segmentation

3.1. On- and Off-line Analysis

At the Thoraxcenter an in-house produced Semi-automated contour detection program for cross-sectional and volumetric quantification of 3-D ICUS data sets is used [6,7]. This program will be integrated into the software of the 3-D image acquisition system. Due to the fact that the 3-D image acquisition software runs under DOS and the analysis software under windows, rebooting of the machine is momentarily necessary. After the initiating sequence to start the analysis software the raw ICUS images can be loaded into the computer memory with a maximum limitation of 200 images. It took 9 $\pm$ 3 minutes for an experienced operator to perform an on-line ICUS analysis of a coronary segment with typical acquisition parameters as mentioned in paragraph 2.1.

3.2. Clinical Results

Two comparison studies have been carried out to see if the described approach results in more accurate vessel dimension analysis. Coronary vessel analysis of ICUS image data sets acquired ECG-triggered vs. Non-triggered were compared and dynamic vessel dimension changes over the R-R interval within the same coronary segment were investigated. In figure 4 longitudinal cross-sections of a Non-triggered acquisition of a coronary segment can be seen.

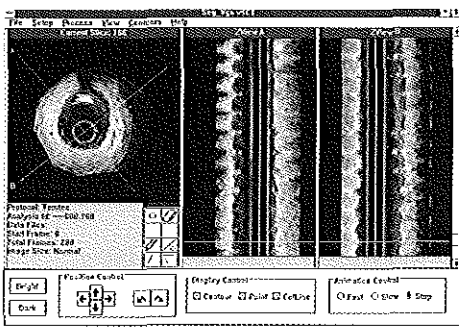

Figure 4 Non-gated pullback

It is clear in this figure that in some parts of this coronary segment it is difficult to point out where exactly the luminal border is. However for a true perception the images should be viewed on a high-resolution monitor instead of the limited space and quality of printed images.

Figure 5 shows a coronary segment from the same patient but now ECG-Triggered.

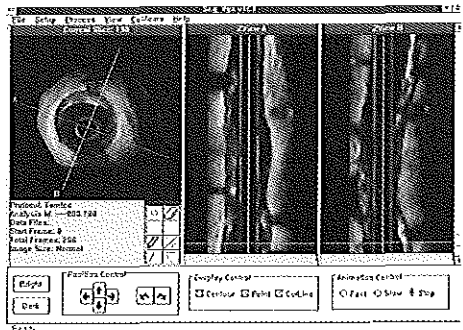

Figure 5 ECG-gated pullback

In this image it is better visible where the luminal border is. The sharper defined edges and the lack of motion from left to right of the vessel wall helps to decrease the analysis time into half the time needed for non-triggered data sets. This is mainly due to the fact that less manual interactions to correct the automated found contours are necessary.

For the volumetric quantification study 28 angiographally straight atherosclerotic segments during 19 diagnostic and 7 procedures after coronary intervention (26 patients; 21 male; 54.9 $\pm$ 9.1 years) were examined. Segments were located in the left anterior descending (15), right (11) and circumflex (2) arteries. At a maximum rate of 5 images per mm a total of 110 $\pm$ 39 images per segment were sampled (40 ms after the R-top) and digitised (48-194 images/segment; corresponding length: 9.6-38.8 mm). The results showed a high intraobserver (IAO) and interobserver (IRO) reproducibility : the mean values (delta) ranged from 0.14% to 1.51%. Earlier studies using non-triggered data sets digitised off-line from videotape showed variation coefficients for lumen volume of 3 % and for plaque volume of 1.8% [7].

The study for dynamic changes in vessel dimensions was performed in 13 patients after catheter-based coronary intervention. Longitudinal step resolution varied from 0.1 to 0.25 mm (ca. From 10 down to 4 images/mm), the scan length varied from 2 to 5 cm. The comparison of the end-diastole (ED) and the end-systole (ES) volumetric analysis showed no significant difference in the mean values of vessel dimensions, but showed a large standard deviation of the difference (delta) : Luminal volume : 160 $\pm$ 151 mm^3 (ED) vs. 162 $\pm$ 159 mm^3 (ES), -2 $\pm$ 8 mm^3 (Δ); Plaque volume : 117 $\pm$ 101 mm^3 (ED) vs. 118 $\pm$ 96 mm^3 (ES), -0.8 $\pm$ 5 mm^3 (Δ); Luminal area : 6.5 $\pm$ 3.9 mm^2 (ED) vs. 6.6 $\pm$ 4 mm^2 (ES), -0.06 $\pm$ 0.38 mm^2 (Δ). So on average it seems that systolic-diastolic changes of vessel dimensions are smoothened out, but in individual cases a large difference in vessel dimensions can be found. This indicates that for

research purposes in which high accurate vessel analysis is necessary, such as pro/regression studies, the described method could maybe provide higher accuracy than the current widespread used techniques.

4. Limitations

The proposed technique suffers from the following limitations :

- No spatial movement information of the echotransducer is currently registered (ea. straight pipe representation).
- The resolution of the ICUS transducers determines the upper resolution limit of 3-D reconstruction's and analysis.
- The acquisition time is longer compared with uniform velocity pullbacks.
- The technique is more costly than the currently widespread used techniques.

5. Future Developments

The most important improvement could be found in registering the spatial movement of the echotransducer during a pullback sequence, ea. tracking the tip of the catheter. This could provide also true length measurements. Work on this subject has been carried out at the Thoraxcenter [8]. This method works momentarily with a very time consuming technique of off-line digitisation of the spatial movement of the cathetertip from BI-plane angiographic films. Currently work is under construction to produce an image acquisition station, which can acquire BI-plane angiographic images simultaneously with ICUS images. This could be a major improvement of speeding up the process to reconstruct a coronary segment with his true curvature.

6. Conclusion

The feasibility of ECG-gated pullbacks for producing accurate analysis of vessel dimensions could be demonstrated. High-quality ICUS data sets were obtained, not showing cyclic saw-shaped artifacts as seen by non-gated approaches. Therefore this method is warranted in progression/regression of atherosclerosis studies.

References

[1] Roelandt JRTC, Di Mario C, Pandian NG, Li W, Keane D, Slager CJ, de Feyter PJ, Serruys PW. Three-dimensional reconstruction of intracoronary ultrasound images: rationale, approaches, problems, and directions. Circulation 1994; 90:1044-1055.

[2] Karson TH, Zepp RC, Chandra S, Hill RM, Waitz AS, Patten JP, Obuchowski NA. European Heart Journal 1996; volume 16 (abstract supplement): 270.

[3] Di Mario C, von Birgelen C, Prati F, Soni B, Li W, Bruining N, de Jaegere PJ, de Feyter PJ, Serruys PW. Three-dimensional reconstruction of intracoronary ultrasound: clinical of research tool? Br Heart J 1995; 73 (suppl. 2):26-32

[4] von Birgelen C, Di Mario C, Prati F, Bruining N, Li W, de Feyter PJ, Roelandt JRTC. Intracoronary ultrasound: Three-dimensional reconstruction techniques. In: de Feyter PJ, Di Mario C, Serruys PW, eds. Quantitative coronary imaging. Rotterdam: Barjesteh, Meeuwse & Co. 1995: 181-197.

[5] Bruining N, von Birgelen C, Di Mario C, Prati F, Li W, Den Hoed W, Patijn M, de Feyter PJ, Serruys PW, Roelandt JRTC. Dynamic Three-dimensional Reconstruction of ICUS Images[4]Based on an ECG-Gated Pullback Device. In: Computers In Cardiology 1995. Los Alamitos : IEEE Computer Society Press, 1995:633-636.

[6] Li W, von Birgelen C, Di Mario C, Boersma E, Gussenhoven EJ, van der Putten N, Bom N. Semi-Automatic Contour Detection for Volumetric Quantification of Intracoronary Ultrasound. In: Computers In Cardiology 1994. Los Alamitos : IEEE Computer Society Press, 1994:277-280.

[7] von Birgelen C, Di Mario C, Li W, Camenzind E, Ozaki Y, de Feyter PJ, Bom N, Roelandt JRTC. Volumetric quantification in intracoronary ultrasound: validation of a new automatic contour detection method with integrated user interaction. Circulation 1994; 90: I-550.

[8] Laban M, Oomen JA, Slager CJ, Wentzel JJ, Krams R, Schuurbiers JHC, den Boer A, von Birgelen C, Serruys PW, de Feijter PJ. ANGUS: A New Approach to Three-Dimensional Reconstruction of Coronary Vessels by Combined Use of Angiography and Intravascular Ultrasound. In : Computers in Cardiology 1996. Los Alamitos : IEEE Computer Society Press, 1995:325-328.

Address for correspondence.

Bruining N.
Thoraxcenter, University Hospital Rotterdam Dijkzigt
Room BD308b
Dr. Molewaterplein 40
3015 GD Rotterdam
The Netherlands
Tel.:(31)104635334
Fax.:(31)104634444
E-mail: bruining@thch.azr.nl

CHAPTER 8

ECG-Gated versus Nongated Three-Dimensional Intracoronary Ultrasound Analysis: Implications for Volumetric Measurements

N. Bruining, C. von Birgelen, P.J. de Feyter, J. Ligthart, W. Li, P.W. Serruys and J.R.T.C. Roelandt

Catheterization and Cardiovascular Diagnosis, 1998; 43: 254-59
As part presented at the AHA, November 11, 1997, Orlando, USA
As part presented at the ESC, August 28, 1997, Stockholm, Sweden

ECG-Gated Versus Nongated Three-Dimensional Intracoronary Ultrasound Analysis: Implications for Volumetric Measurements

Nico Bruining, BSc, Clemens von Birgelen, MD, Pim J. de Feyter, MD, PhD, Jurgen Ligthart, Wenguang Li, MSc PhD, Patrick W. Serruys, MD, PhD, and Jos R.T.C. Roelandt,* MD, PhD

The quantitative analysis of a three-dimensional (3-D) intracoronary ultrasound (ICUS) image data set permits a more comprehensive assessment of coronary arterial segments. The 3-D image sets are generally acquired during continuous motorized pullbacks. However, the cyclic changes of vascular dimensions and the cyclic spatial displacement of the ICUS transducer relative to the vessel wall can result in characteristic image artifacts, which may limit the applicability of quantitative automated analysis systems. This limitation may be overcome by an ECG-gated image acquisition. In the present study we acquired in vivo (1) nongated and (2) ECG-gated 3-D ICUS image sets of 15 human atherosclerotic coronary arteries and performed a computer-assisted contour detection of the lumen and total vessel boundaries. Total vessel and lumen volumes measured significantly larger in the nongated versus ECG-gated end-diastolic image sets (753 ± 307 mm^3 vs. 705 ± 305 mm^3; 411 ± 154 mm^3 vs. 388 ± 165 mm^3, both: $P < 0.05$). Both end-diastolic and systolic measurements were available in nine arteries, showing a larger total vessel and lumen volume at systole (664 ± 221 mm^3 vs. 686 ± 227 mm^3, $P = 0.03$; 384 ± 164 mm^3 vs. 393 ± 170 mm^3, $P = 0.08$). The differences observed may be of particular interest for volumetric ICUS studies, addressing presumably small differences in vessel or lumen dimensions. *Cathet. Cardiovasc. Diagn. 43:254–260, 1998.*
© 1998 Wiley-Liss, Inc.

Key words: intravascular ultrasound; image processing; three-dimensional reconstruction; coronary artery disease

INTRODUCTION

The assessment of coronary arteries by intracoronary ultrasound (ICUS) imaging [1,2], allows the evaluation of the geometry of both lumen and vessel wall, as well as careful assessment of the results of catheter-based interventions [3–5]. Recently, three-dimensional (3-D) image reconstruction and analysis systems have been introduced [3,4,6–14], which can be used for quantitative analyses of ICUS image data. Such 3-D systems generally acquire sequences of ICUS images during uniform-speed motorized pullbacks. Image artifacts that result from cyclic changes in coronary dimensions and the movement of the ICUS catheter relative to the vessel wall represent potential limitations for the feasibility of 3-D boundary-detection systems [11]. A novel approach limits cyclic movement artifacts by use of an ECG-gated image acquisition workstation that controls a dedicated pullback device [13,15] and permits the application of an analysis program for automated boundary detection in the 3-D ICUS image sets [12,14]. In this study, we acquired (1) nongated and (2) ECG-gated 3-D image sets of 15 atherosclerotic coronary segments of patients undergoing catheter-based coronary interventions and performed computer-assisted measurements of the lumen and total vessel volumes to evaluate potential differences between the nongated and ECG-gated approach.

METHODS

Study Population

We studied 15 patients (11 male, mean age: 57 ± 11.4 yr) in sinus rhythm. The Medical Ethical Committee of the EMCR approved the study and all patients signed a written informed consent form. The patients received aspirin (250 mg) and heparin (10,000 U) intravenously. If the duration of the entire interventional procedure ex-

Thoraxcenter, Department of Cardiology, Erasmus Medical Center and Erasmus University, Rotterdam, The Netherlands

*Correspondence to: Jos R.T.C. Roelandt, M.D., Thoraxcentre, Erasmus University, P.O. Box 1738, 3000 DR Rotterdam, The Netherlands. E-mail: Roelandt@card.azr.nl

Received 23 July 1997; Revision accepted 7 October 1997

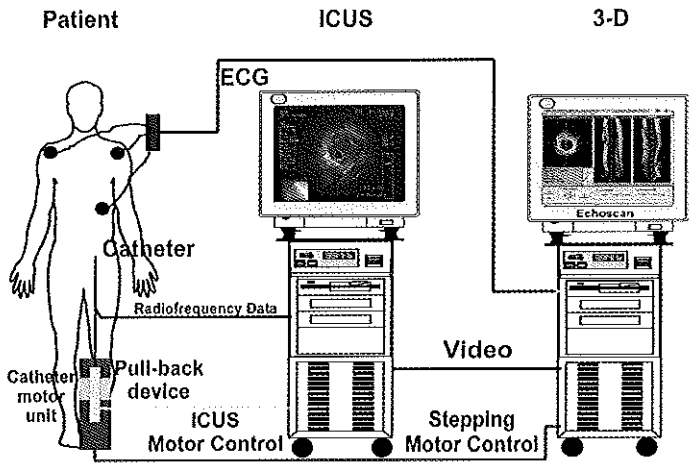

Fig. 1. Equipment setup in the catheterization laboratory. Besides the basic ICUS system, a 3-D image acquisition workstation (EchoScan, TomTec) was used (right). The 3-D reconstruction system receives the video output of the ICUS system and the patient's ECG signal.

ceeded 1 hr, the activated clotting time was measured and intravenous heparin was used to maintain an activated clotting time >300 sec. The coronary segments examined were in the right (n = 3), left anterior descending (n = 7), and left circumflex coronary arteries (n = 5).

ICUS Image Acquisition

Intracoronary nitrates were administered before the segments were examined with ICUS. Two mechanical ICUS systems, ClearView (CardioVascular Imaging Systems, Sunnyvale, CA) and Sonos (Hewlett-Packard, Andover, MA) were used with sheath-based ICUS catheters (MicroView, CVIS). The 30 MHz single-element transducer was withdrawn inside the 2.9F 15-cm-long sonolucent distal sheath, which alternatively housed the guidewire (during catheter introduction), or the transducer (during imaging, after the guidewire had been pulled back). A diagram of the setup of the ICUS system and the 3-D acquisition and analysis system in the catheterization laboratory is shown in Figure 1.

The ECG-gated image acquisition and digitization were performed by a 3-D image acquisition workstation [14,15] (EchoScan, TomTec, Munich, Germany), which received the video signal input from the ICUS machine and the ECG signal from the patient. This system steered the ECG-gated stepping pullback device to withdraw the imaging transducer through the stationary-imaging sheath. The workstation considered the heart rate variability and only acquired images from cycles meeting a predetermined range; premature beats were rejected.

In brief, before image acquisition, the R-R intervals were measured over a period of 2 min to define the range of the R-R intervals of cardiac cycles to be sampled (mean value ± 100 ms). The 3-D acquisition station was capable of acquiring a maximum of 25 frames per cardiac cycle at a given site. Images coinciding with the peak of the R-wave were used for quantitative analysis (end-diastolic phase). If an R-R interval failed to meet the preset range, the ICUS catheter remained at the same site until a cardiac cycle met the predetermined R-R range. Then, the ICUS transducer was withdrawn 0.2 mm and images were recorded at the next site in the same way. In this study, an average of six frames per cardiac cycle at one site were recorded; image acquisition required on average 1 min per centimeter axial length. Nongated image acquisition was performed with the same technical equipment at a speed of 0.5 mm/sec ("conventional approach").

Image Analysis System

A Microsoft Windows®-based contour detection program, developed at the Thoraxcenter Rotterdam, was used for the automated 3-D analysis of up to 200 ICUS images. Two longitudinal sections were constructed from the data set and the contours corresponding to the lumen-intima and the media-adventitia boundaries were

identified using a minimum-cost based analysis system [12,13]. These longitudinal contours were used to define regions-of-interest in the individual cross-sectional ICUS images. These regions-of-interest guided the automated contour detection in the planar ICUS images. The location of an individual cross-sectional image was indicated by a cursor on the longitudinal sections, which allowed scrolling through the entire set of planar ICUS images to check the contours. Corrections could be performed interactively by "forcing" the contour through visually identified points, and then the entire data set was updated (dynamic programming). The performance of this analysis system has been validated in a tubular phantom [12], and a comprehensive histologic validation has been performed [16]. The intraobserver and interobserver variability in nongated (<0.8%, SD < 2.06%) [12] and gated (<0.4%, SD < 3.2%) [14] 3-D ICUS image sets of atherosclerotic coronary arteries in vivo have been reported previously.

ICUS Image Analysis

The analyst traced the lumen-intima and the media-adventitia boundaries. In the presence of calcium deposits, the obscured media-adventitia border was extrapolated using the information of adjacent ICUS cross-sections [14]. By these tracings, the total vessel area (encompassing the media-adventitia border) and the lumen area were determined. The plaque burden (%) was calculated as total vessel area minus lumen area divided by the total vessel area. *Volumes* of total vessel and lumen were calculated as: $V = \Sigma_{i=1}^{n} Ai \cdot H$, where V = volume, A = area of total vessel or lumen in a given cross-sectional ultrasound image, H = the thickness of the coronary artery slice, that is represented by this digitized cross-sectional ICUS image; and n = the number of digitized cross-sectional images encompassing the volume to be measured. *Segment length* was calculated as the number of images analyzed, multiplied by the distance between two adjacent images. *Longitudinal catheter displacement* during the cardiac cycle was measured as the maximal systolic-diastolic movement of the ICUS transducer relative to a landmark (side branch or characteristic calcium deposit) in computed longitudinal sections.

Statistical Analysis

Quantitative data are presented as mean ± standard deviation (SD). ECG-gated 3-D image sets, acquired at the peak of the R-wave (end-diastole), were compared with both conventional nongated 3-D image sets and systolic 3-D image sets (provided by the ECG-gated approach), using the two-tailed paired Student's t-test. A P value <0.05 was considered statistically significant.

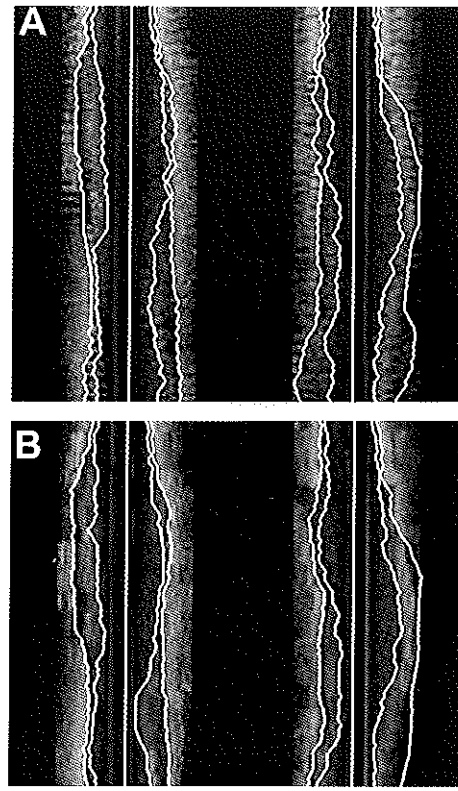

Fig. 2. Longitudinal views reconstructed from nongated (A) and ECG-gated (B) ICUS image sets. In the nongated example, a saw-blade shape appearance of the vascular structures can be appreciated. The ECG-gated approach provided smooth longitudinal vessel contours. Inner and outer contours represent the luminal and external vascular boundaries.

RESULTS

Nongated Versus ECG-Gated (end-diastolic) Measurements

Lumen and vessel contours in ECG-gated image sets were much smoother than those in nongated image sets. Figure 2 shows an example of longitudinal sections from the nongated and the ECG-gated 3-D ICUS image sets (corresponding area measurements are given in Fig. 3). The movement of the catheter and systolic-diastolic changes of vessel dimensions during the cardiac cycle

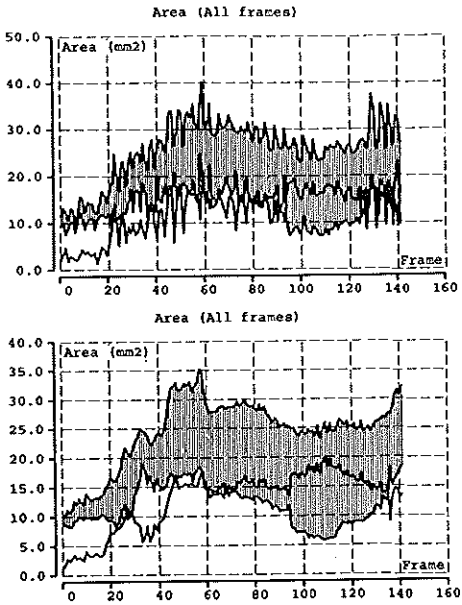

Fig. 3. Cross-sectional area measurements along a coronary segment (displayed in Fig. 2). Measurements were obtained from nongated (top) and ECG-gated (bottom) image sets. The upper and lower boundaries of the gray zone represent the total vessel and lumen cross-sectional area measurements. Note the saw-blade shape appearance of the measurements in the nongated image sets (top).

TABLE I. Nongated vs. ECG-Gated (end-diastolic) Measurements (n = 15)

	Nongated	ECG-gated (end-diastolic)	*P*
Total vessel volume (mm^3)	753.0 ± 307.3	704.5 ± 304.5	*0.04*
Lumen volume (mm^3)	410.7 ± 153.8	387.8 ± 164.5	*0.02*
Images/segment	163 ± 19	154 ± 29	NS
Mean plaque burden (%)	43.0 ± 9.1	42.8 ± 9.1	NS
Segment length (mm)	48.4 ± 16.9	47.5 ± 16.3	NS
Longitudinal catheter displacement (mm)	[a]	0.8 ± 0.9	

[a]Parameter measured in ECG-gated image sets only.
NS = not significant.

caused the saw-blade shape image artifact in the nongated images. The length of the coronary segments analyzed was 48.4 ± 16.9 mm (range: 30–80 mm). Both total vessel and lumen volumes (Table I) in nongated image sets were significantly higher than those measured in the corresponding ECG-gated image sets (753 ± 307 mm^3 vs. 705 ± 305 mm^3, $P = 0.04$, and 411 ± 154 mm^3 vs. 388 ± 165 mm^3, $P = 0.02$). Figure 4 displays the absolute luminal volumetric differences between measurements in nongated and ECG-gated image sets. Results of the linear regression analyses are given in Figure 5.

End-Diastolic Versus Systolic Measurements (both ECG-gated approach)

In nine patients, image sets that were acquired in systole could be compared with those obtained at the peak of the R-wave (end-diastole). Measurements were for the total vessel volume 686 ± 227 mm^3 and 664 ± 221 mm^3 ($P = 0.03$, variation 3.4 ± 3.8%) and for the lumen volume 393 ± 170 mm^3 and 384 ± 164 mm^3 ($P = 0.08$; variation 2.7 ± 4.4%) (Table II). Results of the linear regression analyses comparing systolic and end-diastolic measurements are given in Figure 6.

DISCUSSION

Image acquisition for the purpose of 3-D reconstruction is generally performed during continuous nongated motorized pullbacks, but the cyclic changes of the vascular dimensions and the displacement of the ultrasound transducer relative to the vessel wall can result in significant saw-blade shape image artifacts in longitudinally reconstructed sections. ECG-gated image acquisition with a novel method [15] allows compilation of images of the same phase of the cardiac cycle in the 3-D image sets. This results in much smoother contours of both lumen and vascular wall in reconstructed longitudinal views and facilitates automated contour-detection with the computerized analysis system applied [14]. In addition, measurements can be performed at different phases of the cardiac cycle.

The present study was the first to evaluate the potential difference in volumetric measurements between the conventional nongated and the novel ECG-gated approach. Our data demonstrate that conventional nongated vessel and lumen volume measurements were significantly higher than the corresponding measurements in end-diastolic image sets, derived from the ECG-gated image acquisition. In addition, comparison of volumetric measurements in end-diastolic image sets (peak of the R-wave) and systolic image sets revealed higher volumes during systole, confirming previous observations with conventional planar ICUS [17]. The natural history and the progression or regression of coronary atherosclerosis most often have been assessed by quantitative coronary angiography [18,19], but the quantitative angiographic analysis is limited to the assessment of luminal silhouettes and early atherosclerosis remains undetected [2,3].

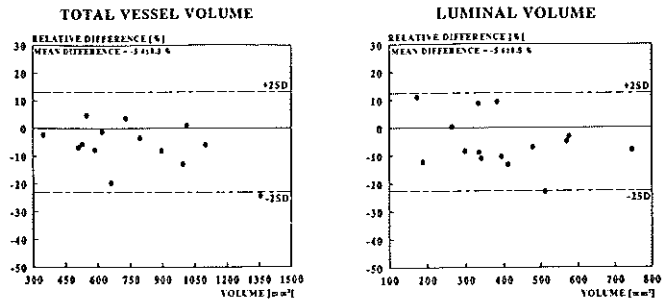

Fig. 4. Relative differences of total vessel (left) and lumen volume measurements (rights) in nongated vs. ECG-gated (end-diastolic) image sets.

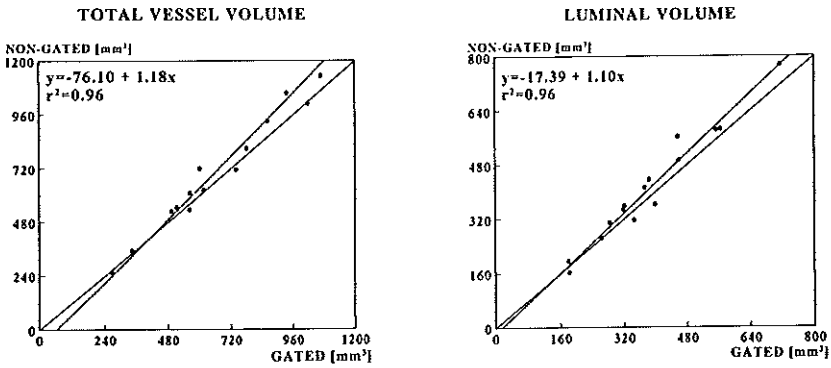

Fig. 5. Linear regression analyses comparing total vessel (left) and lumen volume measurements (right) in nongated vs. ECG-gated (end-diastolic) image sets.

TABLE II. Nongated and Both End-Diastolic and Systolic (ECG-gated) Measurements (n = 9)

	Nongated	ECG-gated End-diastolic	ECG-gated Systolic	*P*, End-diastolic vs. Systolic
Total vessel volume (mm³)	684.5 ± 239.6	663.8 ± 220.8	685.7 ± 227.4	*0.03*
Lumen volume (mm³)	396.1 ± 178.3	383.6 ± 164.2	393 ± 170.2	0.08

ICUS depicts even early atherosclerotic changes. Recently, volumetric ICUS measurements have been suggested to evaluate the progression-regression of atherosclerosis during pharmacological or nonpharmacological interventions [20]. However, the volumetric changes as observed in such studies may be small. The findings of the presented study should be considered particularly when addressing small changes, as expected in progression-regression studies of atherosclerosis.

Limitations and Potential Sources of Error

The heart rate shows physiological variability and the ECG-gated method acquired images from cardiac cycles with different R-R intervals (mean R-R interval ± 100 ms); the length of cardiac cycles in these data sets can differ by up to 200 ms. Thus systolic data sets contain images that are not always acquired with exactly identical timing, which may cause image artifacts and may affect the accuracy of systolic measurements (see Fig. 7).

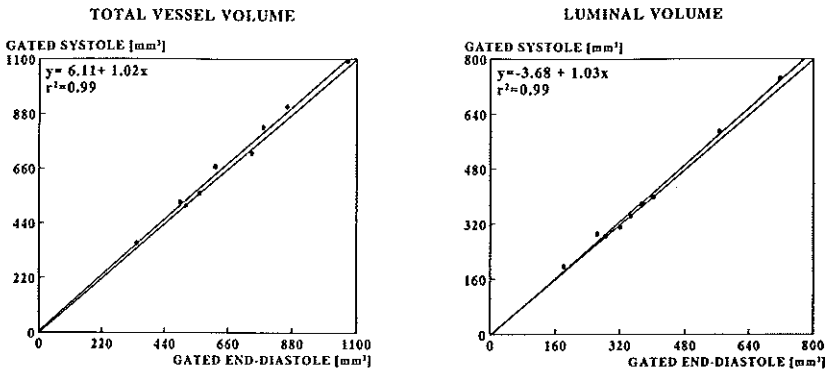

Fig. 6. Linear regression analyses, comparing total vessel (left) and lumen volume measurements (right) in end-diastolic vs. systolic image sets, both obtained from ECG-gated image acquisition.

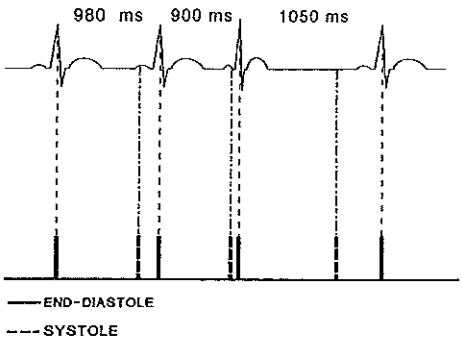

Fig. 7. ECG-gated image acquisition diagram. When applying ECG-gating for image acquisition, the first image is acquired after detecting the peak of the R-wave (solid line), corresponding to the end-diastolic phase (ED) of the cardiac cycle. The heart rate shows a physiological variability and images from cardiac cycles with different R-R intervals are acquired (range: mean R-R interval ± 100 ms); the length of cardiac cycles in these data sets can differ by up to 200 ms. Therefore, systolic data sets (thick short dotted line) contain images that are not always acquired with exactly the same timing, which can result in image artifacts and may affect the accuracy of systolic volumetric ICUS measurements.

ECG-gated image acquisition results in an extended duration of the ICUS imaging runs, which may limit its preintervention use in patients with severe luminal obstructions.

Nonuniform transducer rotation of mechanical ICUS catheters, eccentric catheter position, or vascular curvatures may affect the accuracy of 3-D reconstruction and analysis [21–23]. Approaches that combine both radiographic and ICUS data have been proposed to solve most of these problems, but these techniques are laborious and still restricted to research [21,24].

Testing in an in-vitro phantom may allow to obtain additional insights into the accuracy of nongated volumetric measurements vs. ECG-gated measurements. However, to produce a model that simulates the complex 3-D motion of the heart combined with the patients respiration and the dynamic changes of vessel dimensions is extremely difficult and even may be impossible.

Conclusion

Volumetric ICUS measurements in nongated image sets differ significantly from those in end-diastolic ECG-gated image sets. This should be considered particularly when addressing potentially small volumetric changes, such as expected in progression-regression studies of atherosclerosis.

ACKNOWLEDGMENTS

C.v.B. is the recipient of a fellowship of the German Research Society, Bonn, Germany.

REFERENCES

1. Fitzgerald PJ, St. Goar FG, Connolly AJ, Pinto FJ, Billingham ME, Popp RL, Yock PG: Intravascular ultrasound imaging of coronary arteries: Is three layers the norm? Circulation 86:154–158, 1992.

2. Mintz GS, Painter JA, Pichard AD, Kent KM, Satler LF, Popma JJ, Chuang YC, Bucher TA, Sokolowicz LE, Leon MB: Atherosclerosis in angiographically "normal" coronary artery reference segments: An intravascular ultrasound study with clinical correlations. J Am Coll Cardiol 25:1479–1485, 1995.
3. Erbel R, Ge J, Bockisch A, Kearney P, Gorge G, Haude M, Schumann D, Zamorano J, Rupprecht HJ, Meyer J: Value of intracoronary ultrasound and Doppler in the differentiation of angiographically normal coronary arteries: A prospective study in patients with angina pectoris. Eur Heart J 17:880–889, 1996.
4. von Birgelen C, Gil R, Ruygrok P, Prati F, Di Mario C, van der Giessen WJ, de Feyter PJ, Serruys PW: Optimized expansion of the Wallstent compared with the Palmaz-Schatz stent: On-line observations with two- and three-dimensional intracoronary ultrasound after angiographic guidance. Am Heart J 131:1067–1075, 1996.
5. Dussaillant GR, Mintz GS, Pichard AD, Kent KM, Satler LF, Popma JJ, Wong SC, Leon MB: Small stent size and intimal hyperplasia contribute to restenosis: A volumetric intravascular ultrasound analysis. J Am Coll Cardiol 26:720–724, 1995.
6. Rosenfield K, Losordo DW, Ramaswamy K, Pastore JO, Langevin RE, Razvi S, Kosowsky BD, Isner JM: Three-dimensional reconstruction of human coronary and peripheral arteries from images recorded during two-dimensional intravascular ultrasound examination. Circulation 84:1938–1956, 1991.
7. Coy KM, Park JC, Fishbein MC, Laas T, Diamond GA, Adler L, Maurer G, Siegel RJ: In vitro validation of three-dimensional intravascular ultrasound for the evaluation of arterial injury after balloon angioplasty. J Am Coll Cardiol 20:692–700, 1992.
8. Mintz GS, Pichard AD, Satler LF, Popma JJ, Kent KM, Leon MB: Three-dimensional intravascular ultrasonography: Reconstruction of endovascular stents in vitro and in vivo. J Clin Ultrasound 21:609–615, 1993.
9. Matar FA, Mintz GS, Douek P, Farb A, Virmani R, Javier SP, Popma JJ, Pichard AD, Kent KM, Satler LF, Leller M, Leon MB: Coronary artery lumen volume measurement using three-dimensional intravascular ultrasound: Validation of a new technique. Cathet Cardiovasc Diagn 33:214–220, 1994.
10. Sonka M, Liang W, Zhang X, De Jong S, S.M. C, McKay CR: Three-dimensional automated segmentation of coronary wall and plaque from intravascular ultrasound pullback sequences, Computers in Cardiology, Vienna. IEEE Computer Society Press, 637–640, 1995.
11. Roelandt JR, di Mario C, Pandian NG, Wenguang L, Keane D, Slager CJ, de Feyter PJ, Serruys PW: Three-dimensional reconstruction of intracoronary ultrasound images: Rationale, approaches, problems, and directions. Circulation 90:1044–1055, 1994.
12. von Birgelen C, di Mario C, Li W, Schuurbiers JC, Slager CJ, de Feyter PJ, Roelandt JR, Serruys PW: Morphometric analysis in three-dimensional intracoronary ultrasound: An in vitro and in vivo study performed with a novel system for the contour detection of lumen and plaque. Am Heart J 132:516–527, 1996.
13. von Birgelen C, Mintz GS, Nicosia A, Foley DP, van der Giessen WJ, Bruining N, Airiian SG, Roelandt JRTC, de Feyter PJ, Serruys PW: Electrocardiogram-gated intravascular ultrasound image acquisition after coronary stent deployment facilitates on-line three-dimensional reconstruction and automated lumen quantification. J Am Coll Cardiol 30:436–443, 1997.
14. von Birgelen C, de Vrey EA, Mintz GS, Nicosia A, Bruining N, Li W, Slager CJ, Roelandt JRTC, Serruys PW, de Feyter PJ: ECG-gated three-dimensional intravascular ultrasound: Feasibility and reproducibility of an automated analysis of coronary lumen and atherosclerotic plaque dimensions in humans. Circulation 1997 (in press).
15. Bruining N, von Birgelen C, Di Mario C, Prati F, Li W, den Hoed W, Patijn M, de Feyter PJ, Serruys PW, Roelandt JRTC: Dynamic three-dimensional reconstruction of ICUS images based on an ecg-gated pull-back device, Computers in Cardiology, Vienna. IEEE Computer Society Press, 633–636, 1995.
16. von Birgelen C, van der Lugt A, Nicosia A, Mintz GS, Gussenhoven EJ, de Vrey E, Mallus MT, Roelandt JRTC, Serruys PW, de Feyter PJ: Computerized assessment of coronary lumen and atherosclerotic plaque dimensions in three-dimensional intravascular ultrasound correlated with histomorphometry. Am J Cardiol 78:1202–1209, 1996.
17. Ge J, Erbel R, Gerber T, Gorge G, Koch L, Haude M, Meyer J: Intravascular ultrasound imaging of angiographically normal coronary arteries: A prospective study in vivo. Br Heart J 71:572–578, 1994.
18. de Feyter PJ, Serruys PW, Davies MJ, Richardson P, Lubsen J, Oliver MF: Quantitative coronary angiography to measure progression and regression of coronary atherosclerosis: Value, limitations, and implications for clinical trials. Circulation 84:412–423, 1991.
19. Waters D, Lesperance J, Craven TE, Hudon G, Gillam LD: Advantages and limitations of serial coronary arteriography for the assessment of progression and regression of coronary atherosclerosis. Implications for clinical trials. Circulation 87:II38–47, 1993.
20. von Birgelen C, Slager CJ, di Mario C, de Feyter PJ, Serruys PW: Volumetric intracoronary ultrasound: A new maximum confidence approach for the quantitative assessment of progression-regression of atherosclerosis? Atherosclerosis 118:S103–113, 1995.
21. von Birgelen C, Mintz GS, de Feyter PJ, Bruining N, Nicosia A, Di Mario C, Serruys PW, Roelandt JRTC: Reconstruction and quantification with three-dimensional intracoronary ultrasound: An update on techniques, challenges, and future directions. Eur Heart J 18:1056–1067, 1996.
22. Chae JS, Brisken AF, Maurer G, Siegel RJ: Geometric accuracy of intravascular ultrasound imaging. J Am Soc Echocardiogr 5:577–587, 1992.
23. Di Mario C, Madretsma S, Linker D, The SH, Bom N, Serruys PW, Gussenhoven EJ, Roelandt JR: The angle of incidence of the ultrasonic beam: A critical factor for the image quality in intravascular ultrasonography. Am Heart J 125:442–448, 1993.
24. Evans JL, Ng KH, Wiet SG, Vonesh MJ, Burns WB, Radvany MG, Kane BJ, Davidson CJ, Roth SI, Kramer BL, Meyers SN, McPherson DD: Accurate three-dimensional reconstruction of intravascular ultrasound data. Spatially correct three-dimensional reconstructions. Circulation 93:567–576, 1996.

Editorial Comment

What's New With IVUS?

Jonathan M. Tobis, MD
Division of Cardiology,
University of California Medical Center,
Irvine and Los Angeles, California

Bruining et al. should be congratulated on their informative paper demonstrating that electrocardiogram (ECG) gating improves volumetric measurements from three-dimensional intracoronary ultrasound images [1]. The ECG gating not only smooths the longitudinal image and makes it visually more pleasing, it also improves the quantitative analysis. The volumes of the artery lumen and the vessel (i.e., the area bounded by the media) were larger when measured by a nongated computer edge-detection program as compared with the ECG-gated program. The major downside to this method is that the image acquisition rate is slow at 1 min/cm of artery. This rate may be feasible for dedicated IVUS researchers, but the casual user of intravascular ultrasound may find this too laborious. However, the longitudinal images more closely approximates an angiographic view and therefore is a more familiar presentation for the interventional cardiologist. As the authors have pointed out, the ECG-gating technique may be more appropriate for serial studies that attempt to look at the volume of atherosclerotic plaque over time.

This article reminds us that, in addition to ECG gating, there are new developments in the field of intravascular ultrasound imaging. Perhaps the most significant advance is complete digital storage of all the cross-sectional ultrasound images. With this new capability, the operator will be able to scroll through the database of images to review all cross-sectional information and the long-axis reconstructed projections. The ability to recall the images from a digital format will prevent the loss in image quality that occurs from digital-to-analog conversion and playback from the videotape. Although videotape will still be used as a storage medium, there will be the capacity to download the digital images to the hard drive and then to a writable compact disk (CD) that can store up to 650 megabytes of data. Several cases can thus be stored on a single CD. The digital format will also facilitate reports by incorporating the quantitative results measured from the digital images and by providing the ability to embed the ultrasound images directly into the report printout.

The second area of significant improvement is in catheter design. Boston Scientific will be coming out with a smaller 2.6-French monorail design catheter using a 40-MHz transducer. Although the reflections from blood are slightly annoying, the lower profile of this catheter permits its entrance into smaller lesions that could not be passed with the 3.2-French catheter. Endosonics has also dramatically improved their images along with their 64-element transducer tipped catheter. Hewlett-Packard has improved the pull-back device for operators that like to acquire data in a continuous fashion. The newer pull-back devices are smaller and more user friendly. This should make the ECG-gating technique described by Bruining et al. even more feasible.

It is encouraging to see these impressive improvements in catheter design, image quality, and digital image manipulation, which demonstrate a healthy commitment by industry to the future progress of intravascular ultrasound.

REFERENCE

1. Bruining N, von Birgelen C, de Feyter P, Ligthart J, Li W, Serruys P, Roelandt J: ECG-gated versus non-gated three-dimensional intracoronary ultrasound analysis: Implications for volumetric measurements. Cathet Cardiovasc Diagn, 1997.

CHAPTER 9

ECG-Gated Three-Dimensional Intravascular Ultrasound Feasibility and Reproducibility of the Automated Analysis of Coronary Lumen and Atherosclerotic Plaque Dimensions in Humans

C. von Birgelen, E. de Vrey, G.S. Mintz, A. Nicosia, N. Bruining, W. Li, C.J. Slager, J.R.T.C. Roelandt, P.W. Serruys and P.J. de Feyter

Circulation, 1997; 96: 2944-52

—

ECG-Gated Three-dimensional Intravascular Ultrasound

Feasibility and Reproducibility of the Automated Analysis of Coronary Lumen and Atherosclerotic Plaque Dimensions in Humans

Clemens von Birgelen, MD; Evelyn A. de Vrey, MD; Gary S. Mintz, MD; Antonino Nicosia, MD; Nico Bruining, BSc; Wenguang Li, MSc; Cornelis J. Slager, MSc; Jos R.T.C. Roelandt, MD, PhD; Patrick W. Serruys, MD, PhD; Pim J. de Feyter, MD, PhD

Background Automated systems for the quantitative analysis of three-dimensional (3D) sets of intravascular ultrasound (IVUS) images have been developed to reduce the time required to perform volumetric analyses; however, 3D image reconstruction by these nongated systems is frequently hampered by cyclic artifacts.

Methods and Results We used an ECG-gated 3D IVUS image acquisition workstation and a dedicated pullback device in atherosclerotic coronary segments of 30 patients to evaluate (1) the feasibility of this approach of image acquisition, (2) the reproducibility of an automated contour detection algorithm in measuring lumen, external elastic membrane, and plaque+media cross-sectional areas (CSAs) and volumes and the cross-sectional and volumetric plaque+media burden, and (3) the agreement between the automated area measurements and the results of manual tracing. The gated image acquisition took 3.9±1.5 minutes. The length of the segments analyzed was 9.6 to 40.0 mm, with 2.3±1.5 side branches per segment. The minimum lumen CSA measured 6.4±1.7 mm^2, and the maximum and average CSA plaque+media burden measured 60.5±10.2% and 46.5±9.9%, respectively. The automated contour-detection required 34.3±7.3 minutes per segment. The differences between these measurements and manual tracing did not exceed 1.6% (SD<6.8%). Intraobserver and interobserver differences in area measurements (n=3421; r=.97 to.99) were <1.6% (SD<7.2%); intraobserver and interobserver differences in volumetric measurements (n=30; r=.99) were <0.4% (SD<3.2%).

Conclusions ECG-gated acquisition of 3D IVUS image sets is feasible and permits the application of automated contour detection to provide reproducible measurements of the lumen and atherosclerotic plaque CSA and volume in a relatively short analysis time. (*Circulation*. 1997;96:2944-2952.)

Key Words • ultrasonics • coronary disease • imaging

Intravascular ultrasound allows transmural, tomographic imaging of coronary arteries in humans in vivo and provides insights into the pathology of coronary artery disease by defining vessel wall geometry and the major components of the atherosclerotic plaque.[1-7] Although invasive, IVUS is safe[8,9] and allows a more comprehensive assessment of the atherosclerotic plaque than the "luminal silhouette" furnished by coronary angiography.[10-14] Nevertheless, conventional IVUS analysis is a planar technique. Volumetric analysis of conventionally obtained IVUS images using Simpson's rule and planar analysis of multiple image slices is possible and may yield additional information, although it is time-consuming. To reduce the time for volumetric analysis[15] of IVUS images, automated 3D image reconstruction systems have been developed.[16-27] However, these systems have limitations, including (1) an inconsistent ability to detect the external arterial boundary and (2) imaging artifacts produced by cyclic changes in vascular dimensions and by movement of the IVUS catheter relative to the vessel.[20,22,24]

As a consequence, we have developed an analysis system that (1) uses 3D IVUS image sets acquired with an ECG-gated image acquisition workstation and pullback device to limit cyclic artifacts[28] and (2) detects both the luminal and external vascular boundaries of atherosclerotic coronary arteries to permit plaque volume measurement.[10,29-31] We report the feasibility of IVUS image acquisition and the reproducibility of analysis with this methodology.

Received January 8, 1997; revision received May 8, 1997; accepted May 28, 1997.

From the Thoraxcenter, Division of Cardiology, University Hospital Rotterdam-Dijkzigt and Erasmus University, Rotterdam (C. von B., E. de V., A.N., N.B., W.L., C.J.S., J.R.T.C.R., P.W.S., P.J. de F.), and the Interuniversity Cardiology Institute (W.L., P.W.S.), Netherlands; and the Washington (DC) Hospital Center (G.S.M.). Dr von Birgelen is now at the Department of Cardiology, University Hospital Essen, Germany.

Correspondence to Pim J. de Feyter, MD, PhD, Thoraxcenter, Bd 381, PO Box 1738, 3000 DR Rotterdam, Netherlands.

© 1997 American Heart Association, Inc.

Methods

Patient Population

Between August 1, 1995, and February 29, 1996, we examined 28 patients with ECG-gated 3D IVUS, which represented a consecutive series of patients investigated with this approach. There were 23 men and 5 women who ranged in age from 38 to 72 years (mean, 55.3±8.9 years). All but 3 of them, studied at routine follow-up after previous catheter-based interventions, were symptomatic and/or had revealed signs of myocardial ischemia during noninvasive functional testing. Reasons for cardiac catheterization were either for diagnostic evaluation

Selected Abbreviations and Acronyms
CSA = CSA
3D = three-dimensional
EEM = external elastic membrane
IVUS = intravascular ultrasound

(n=20) or for follow-up study after a previous angioplasty procedure (n=8). Of the 20 patients examined during diagnostic catheterizations, 6 had one-vessel, 8 had two-vessel, and 1 had three-vessel disease. All patients with one- and two-vessel disease subsequently underwent successful catheter-based interventions (balloon angioplasty, n=3; directional atherectomy, n=2; stenting, n=9). Bypass surgery was performed in the patient with three-vessel disease. Of the 8 patients investigated at follow-up after previous interventions (after balloon angioplasty, n=5; directional atherectomy, n=3), 3 patients showed a significant restenosis and were successfully treated by repeat balloon angioplasty.

Thirty atherosclerotic coronary segments located in the left anterior descending coronary artery (n=15), right coronary artery (n=12), and left circumflex coronary artery (n=3) were analyzed; 13 segments were proximal, 15 mid, and 2 distal. As a condition for inclusion, segments had to be angiographically relatively straight (in at least two angiographic views from opposite projections). An exclusion criterion was calcification encompassing >180° of the arterial circumference over a ≥5-mm-long axial segment. This study was approved by the Local Council on Human Research. All patients signed a written informed consent form approved by the Medical Ethical Committee of the University Hospital Rotterdam-Dijkzigt.

IVUS Imaging

All patients received 250 mg aspirin and 10 000 U heparin IV. If the duration of the entire catheterization procedure exceeded 1 hour, the activated clotting time was measured, and intravenous heparin was administered to maintain an activated clotting time of >300 seconds. After intracoronary injection of 0.2 mg nitroglycerin, the atherosclerotic coronary segment to be reconstructed was examined with a mechanical IVUS system (ClearView, CardioVascular Imaging Systems Inc) and a sheath-based IVUS catheter incorporating a 30-MHz beveled, single-element transducer rotating at 1800 rpm (MicroView, CardioVascular Imaging Systems Inc). This catheter is equipped with a 2.9F 15-cm-long sonolucent distal sheath with a common lumen that alternatively houses the guidewire (during catheter introduction) or the transducer (during imaging after the guidewire has been pulled back), but not both. This design avoids direct contact of the IVUS imaging core with the vessel wall. The IVUS transducer was withdrawn through the stationary imaging sheath by an ECG-triggered pullback device with a stepping motor developed at the Thoraxcenter Rotterdam.[28]

ECG-Gated 3D IVUS Image Acquisition

The ECG-gated image acquisition and image digitization was performed by a workstation initially designed for the 3D reconstruction of echocardiographic images[28] (Echoscan, TomTec). This workstation received input from the IVUS machine (video) and the patient (ECG signal) and on the other hand, controlled the motorized transducer pullback device.

The steering logic of the workstation considered the heart rate variability and checked for the presence of extrasystoles during image acquisition and digitization (Fig 1). First, the RR intervals were measured over a 2-minute period to define the upper and lower limits of the range of acceptable RR intervals (mean value±50 ms). IVUS images were acquired 40 ms after the peak of the R wave. When the length of the RR interval met the preset range, the IVUS image was stored in the computer memory. Consecutively, the IVUS transducer was withdrawn 200 μm to acquire the next image. Although the longitudinal resolution available with this technical setup is 100 μm,[28] in the present study only one IVUS image per 200 μm axial arterial length was acquired. Thus, an average of 114 images per segment were digitized and analyzed (range, 48 to 200 images per segment; corresponding segment length, 9.6 to 40.0 mm).

IVUS Analysis Protocol

Each set of digitized IVUS images was analyzed off-line by two independent observers using an automated, computerized contour detection algorithm.[29-31] These measurements (Ia and II) were compared to study the interobserver variability. Blinded analyses were repeated by the first observer after an

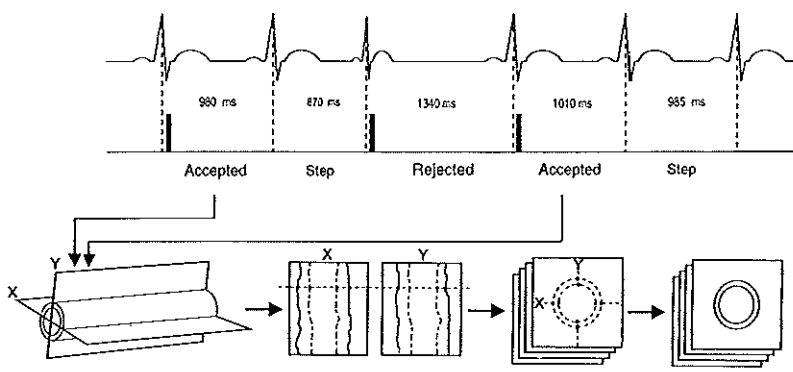

FIG 1. IVUS images were acquired 40 ms after peak of R wave and stored (accepted) in computer memory only if RR intervals met predefined range (top). Consecutively, transducer was withdrawn 200 μm to adjacent acquisition site (step) to acquire next image. If an RR interval did not meet range, image was not stored (rejected), and transducer was kept at that site until an image was acquired. Image acquisition and motorized pullback were controlled by steering logic of image acquisition workstation. Automated detection of intimal and medial boundaries was first performed on two perpendicular longitudinal sections (X, Y) reconstructed from image data of entire 3D stack of images (bottom); edge information of these longitudinal contours was represented as points on planar images, defining there the center and range of final automated contour detection process.

interval of at least 6 weeks. These measurements (Ia and Ib) were compared to study the intraobserver variability.

Two hundred planar images were randomly selected for "manual" analysis by a third investigator (MA-III) who was experienced in IVUS image analysis but blinded to the (above) automated contour detection results. This analyst could review the videotape to ensure a maximum accuracy of contour tracing, performed within an average of 4.1 minutes per image. Validation of manual CSA measurements by IVUS has been reported previously.[32-34] These measurements were compared with the automated contour detection analysis made by observer I.

Data Analysis

The CSA measurements included the lumen and EEM CSA. Plaque+media CSA was calculated as EEM minus lumen CSA, and the CSA plaque+media burden was calculated as plaque+media CSA divided by EEM CSA. The EEM CSA (which represents the area within the border between the hypoechoic media and the echoreflective adventitia) has been shown to be a reproducible measure of the total arterial CSA. As in many previous studies using IVUS, plaque+media CSA was used as a measure of atherosclerotic plaque, because ultrasound cannot measure media thickness accurately.[35] Lumen, EEM, and plaque+media volumes were calculated as

$$\text{Volume} = \sum_{i=1}^{n} \text{CSA}_i \times H$$

where H is the thickness of a coronary artery slice, represented by a single tomographic IVUS image, and n is the number of IVUS images in the 3D data set. The volumetric plaque+media burden was calculated as plaque+media volume divided by EEM volume.

Plaque composition was assessed visually to identify lesion calcium. Calcium produced bright echoes (brighter than the reference adventitia), with acoustic shadowing of deeper arterial structures. The largest arc(s) of target lesion calcium was identified and measured in degrees with a protractor centered on the lumen. The overall length (in mm) of lesion calcium was measured by use of the length measurements provided by the 3D reconstruction.

Computerized Contour Detection in ECG-Gated 3D IVUS

Steps Involved in Image Analysis

Two longitudinal sections were constructed, and contours corresponding to the lumen-tissue and media-adventitia interfaces were automatically identified (Fig 1). The necessity to manually edit these contours was significantly reduced, because cyclic "saw-shaped" image artifacts that can hamper the automated detection in nongated image sets were virtually abolished (Fig 2). The sufficiency of the contour detection was visually checked, requiring an average of 5 minutes. If necessary, these longitudinal contours were edited with computer assistance (see below) within <1 minute. The longitudinal contours were transformed to individual edge points on the planar images, defining center and range of the automated boundary search on the planar images.

Subsequently, contour detection of the planar images was performed. The axial location of an individual planar image was indicated by a cursor, which was used to scroll through the entire set of planar images while the detected contours were visually checked. Correct detection of the longitudinal contours minimized the need for computer-assisted editing of the cross-sectional contours. Careful checking and editing of the contours of the planar images was performed within an average of 25 minutes. Finally, the contour data of the planar images were used for the computation of the results.

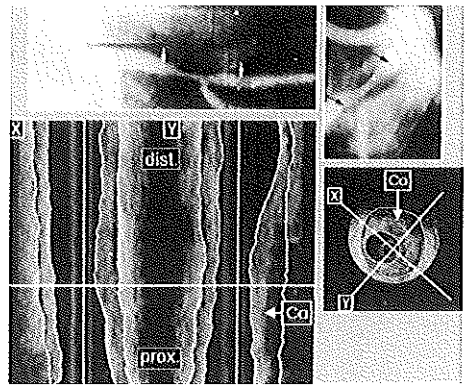

FIG 2. Example of automated 3D contour detection analysis in diseased left anterior descending coronary artery. Range of 14.6-mm-long IVUS reconstruction and analysis is indicated by arrowheads in angiograms (top) taken from opposite angiographic projections. Cut planes of two reconstructed longitudinal sections (X, Y; lower left) are indicated on planar IVUS image (lower right), depicting calcification (Ca) of atherosclerotic plaque. Horizontal cursor on longitudinal sections can be used to scroll from distal (dist.) to proximal (prox.) through planar images. Thickness of that cursor is artificially increased to improve visibility (true thickness=half a scan line). 3D approach permitted interpretation in longitudinal dimension and facilitated tracing of estimated external vascular contour in acoustic shadowing behind calcium. Angiograms (top) and radiographic image of ultrasound catheter during image acquisition (insert, top left) illustrate that analyzed arterial segment was relatively straight and showed no more than mild vessel curvatures. As linear 3D analysis systems do not account for vascular curvatures, this premise was important because it limits curve distortion–induced deviation of volumetric measurements.

Minimum-Cost Algorithm and Computer-Assisted Contour Editing

A minimum-cost algorithm was used to detect the luminal and external vessel boundaries.[29] Each digitized IVUS image was resampled in a radial format (64 radii per image); a cost matrix representing the edge strength was calculated from the image data. For the boundary between lumen and plaque, the cost value was defined by the spatial first derivative.[36] For the external vessel boundary, a cross-correlation pattern matching process was used for the cost calculations. The path with the smallest accumulated value was determined by dynamic programming techniques.[29] The computer-assisted editing differed considerably from conventional manual contour tracing. The computer mouse was pointed on the correct boundary to give that site a very low value in the cost matrix, and subsequently the automated detection of the minimum cost path was updated within <1 second. Editing the contour of a single slice caused the entire data set to be updated (dynamic programming).

Handling of Side Branches and Calcification

Side branches with a relatively small ostium were generally ignored by the algorithm as a result of its robustness, which means that the automated contour detection did not follow every abrupt change in the cost path. However, in branches with a large ostium, the contour did follow the lumen and vessel boundaries of the side branch. This was corrected by displaying the side branch in one of the longitudinal sections and interpolating the longitudinal vessel contours as straight

TABLE 1. Feasibility and Processing Time

Seg	ECG Gating	Image Quality	Images/ Seg, n	Acquisition Time/Seg, min	Acquisition Time/Image, s	Analysis Time/Seg, min	Analysis Time/Image, min
1	+++	++	123	4.2	2.0	34.6	0.3
2	+++	++	66	2.1	1.9	22.4	0.3
3	+++	+++	146	4.7	1.9	36.9	0.3
4	+++	+++	200	6.9	2.1	42.3	0.2
5	+++	+	71	2.7	2.3	38.2	0.5
6	+++	++	194	6.8	2.1	47.8	0.3
7	+++	+++	84	2.9	2.0	28.6	0.3
8	+++	++	74	2.7	2.2	29.7	0.4
9	+++	+++	150	4.7	1.9	37.3	0.3
10	+++	++	94	3.1	2.0	31.7	0.3
11	+++	++	48	1.5	1.9	21.3	0.4
12	++	+	129	4.9	2.3	48.4	0.4
13	+++	++	127	4.3	2.0	35.0	0.3
14	+++	+	147	5.7	2.3	46.4	0.3
15	+++	++	194	6.6	2.0	39.4	0.2
16	+++	++	106	3.5	2.0	36.9	0.4
17	+++	++	129	4.6	2.2	44.8	0.4
18	+++	++	150	5.4	2.2	37.3	0.3
19	+++	+++	148	4.5	1.8	37.1	0.3
20	+++	+++	152	5.2	2.0	37.5	0.3
21	+++	++	88	2.9	2.0	31.1	0.4
22	+++	++	110	3.1	1.7	33.3	0.3
23	+++	++	94	3.4	2.2	31.7	0.3
24	+++	++	100	3.5	2.1	33.1	0.3
25	+++	++	75	2.6	2.0	29.8	0.4
26	+++	+++	126	4.2	2.0	34.9	0.3
27	+++	+++	79	2.7	2.0	27.1	0.3
28	+++	+++	69	2.4	2.1	23.8	0.3
29	+++	+++	75	2.4	1.9	25.8	0.3
30	+++	+++	73	2.5	2.0	24.4	0.3
Mean	...	...	114.0	3.9	2.0	34.3	0.3
SD	...	...	41.1	1.5	0.1	7.3	0.1
n	...	...	30	30	30	30	30

Seg indicates segment. ECG gating: +++, easy performance without image artifacts; ++, easy performance with a few cyclic image artifacts. Image quality: +++, excellent; ++, good; +, mediocre.

lines. As a result, the side branch was outside the region of interest on the planar images. Similarly, small calcific portions of the plaque did not affect the detection of the external vessel boundary because of the robustness of the algorithm. In case of marked vessel wall calcification, the automated approach fails to detect the external vessel boundary. However, the 3D approach of the analysis system allowed interpretation of the external vessel boundary in the longitudinal dimension and facilitated tracing of a straight contour line behind the calcium.

Previous Validation In Vitro and In Vivo

In vitro, the algorithm has been validated in a tubular phantom consisting of several segments. The automated measurements revealed a high correlation with the true phantom areas and volumes (r=.99); mean differences were −0.7% to 3.9% (SD<2.6%) for the areas and 0.3% to 1.7% (SD<3.8%) for the volumes of the various segments.[30] A comparison between automated 3D IVUS measurements in 13 atherosclerotic coronary specimen (area plaque+media burden <40%) in vitro and morphometric measurements on the corresponding histological sections revealed good correlations for measurements of lumen, EEM, plaque+media, and plaque+media burden (r=.94,.88,.80, and.88 for areas and.98,.91,.83, and.91 for volumes).[31] In vitro, both area and volume measurements by the automated system agreed well with results obtained by manual tracing of IVUS images, showing low (−3.7% to 0.3%) mean between-method differences with SD <6% and high correlation coefficients (r≥.97 for areas and r=.99 for volumes).[31] In vivo, using 3D IVUS image sets acquired during nongated continuous pullbacks through 20 diseased coronary segments, intraobserver and interobserver comparisons revealed high correlations (r=.95 to.98 for area and r=.99 for volume)[30] and small mean differences (−0.9% to 1.1%), with SD of lumen, EEM, and plaque+media not exceeding 7.3%, 4.5%, and 10.9% for areas and 2.7%, 0.7%, and 2.8% for volumes. The time of (automated) analysis in that study was 69±19 minutes. Importantly, that study did not include segments with more than focal calcification, more than one side branch, or extensive systolic-diastolic movement artifacts in the longitudinally constructed images.

Statistical Analysis

Quantitative data were given as mean±SD; qualitative data were presented as frequencies. According to Bland and Altman,[37] the intraobserver and interobserver agreement (reproducibility) of the contour detection method was assessed by determining the mean and SD of the between-observation and between-observer differences, respectively. The results of the repeated contour analyses (Ia versus Ib), the independent contour detection analyses (Ia versus II), and the manual versus the contour analyses (III-MA versus Ia) were compared by the two-tailed Student's t test for paired data analysis and linear regression analysis; values of P<.05 were considered statistically significant.

Results

Feasibility and Acquisition and Processing Time

The gated IVUS image acquisition required 3.9±1.5 minutes (1.5 to 6.9 minutes) per coronary segment,

TABLE 2. Characteristics of Coronary Segments

Seg	Vessel	MLCSA, mm²	CSA P+M Burden, %		Side Branches, n	Calcium		
			Max	Mean		Presence	Max Arc, °	Length, mm
1	Prox LAD	6.6	54.2	47.0	2	Multiple	60	<1
2	Mid LAD	6.4	44.8	36.6	3	...	...	...
3	Prox LCx	7.4	71.4	65.9	1	Single	180	1.6
4	Distal RCA	5.7	72.1	61.1	5	...	...	...
5	Prox LCx	8.1	31.7	22.8	0	...	...	...
6	Prox LCx	6.2	62.1	51.3	1	...	...	...
7	Mid LAD	6.8	43.5	28.8	4	...	...	...
8	Mid LAD	8.5	51.9	40.1	1	Single	95	<1
9	Mid RCA	4.1	69.5	44.6	3	...	...	...
10	Prox LAD	5.5	66.0	50.6	4	Single	180	1.6
11	Prox LAD	9.6	60.2	48.1	1	Single	100	4.4
12	Prox RCA	4.3	66.4	49.3	1	Multiple	180	1.4
13	Mid RCA	4.7	77.7	58.6	2	Multiple	190	<1
14	Mid RCA	4.2	65.4	50.8	1	Multiple	180	<1
15	Mid RCA	6.4	68.4	58.9	1	Multiple	125	<1
16	Prox LAD	4.3	60.4	36.0	2	...	...	...
17	Prox LAD	5.3	64.8	51.1	1	...	...	...
18	Mid RCA	5.7	65.3	54.2	3	Multiple	50	<1
19	Mid RCA	6.4	66.7	47.9	6	...	...	...
20	Mid RCA	7.2	68.1	53.0	3	...	...	...
21	Prox RCA	9.7	56.9	33.2	0	Single	60	<1
22	Prox LAD	3.5	67.3	49.6	1	...	...	...
23	Prox LAD	6.8	59.1	51.0	2	Single	70	4.6
24	Distal LAD	7.1	50.0	36.6	5	Multiple	100	<1
25	Mid LAD	7.0	57.0	39.6	2	Single	95	<1
26	Mid RCA	5.4	51.9	38.1	4	Single	90	<1
27	Mid RCA	5.9	49.3	39.2	3	...	...	...
28	Prox LAD	9.7	59.4	45.6	2	Single	85	<1
29	Mid LAD	8.0	57.9	46.1	4	...	...	...
30	Mid LAD	5.8	75.6	58.9	2	Single	95	4.8
Mean	...	6.4	60.5	46.5	2.3	...	113.8	...
SD	...	1.7	10.2	9.9	1.5	...	48.8	...
n	...	30	30	30	30	...	17	...

Seg indicates segment; MLCSA, minimal luminal CSA; P+M, plaque+media; Prox, proximal; LAD, left anterior descending coronary artery; LCx, left circumflex coronary artery; and RCA, right coronary artery.

which corresponds to 2.0±0.1 seconds (1.7 to 2.3 seconds) per image (Table 1). All segments could be analyzed by the computerized contour detection system during an analysis time of 34.3±7.3 minutes per segment (21.3 to 48.4 minutes), corresponding to 0.3±0.1 minutes (0.2 to 0.5 minutes) per computerized IVUS image analysis.

IVUS Segment Characteristics

All but two of the segments (93%) contained at least one side branch (Table 2). The average number of side branches per segment was 2.3±1.5 (range, 0 to 6). Calcification was present in 17 segments (57%), 11 (37%) showed a single calcium deposit, and 6 (20%) contained multiple calcium deposits. The maximum arc of calcium was 114±49° (50° to 190°); in 6 segments, the length of the calcified portion exceeded 1 mm.

The minimal lumen CSA as measured by the contour detection system was 6.4±1.7 mm² (3.5 to 9.7 mm²). The maximum and average CSA plaque+media burden were 60.5±10.2% (31.7% to 77.7%) and 46.5±9.9% (22.8% to 65.9%).

Manual Tracing Versus Automated Contour Detection

In the 200 randomly selected image slices, the measurements of the lumen, EEM, and plaque+media CSAs and the CSA plaque+media burden obtained with the automated contour detection system (9.37±3.09 mm², 18.33±6.70 mm², 8.95±5.16 mm², and 46.03±13.46%, respectively) were similar to the results obtained by manual tracing (9.35±3.18 mm², 18.37±6.62 mm², 9.02±5.08 mm², and 46.53±13.41%; n=200). Between-method differences were 0.4±4.3%, −0.4±3.6%, −1.6±9.1%, and −1.2±6.8%, respectively (all P=NS). The correlations between the measurements provided by both methods were high ($r \geq .98$; Fig 3).

Reproducibility of the Contour Detection Analysis

For measurements of lumen, EEM, and plaque+media CSA and the CSA plaque+media burden (n=3421), both intraobserver (−0.4±2.7%, −0.4±1.8%, −0.4±5.1%, and −0.0±4.2%) and interobserver (0.4±5.2%, −0.9±2.7%, −1.5±7.2%, and −1.5±6.9%; all $P<.001$) differences were low. Correlation coefficients were high for repeated measurements by the same observer ($r=.99$) and measurements by the two observers ($r \geq .97$; Fig 4). For the corresponding volumetric measurements (n=30), the intraobserver (−0.4±1.1%, −0.4±0.6%, −0.3±1.0%, and 0.0±0.4%) and interobserver (0.6±2.9%, −0.8±1.0%, −2.5±3.2%, and 0.8±1.5%; $P<.05$) differences were also low, and high correlations were found for both intraobserver and interobserver comparisons ($r=.99$; Fig 5).

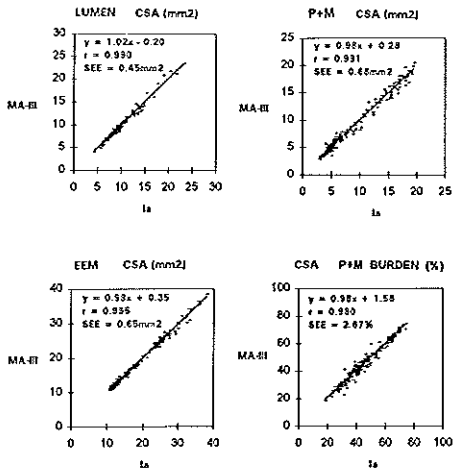

FIG 3. Correlation between results of measurements of lumen, EEM, and plaque+media (P+M) CSA and CSA P+M burden by automated contour detection (Ia) and conventional manual tracing (MA-III).

Discussion

The present study demonstrates that (1) ECG-gated acquisition of 3D IVUS images is feasible, (2) there is a good agreement between the results provided by the automated contour detection method and manual border tracing, and (3) the automated contour detection analysis can be performed in a relatively short analysis time with a high degree of reproducibility.

3D reconstruction of IVUS images was first used to visually assess the spatial configuration of plaques, dissections, and stents and to perform basic measurements.[16,17,19] More recently, the 3D reconstruction systems have included algorithms for automated quantification of lumen dimensions.[16-21,25-27] The contour detection system used in the present study can be used for the detection of both the tissue-lumen boundary and the media-adventitia (EEM) boundary, and therefore plaque volume can be measured.

Feasibility

Non–ECG-gated image acquisition is frequently marred by cardiac cycle–linked coronary artery vasomotion and IVUS catheter motion, which produce sawtooth artifacts in the reconstructed 3D images that can interfere with automated contour detection (both the ease of use and, presumably, reproducibility). Conversely, in the present ECG-gated image sets, the longitudinal contours were smooth and without such artifacts. Therefore, there was much less need to manually edit the automatically detected longitudinal contours. Moreover, the accuracy of the derived edge information improved the performance of the second automated contour detection step on the planar IVUS images. This reduction in manual editing time on both longitudinal and planar images accounts for the low time of analysis compared with a previous study using nongated image acquisition[30]

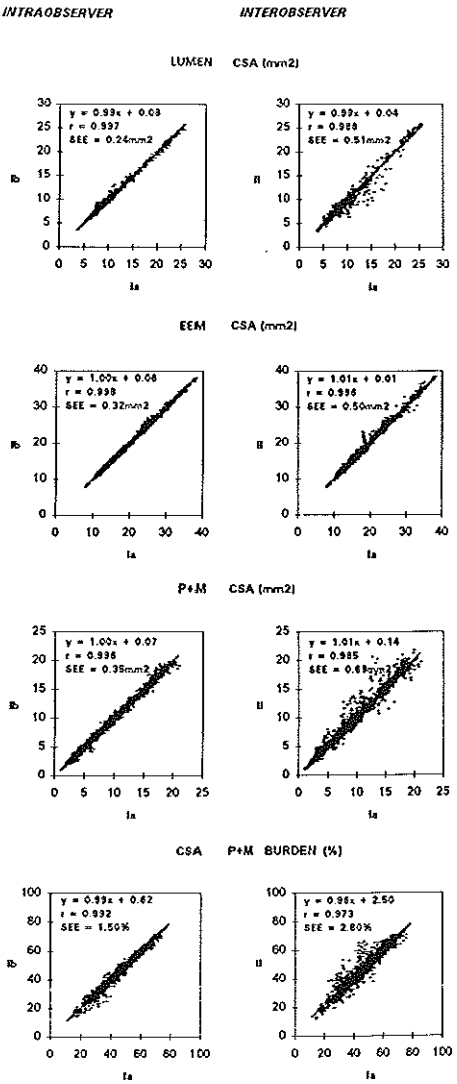

FIG 4. Intraobserver variability (left; first [Ia] vs second [Ib] observation) and interobserver variability (right; first [Ia] vs second [II] observer) of measurements of lumen, EEM, and plaque+media (P+M) CSA and CSA P+M burden by automated contour detection analysis system.

(34 minutes and 69 minutes, respectively). Indeed, this represents a significant reduction in analysis time and as a consequence reduces the cost of the analysis. However, the ECG-gated 3D IVUS acquisition in the present study required a longer acquisition time than conventional motorized pullback (eg, non–ECG-triggered pull-

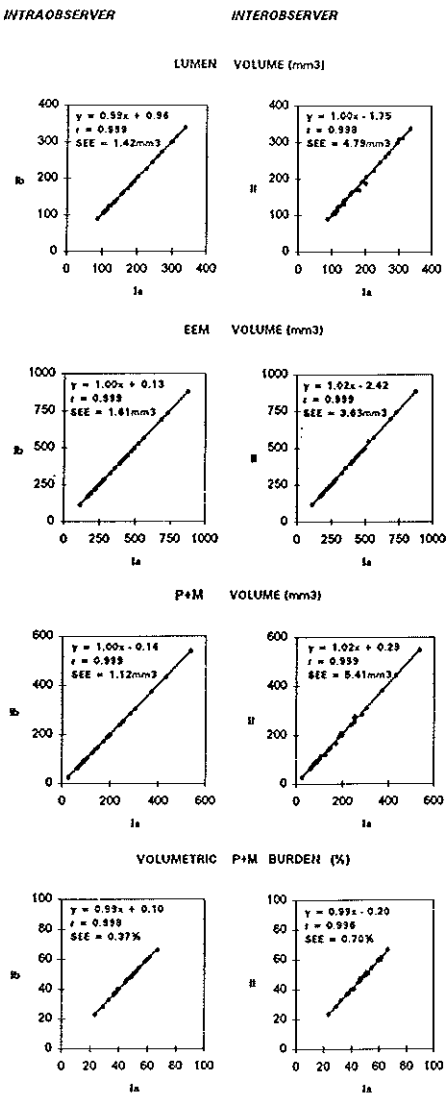

FIG 5. Intraobserver variability (left; first [Ia] vs second [Ib] observation) and interobserver variability (right; first [Ia] vs second [II] observer) of measurements of lumen, EEM, and plaque+media (P+M) volume and volumetric P+M burden by automated contour detection analysis system.

back at 0.5 mm/s). On average, only a 6-mm-long coronary segment could be imaged in 1 minute.

Reproducibility of the Contour Detection

In the present study, the measurement of the lumen, EEM, and plaque+media CSA differed little from the results obtained by manual contour tracing of these borders; there were only small interobserver and intraobserver differences in both the planar and volumetric analyses. However, the reproducibility of the plaque+media measurements was lower than for the other measures, which may reflect the combined variability of both the luminal and the EEM contours, confirming previous in vitro[31] and in vivo data (nongated patient data)[30] and findings of others.[35] The reproducibility of the volumetric measurements was higher than for the CSA measurements, which may be a result of an averaging of the differences between the individual CSA measurements.

Although the segments in this ECG-gated contour detection study were nonselected and included calcified segments with some side branches, the reproducibility of the CSA measurements was consistently better than observed in a previous study using nongated contour detection.[30] We believe that the key factors explaining the overall high reproducibility of automated contour detection observed in this study are (1) the integrated analyses of the conventional cross-sectional image slices with two longitudinal sections and (2) the facilitated and improved detection as a result of the smoothness of the contours on the ECG-gated longitudinal IVUS sections.

Reproducibility of Alternative Methods of Quantitative 3D IVUS

There is very little information on the reproducibility of 3D IVUS measurements using other measurement systems and algorithms. Matar and colleagues[21] reported a Pearson's correlation coefficient of .98 for an intraobserver study of lumen volume measurement by an automated threshold-based IVUS analysis system, confirming the low variability of the volumetric measurements observed in the present study. Another acoustic quantification system[25] performs measurements of lumen CSA and volume, based on the automated detection of the blood pool in single IVUS images acquired at random during the cardiac cycle.[21,25] Because the measurements are based on single-frame analysis, ECG-gated image acquisition may not influence the reproducibility of such systems.

Conversely, 3D contour detection–based analysis approaches benefit from an ECG-gated image acquisition.[20] Sonka and associates[39,40] developed an alternative 3D contour detection system that performs computerized detection of the luminal and external vascular boundaries in 3D sets of planar IVUS images without the additional information provided by the longitudinal contours. In their study,[39] the correlation between automated and manually traced CSA measurements was quite good (r=.91 and.83 for lumen and plaque CSA, respectively). Using ECG-gated 3D IVUS, they found significantly improved results (r=.98 and.94 for lumen and plaque+media CSA, respectively),[40] underlining the significance of ECG-gated IVUS image acquisition. Most likely, other promising contour detection algorithms[41,42] for 3D analyses may also benefit from an ECG-gated image acquisition.

Potential Sources of Error and Study Limitations

Problems related to IVUS in general[43] and to 3D reconstruction in particular[22,23] may influence the contour detection process. The quality of the basic IVUS

images is crucial to both planar and 3D image analysis.[22] Incomplete visualization of the vessel wall, for example as caused by acoustic shadowing[6] from lesion-associated calcium, hampers conventional planar IVUS analyses; however, 3D IVUS allows interpretation in the axial dimension and estimated contour tracing of the external vascular boundary. Image distortion caused by nonuniform transducer rotation or noncoaxial IVUS catheter position in the lumen may create artifacts both in planar images and in 3D reconstruction.[22]

Vessel curvatures may cause differences between the movement of the distal transducer tip and the proximal part of the catheter (although the use of sheath-based IVUS catheters reduces the latter problem) and a significant distortion of the 3D image reconstruction.

Most importantly, linear 3D systems such as used in this study can provide only approximate values of the volumetric parameters[44] because they do not account for vascular curvatures and the real spatial geometry. In curved vascular segments, this results in an overestimation of plaque volume at the inner side (expansion) and an underestimation of plaque volume at the outer side (compression) of the curve.[22] Approaches combining data obtained from angiography and IVUS[45-48] can provide information on the real spatial geometry of the vessel. Unquestionably, the combined approaches have a unique potential, but currently these sophisticated techniques are still laborious, restricted to research applications, and not yet useful for routine off-line analysis of clinical IVUS examinations. In the present study, only relatively straight coronary segments, showing no more than mild vessel curvatures, were included. We felt that this premise was important to limit curve distortion–induced deviation of volumetric measurement,[44] because linear 3D analysis systems do not account for vascular curvatures.

Compared with conventional motorized transducer pullback at a uniform speed, ECG-gated image acquisition takes longer, which may limit its use before intervention, especially in patients with very severe coronary stenoses. Therefore, we currently perform ECG-gated IVUS examinations during diagnostic or follow-up catheterizations and at the presumed end point of coronary interventions.

Clinical Implications

The examination of coronary arteries by IVUS permits the comprehensive assessment of atherosclerosis[1-3,6,7,10,11] and the evaluation of the instantaneous[27,49] and long-term effects of catheter-based interventions on the coronary lumen and plaque. To quantify these changes, anatomic landmarks such as side branches or spots of calcium can be used to define specific anatomic image slices for comparative analysis in serial studies.

The proposed 3D IVUS method, which permits reproducible and reliable contour detection of both lumen and plaque, may facilitate volumetric measurements[10,30,31] and obviate the need for laborious analyses based on Simpson's rule.[15] Furthermore, the use of ECG-gated image acquisition[28] increases the applicability of the contour detection algorithm by shortening the analysis time[49] and increasing the reproducibility of the method. These advantages may be most significant in studies that are expected to show only small changes in plaque and/or lumen over time (eg, in trials evaluating the progression or regression of atherosclerosis during pharmacological therapy[10]). In addition, because the time from the peak of the R wave to image acquisition can be varied, this method can be used to study the cyclic (systole versus diastole) changes in vessel dimensions.

Conclusions

ECG-gated acquisition of 3D IVUS image sets is feasible and permits the application of automated contour detection to provide reproducible measurements of the lumen and atherosclerotic plaque CSA and volume in a relatively short analysis time.

Acknowledgment

Dr von Birgelen is the recipient of a fellowship of the German Research Society (DFG, Bonn, Germany).

References

1. Yock PG, Linker DT. Intravascular ultrasound: looking below the surface of vascular disease. *Circulation*. 1990;81:1715-1718.
2. Nissen SE, Gurley JC, Grines CL, Booth DC, McClure R, Berk M, Fischer C, DeMaria AN. Intravascular ultrasound assessment of lumen size and wall morphology in normal subjects and patients with coronary artery disease. *Circulation*. 1991;84:1087-1099.
3. Fitzgerald PJ, St Goar FG, Connolly AJ, Pinto FJ, Billingham ME, Popp RL, Yock PG. Intravascular ultrasound imaging of coronary arteries: is three layers the norm? *Circulation*. 1992;86:154-158.
4. Ge J, Erbel R, Rupprecht HJ, Koch L, Kearney P, Görge G, Haude M, Meyer J. Comparison of intravascular ultrasound and angiography in the assessment of myocardial bridging. *Circulation*. 1994;89:1725-1732.
5. Lee DY, Eigler N, Nishioka T, Tabak SW, Forrester JS, Siegel RJ. Effect of intracoronary ultrasound imaging on clinical decision making. *Am Heart J*. 1995;129:1084-1093.
6. Mintz GS, Painter JA, Pichard AD, Kent KM, Satler LF, Popma JJ, Chuang YC, Bucher TA, Sokolowicz LE, Leon MB. Atherosclerosis in angiographically 'normal' coronary artery reference segments: an intravascular ultrasound study with clinical correlations. *J Am Coll Cardiol*. 1995;25:1479-1485.
7. Erbel R, Ge J, Bockisch A, Kearney P, Görge G, Haude M, Schürmann D, Zamorano J, Rupprecht HJ, Meyer J. Value of intracoronary ultrasound and Doppler in the differentiation of angiographically normal coronary arteries: a prospective study in patients with angina pectoris. *Eur Heart J*. 1996;17:880-889.
8. Pinto FJ, St Goar FG, Gao SZ, Chenzbraun A, Fischell TA, Alderman EL, Schroeder JS, Popp RL. Immediate and one-year safety of intracoronary ultrasonic imaging: evaluation with serial quantitative angiography. *Circulation*. 1993;88:1709-1714.
9. Hausmann D, Erbel R, Alibelli-Chemarin MJ, Alibelli-Chemarin MJ, Boksch W, Caracciolo E, Cohn JM, Culp SC, Daniel WG, De Scherder I, Di Mario C, Ferguson JJ III, Fitzgerald PJ, Friedrich G, Ge J, Görge G, Hanrath P, Hodgson J McB, Isner JM, Jain S, Maier-Rudolph W, Mooney M, Moses JW, Mudra H, Pinto FJ, Smalling RW, Talley JD, Tobis JM, Walter PD, Weidinger F, Werner GS, Yeung AC, Yock PG. The safety of intracoronary ultrasound: a multicenter survey of 2207 examinations. *Circulation*. 1995;91:623-630.
10. von Birgelen C, Slager CJ, Di Mario C, de Feyter PJ, Serruys PW. Volumetric intracoronary ultrasound: a new maximum confidence approach for the quantitative assessment of progression-regression of atherosclerosis? *Atherosclerosis*. 1995;118(suppl):S103-S113.
11. Mintz GS, Popma JJ, Pichard AD, Kent KM, Satler LF, Chuang YC, DeFalco RA, Leon MB. Limitations of angiography in the assessment of plaque distribution in coronary artery disease: a systematic study of target lesion eccentricity in 1446 lesions. *Circulation*. 1996;93:924-931.
12. de Feyter PJ, Serruys PW, Davies MJ, Richardson P, Lubsen J, Oliver MF. Quantitative coronary angiography to measure progression and regression of coronary atherosclerosis: value, limitations, and implications for clinical trials. *Circulation*. 1991;84:412-423.
13. Serruys PW, de Jaegere P, Kiemeneij F, Macaya C, Rutsch W, Heyndrickx G, Emanuelsson H, Marco J, Legrand V, Materne P, Belardi J, Sigwart U, Colombo A, Goy JJ, van der Heuvel P, Delcan J, Morel AA, for the Benestent Study Group. A comparison of balloon expandable stent implantation with balloon angioplasty in patients with coronary artery disease. *N Engl J Med*. 1994;331:489-495.

14. von Birgelen C, Umans V, Di Mario C, Keane D, Gil R, Prati F, de Feyter PJ, Serruys PW. Mechanism of high-speed rotational atherectomy and adjunctive balloon angioplasty revisited by quantitative coronary angiography: edge detection versus videodensitometry. *Am Heart J.* 1995;130:405-412.
15. Dussaillant GR, Mintz GS, Pichard AD, Kent KM, Satler LF, Popma JJ, Wong SC, Leon MB. Small stent size and intimal hyperplasia contribute to restenosis: a volumetric intravascular ultrasound analysis. *J Am Coll Cardiol.* 1995;26:720-724.
16. Rosenfield K, Losordo DW, Ramaswamy K, Pastore JO, Langevin RE, Razvi S, Kosowsky BD, Isner JM. Three-dimensional reconstruction of human coronary and peripheral arteries from images recorded during two-dimensional intravascular ultrasound examination. *Circulation.* 1991;84:1938-1956.
17. Coy KM, Park JC, Fishbein MC, Laas T, Diamond GA, Adler L, Maurer G, Siegel RJ. In vitro validation of three-dimensional intravascular ultrasound for the evaluation of arterial injury after balloon angioplasty. *J Am Coll Cardiol.* 1992;20:692-700.
18. Rosenfield K, Kaufman J, Pieczek A, Langevin RE, Razvi S, Ilsner JM. Real-time three-dimensional reconstruction of intravascular ultrasound images of iliac arteries. *Am J Cardiol.* 1992;70:412-415.
19. Mintz GS, Pichard AD, Satler LF, Popma JJ, Kent KM, Leon MB. Three-dimensional intravascular ultrasonography: reconstruction of endovascular stents in vitro and in vivo. *Clin Ultrasound.* 1993; 21:609-615.
20. Dhawale PJ, Wilson DL, Hodgson J McB. Optimal data acquisition for volumetric intracoronary ultrasound. *Cathet Cardiovasc Diagn.* 1994;32:288-299.
21. Matar FA, Mintz GS, Douek P, Farb A, Virmani R, Saturnino PJ, Popma JJ, Pichard AD, Kent KM, Satler LF, Keller M, Leon MB. Coronary artery lumen volume measurement using three-dimensional intravascular ultrasound: validation of a new technique. *Cathet Cardiovasc Diagn.* 1994;33:214-220.
22. Roelandt JRTC, Di Mario C, Pandian NG, Li W, Keane D, Slager CJ, de Feyter PJ, Serruys PW. Three-dimensional reconstruction of intracoronary ultrasound images: rationale, approaches, problems, and directions. *Circulation.* 1994;90:1044-1055.
23. Di Mario C, von Birgelen C, Prati F, Soni B, Li W, Bruining N, de Jaegere PJ, de Feyter PJ, Serruys PW, Roelandt JRTC. Three-dimensional reconstruction of two-dimensional intracoronary ultrasound: clinical or research tool? *Br Heart J.* 1995;73(suppl 2):26-32.
24. von Birgelen C, Di Mario C, Serruys PW. Structural and functional characterization of an intermediate stenosis with intracoronary ultrasound: a case of 'reverse glagovian modeling.' *Am Heart J.* 1996;132:694-696.
25. von Birgelen C, Kutryk MJB, Gil R, Ozaki Y, Di Mario C, Roelandt JRTC, de Feyter PJ, Serruys PW. Quantification of the minimal luminal cross-sectional area after coronary stenting by two- and three-dimensional intravascular ultrasound versus edge detection and videodensitometry. *Am J Cardiol.* 1996;78:520-525.
26. Gil R, von Birgelen C, Prati F, Di Mario C, Ligthart J, Serruys PW. Usefulness of three-dimensional reconstruction for interpretation and quantitative analysis of intracoronary ultrasound during stent deployment. *Am J Cardiol.* 1996;77:761-764.
27. von Birgelen C, Gil R, Ruygrok P, Prati F, Di Mario C, van der Giessen WJ, de Feyter PJ, Serruys PW. Optimized expansion of the Wallstent compared with the Palmaz-Schatz stent: online observations with two- and three-dimensional intracoronary ultrasound after angiographic guidance. *Am Heart J.* 1996;131:1067-1075.
28. Bruining N, von Birgelen C, Di Mario C, Prati F, Li W, Den Hood W, Patijn M, de Feyter PJ, Serruys PW, Roelandt JRTC. Dynamic three-dimensional reconstruction of ICUS images based on an ECG-gated pull-back device. In: *Computers in Cardiology 1995.* Los Alamitos, Calif: IEEE Computer Society Press; 1995:633-636.
29. Li W, von Birgelen C, Di Mario C, Boersma E, Gussenhoven EJ, van der Putten N, Bom N. Semi-automatic contour detection for volumetric quantification of intracoronary ultrasound. In: *Computers in Cardiology 1994.* Los Alamitos, Calif: IEEE Computer Society Press; 1994:277-280.
30. von Birgelen C, Di Mario C, Li W, Schuurbiers JCH, Slager CJ, de Feyter PJ, Roelandt JRTC, Serruys PW. Morphometric analysis in three-dimensional intracoronary ultrasound: an in-vitro and in-vivo study using a novel system for the contour detection of lumen and plaque. *Am Heart J.* 1996;132:516-527.
31. von Birgelen C, van der Lugt A, Nicosia A, Mintz GS, Gussenhoven EJ, de Vrey E, Mallus MT, Roelandt JRTC, Serruys PW, de Feyter PJ. Computerized assessment of coronary lumen and atherosclerotic plaque dimensions in three-dimensional intravascular ultrasound correlated with histomorphometry. *Am J Cardiol.* 1996; 78:1202-1209.
32. Hodgson J McB, Graham SP, Sarakus AD, Dame SG, Stephens DN, Dhillon PS, Brands D, Sheehan H, Eberle MJ. Clinical percutaneous imaging of coronary anatomy using an over-the-wire ultrasound catheter system. *Int J Card Imaging.* 1989;4:186-193.
33. Tobis JM, Mallery JA, Gerrett J, Griffith J, Mahon D, Bessen M, Moriuchi M, McLeay L, McRae M, Henry WL. Intravascular ultrasound cross-sectional arterial imaging before and after balloon angioplasty in vitro. *Circulation.* 1989;80:873-882.
34. Nishimura RA, Edwards WD, Warnes CA, Reeder GS, Holmes DR Jr, Tajik AJ, Yock PG. Intravascular ultrasound imaging: in vitro validation and pathologic correlation. *J Am Coll Cardiol.* 1990; 16:145-154.
35. Mallery JA, Tobis JM, Griffith J, Gessert J, McRae M, Moussabeck O, Bessen M, Moriuchi M, Henry WL. Assessment of normal and atherosclerotic arterial wall thickness with an intravascular ultrasound imaging catheter. *Am Heart J.* 1990;119:1392-1400.
36. Li W, Bosch JG, Zhong Y, van Urk H, Gussenhoven EJ, Mastik F, van Egmond F, Rijsterborgh H, Reiber JHC, Bom N. Image segmentation and 3D reconstruction of intravascular ultrasound images. In: Wei Y, Gu B, eds. *Acoustical Imaging. Vol 20.* New York, NY: Plenum Press; 1993:489-496.
37. Bland JM, Altman DG. Statistical methods for assessing agreement between two methods of clinical measurement. *Lancet.* 1986;2: 307-310.
38. Hausmann D, Lundkvist AJS, Friedrich GJ, Mullen WL, Fitzgerald PJ, Yock PG. Intracoronary ultrasound imaging: intraobserver and interobserver variability of morphometric measurements. *Am Heart J.* 1994;128:674-680.
39. Sonka M, Zhang X, Siebes M, DeJong S, McKay CR, Collins SM. Automated segmentation of coronary wall and plaque from intravascular ultrasound image sequences. In: *Computers in Cardiology 1994.* Los Alamitos, Calif: IEEE Computer Society Press; 1994: 281-284.
40. Sonka M, Liang W, Zhang X, De Jong S, Collins SM, McKay CR. Three-dimensional automated segmentation of coronary wall and plaque from intravascular ultrasound pullback sequences. In: *Computers in Cardiology 1995.* Los Alamitos, Calif: IEEE Computer Society Press; 1995:637-640.
41. Frank RJ, McPherson DD, Chandran KB, Dove EL. Optimal surface detection in intravascular ultrasound using multi-dimensional graph search. In: *Computers in Cardiology 1996.* Los Alamitos, Calif: IEEE Computer Society Press; 1996:45-48.
42. Brathwaite PA, Chandran KB, McPherson DD, Dove EL. Lumen detection in human IVUS images using region-growing. In: *Computers in Cardiology 1996.* Los Alamitos, Calif: IEEE Computer Society Press; 1996:37-40.
43. ten Hoff H, Gussenhoven EJ, Korbijn A, Mastik F, Lancee CT, Bom N. Mechanical scanning in intravascular ultrasound: artifacts and driving mechanisms. *Eur J Ultrasound.* 1995;2:227-237.
44. Waligora MJ, Vonesh MJ, Wiet SP, McPherson DD. Effect of vascular curvatures on three-dimensional reconstruction of intravascular ultrasound images *Circulation.* 1994;90(suppl I):I-227. Abstract.
45. Klein HM, Günther RW, Verlande M, Schneider W, Vorwerk D, Kelch J, Hamm M. 3D-surface reconstruction of intravascular ultrasound images using personal computer hardware and a motorized catheter control. *Cardiovasc Intervent Radiol.* 1992;15:97-101.
46. Koch L, Kearney P, Erbel R, Roth T, Ge J, Brennecke R, Meyer J. Three dimensional reconstruction of intracoronary ultrasound images: roadmapping with simultaneously digitised coronary angiograms. In: *Computers in Cardiology 1993.* Los Alamitos, Calif: IEEE Computer Society Press; 1993:89-91.
47. Laban M, Oomen JA, Slager CJ, Wentzel JJ, Krams R, Schuurbiers JCH, den Boer A, von Birgelen C, Serruys PW, de Feyter PJ. ANGUS: a new approach to three-dimensional reconstruction of coronary vessels by combined use of angiography and intravascular ultrasound. In: *Computers in Cardiology 1995.* Los Alamitos, Calif: IEEE Computer Society Press; 1995:325-328.
48. Evans JL, Ng KH, Wiet SG, Vonesh MJ, Burns WB, Radvany MG, Kane BJ, Davidson CJ, Roth SI, Kramer BL, Meyers SN, McPherson DD. Accurate three-dimensional reconstruction of intravascular ultrasound data: spatially correct three-dimensional reconstructions. *Circulation.* 1996;93:567-576.
49. von Birgelen C, Mintz GS, Nicosia A, Foley DP, van der Giessen WJ, Bruining N, Airiian SG, Roelandt JRTC, de Feyter PJ, Serruys PW. Electrocardiogram-gated intravascular ultrasound image acquisition after coronary stent deployment facilitates on-line three-dimensional reconstruction and automated lumen quantification. *J Am Coll Cardiol.* 1997;30:436-443.

CHAPTER 10

Electrocardiogram-Gated Intravascular Ultrasound Image Acquisition After Coronary Stent Deployment Facilitates On-Line Three-Dimensional Reconstruction and Automated Lumen Quantification

C. von Birgelen, G.S. Mintz, A. Nicosia, D.P. Foley, W.J. van der Giessen, N. Bruining, S. G. Airiian, J.R.T.C. Roelandt, P.J. de Feyter and P.W. Serruys

Reprinted with permission from the American College of Cardiology,
Journal of the American College of Cardiology, 1997; 30: 436-43

Electrocardiogram-Gated Intravascular Ultrasound Image Acquisition After Coronary Stent Deployment Facilitates On-Line Three-Dimensional Reconstruction and Automated Lumen Quantification

CLEMENS VON BIRGELEN, MD,* GARY S. MINTZ, MD, FACC,† ANTONINO NICOSIA, MD, DAVID P. FOLEY, MB, MRCPI, PHD, WIM J. VAN DER GIESSEN, MD, PHD, NICO BRUINING, BSC, SERGEI G. AIRIIAN, MD, JOS R. T. C. ROELANDT, MD, PHD, FACC, PIM J. DE FEYTER, MD, PHD, FACC, PATRICK W. SERRUYS, MD, PHD, FACC

Rotterdam, The Netherlands and Washington, D.C.

Objectives. This study evaluates the feasibility, reliability and reproducibility of electrocardiogram (ECG)-gated intravascular ultrasound (IVUS) image acquisition during automated transducer withdrawal and automated three-dimensional (3D) boundary detection for assessing on-line the result of coronary stenting.

Background. Systolic-diastolic image artifacts frequently limit the clinical applicability of such automated analysis systems.

Methods. In 30 patients, after successful angiography-guided implantation of 34 stents in 30 target lesions, we carried out IVUS examinations on-line with the use of ECG-gated automated 3D analyses and conventional manual analyses of two-dimensional images from continuous pullbacks. These on-line measurements were compared with off-line 3D reanalyses. The adequacy of stent deployment was determined by using ultrasound criteria for stent apposition, symmetry and expansion.

Results. Gated image acquisition was successfully performed in all patients to allow on-line 3D analysis within 8.7 ± 0.6 min (mean ± SD). Measurements by on-line and off-line 3D analyses correlated closely ($r \geq 0.95$), and the minimal stent lumen differed only minimally (8.6 ± 2.8 mm^2 vs. 8.5 ± 2.8 mm^2, p = NS). The conventional analysis significantly overestimated the minimal stent lumen (9.0 ± 2.7 mm^2, $p < 0.005$) in comparison with results of both 3D analyses. Fourteen stents (41%) failed to meet the criteria by both 3D analyses, all of these not reaching optimal expansion, but only 7 (21%) were detected by conventional analysis ($p < 0.02$). Intraobserver and interobserver comparison of stent lumen measurements by the automated approach revealed minimal differences (0.0 ± 0.2 mm^2 and 0.0 ± 0.3 mm^2) and excellent correlations ($r = 0.99$ and 0.98, respectively).

Conclusions. ECG-gated image acquisition after coronary stent deployment is feasible, permits on-line automated 3D reconstruction and analysis and provides reliable and reproducible measurements; these factors facilitate detection of the minimal lumen site.

(J Am Coll Cardiol 1997;30:436–43)

©1997 by the American College of Cardiology

Intravascular ultrasound (IVUS) permits detailed, high quality cross-sectional imaging of the coronary arteries in vivo. The normal coronary artery architecture, the major components of the atherosclerotic plaque and, in particular, changes that occur in coronary artery dimensions and anatomy during and after transcatheter therapy can be studied in vivo in a manner otherwise not possible (1–4). This includes direct visualization of intensely echoreflective (but radiolucent) stainless steel stent struts (5–11). In an attempt to reduce both the analysis time and the variability involved in planar IVUS measurements, automated three-dimensional (3D) image reconstruction and analysis systems have been developed (10–20). However, cyclic changes in coronary dimensions and the movement of the IVUS catheter relative to the coronary vessel wall frequently cause image artifacts (Fig. 1) that generally represent an important limitation to the applicability of 3D systems for quantitative analysis (17,21,22).

One method of limiting cyclic artifacts combines electrocardiogram (ECG)-gated image acquisition (22) and a previously validated program for automated 3D IVUS boundary detection (18,19). We applied this technique to the analysis of 34 coronary stents after successful angiography-guided implantation to determine the feasibility, reliability and reproducibility of this approach to assessing on-line procedural results.

From the Thoraxcenter, Division of Cardiology, University Hospital Rotterdam-Dijkzigt and Erasmus University, Rotterdam, The Netherlands; and †Washington Hospital Center, Washington, D.C. Dr. von Birgelen is the recipient of a fellowship of the German Research Society (DFG, Bonn, Germany).

Manuscript received December 10, 1996; revised manuscript received March 25, 1997, accepted April 16, 1997.

*Present address: Department of Cardiology, University Hospital Essen, Hufelandstrasse 55, 45122 Essen, Germany.

Address for correspondence: Patrick W. Serruys, Thoraxcenter, University Hospital Dijkzigt, P.O. Box 1738, 3000 DR Rotterdam, The Netherlands.

Abbreviations and Acronyms

CSA = cross-sectional area
ECG = electrocardiogram, electrocardiographic
IVUS = intravascular ultrasound
3D = three-dimensional
2D = two-dimensional

Methods

Study patients. The study was approved by the Medical Ethical Committee of the Erasmus University Hospital, Rotterdam. All patients provided written informed consent. The study group consisted of 30 patients (24 men, 6 women, mean age ± SD 59.1 ± 8.4 years) who had 34 stents implanted in 30 target lesions. To simplify the ECG-gated acquisition procedure, we chose for the study only patients who had 1) sinus rhythm, 2) ≤10 extrasystoles/min, and 3) no permanent or temporary pacemaker implantation.

Intervention procedures and coronary angiography. All patients received intravenous aspirin (250 mg) and heparin (10,000 U), and subsequent heparin was administered hourly to maintain an activated clotting time >300 s. The percutaneous transluminal angioplasty procedures were performed by using 8F femoral artery sheaths and 8F guiding catheters. All patients were undergoing elective stent implantation for stable (n = 14) or unstable (n = 16) angina; therefore, conservative balloon predilation was performed to enable stent placement but avoid unnecessary dissection. The stents were placed in the right (n = 20), left anterior descending (n = 9) and left circumflex (n = 5) coronary arteries. The following stents were used: Palmaz-Schatz stent (Johnson & Johnson Interventional Systems, n = 15); Wallstent (Schneider, Bulach, Switzerland, n = 11); Cordis balloon expandable coiled stent (Cordis Corporation, n = 4), Multilink stent (Advanced Cardiovascular Systems, n = 2); AVE Microstent (Applied Vascular Engineering, Edmonton, Alberta, Canada, n = 1); and NIR stent (Medinol, Ltd., Tel Aviv, Israel, n = 1). After the procedure, all patients were treated with an antiplatelet regimen of aspirin and ticlopidine.

On-line quantitative coronary angiography was performed with the CAAS II system (Pie Medical, Maastricht, The Netherlands) according to previously described methodology (10,11). The maximal diameter of the target segment and the interpolated reference diameter were used to select the diameter of the balloon-expandable stents. The interpolated reference diameter of the stented coronary segments ranged from 2.5 to 4.7 mm. The proximal and distal vessel diameter, interpolated reference diameter and lesion length were taken into account to select an appropriately sized self-expanding Wallstent (11). Adjunct balloon angioplasty was performed by using low compliance balloon catheters with a maximal nominal size of 3.74 ± 0.44 mm (balloon/preintervention reference = 1.24 ± 0.21; balloon/postintervention reference = 1.04 ± 0.14) at a maximal pressure of 16.4 ± 1.7 atm.

After IVUS imaging was performed, any further treatment was left to the discretion of the operator. Although additional IVUS examinations were not part of the protocol, and were, in fact, not performed, the operator was free to perform them, if he or she considered them necessary.

Angiographic end points. All procedures had achieved angiographic success before IVUS examinations were performed. A procedure was considered angiographically successful if all of the following three criteria were met: 1) smooth contour of the lumen silhouette in the stented segment, 2) diameter stenosis inside the stent in the "worst" (of at least two orthogonal) views <15% by quantitative on-line analysis, and 3) no inflow or outflow obstruction. IVUS examination was then performed.

IVUS imaging. IVUS imaging was performed after bolus injection of intracoronary nitroglycerin with use of a commercially available mechanical sector scanner (CardioVascular Imaging Systems) and 2.9F sheath-based IVUS catheters (MicroView, CardioVascular Imaging Systems). This catheter incorporates a 15-cm long sonolucent distal imaging sheath that alternatively houses the guide wire (during catheter introduction) or, after the guide wire has been pulled back, the 30-MHz beveled single-element transducer (during imaging).

First, a continuous motorized pullback of the IVUS transducer at a pullback speed of 0.5 mm/s (within the imaging sheath) was performed for conventional on-line two-dimensional (2D) cross-sectional IVUS analysis. Next, the transducer was readvanced for ECG-gated image acquisition. The basic settings of the IVUS machine remained unchanged to ensure an equal image quality during both pullbacks. Between both pullbacks there were no significant changes in the patients' heart rate and no differences in the occurrence of arrhythmias. The ECG-triggered pullback device uses a step-

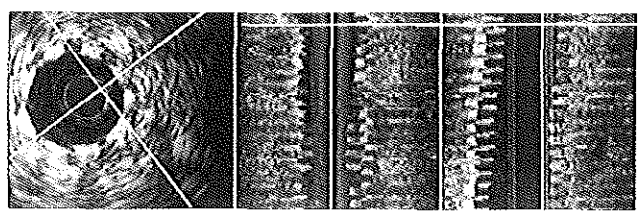

Figure 1. Cyclic artifact in 3D IVUS image set of stented coronary segment. **Center and right panels,** Saw-shaped artifacts in two perpendicular longitudinal sections after *non-gated* image acquisition, resulting from the cyclic movement of the echo-transducer relative to the coronary wall, may limit the on-line applicability of systems for automated contour detection. **Left panel,** Cross-sectional image corresponding to the horizontal cursor in the longitudinal sections.

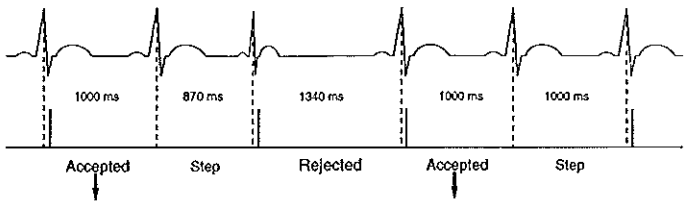

Figure 2. Principle of ECG-gated image acquisition and stepwise pullback. Images were acquired 40 ms after the peak of the R wave and only *accepted* for computer storage (arrows) if the time interval between two successive R waves met a predefined range. This range was based on data (mean RR interval ± 50 ms), taken before imaging was performed. If an RR interval was too long or short, images were *rejected*, and the transducer remained at this site until the image could be acquired during a heart cycle with an appropriate RR interval length. During the following heart cycle, the transducer was withdrawn 200 μm (Step) to the adjacent image acquisition site.

ping motor to withdraw the transducer in 0.2-mm axial increments through the stationary imaging sheath. The ECG-triggered pullback device is controlled by a 3D ultrasound work station (23) (EchoScan, TomTec, Munich, Germany). The work station receives a video input from the IVUS machine and an ECG signal from the patient. It measures the RR intervals over a 2-min period preceding the imaging sequence to define the upper and lower limits of acceptable RR intervals (mean value ± 50 ms). During the imaging sequence it considers heart rate variability and checks for the presence of extrasystoles. If the RR interval meets the preset range, images are 1) acquired 40 ms after the peak of the R wave, 2) digitized (by the work station), and 3) stored in the computer memory. After an image is acquired, the IVUS transducer is withdrawn 0.2 mm to acquire the next image at that site (Fig. 2).

IVUS analysis protocol. All 34 stented lesions were analyzed on-line by two experienced IVUS analysts who had no knowledge of each other's results. One analyst (called the "2D analyst") performed conventional manual tracing of the cross-sectional IVUS images. The second analyst (called the "3D analyst") analyzed the ECG-gated 3D IVUS images (18,19). The senior interventional cardiologists of the department decided that, to be clinically useful, all on-line analyses should be completed within ≤10 min.

After an interval of ≥4 weeks, the 3D analyst performed a blinded off-line reanalysis of the stored ECG-gated image set from all 34 stents. This off-line reanalysis had no time limit. Each image was carefully checked, the videotape was used to confirm the automated measurements, even small deviations were corrected, and the results were approved by two independent cardiologists, experienced in the use and analysis of IVUS imaging. The off-line reanalysis was performed within 28.7 ± 5.9 min and represented the maximal confidence measurements.

Intraobserver and interobserver variability of on-line 3D measurements of the stent cross-sectional area were determined from 10 randomly selected digitized stent image data sets (for a total of 1,112 cross-sectional IVUS images). Because actual on-line conditions cannot be reproduced, this comparison was obtained from simulated on-line conditions, especially a maximal analysis time of 10 min. Intraobserver variability was determined from repeated measurements performed by the 3D analyst; interobserver variability was determined by comparing the measurements of the 3D analyst and those of a third analyst who had no knowledge of previous data.

2D quantitative IVUS analysis. By using previously validated manual contour tracing techniques (24), the minimal lumen cross-sectional area (CSA) within the stented segment was measured and compared with the proximal and distal reference lumen CSA. These reference measurements were obtained from the most normal-looking cross-sections within 5 mm proximal and distal to the stent edges. In addition, the stent symmetry index (minimal/maximal stent diameter) was measured at the minimal lumen CSA site.

3D quantitative IVUS analysis. Quantitative 3D IVUS analysis was performed by using a contour detection program (Fig. 3) developed at the Thoraxcenter, Rotterdam. This system allows the automated analysis of up to 200 IVUS images. Two longitudinal sections are constructed in which contour detection is performed to identify regions of interest (center and range for boundary searching) on planar images. This procedure facilitates automated detection of the lumen boundary on the planar images with use of the minimum cost algorithm (18,19). The axial location of an individual planar image is indicated by a cursor that is used to scroll through the entire set of planar IVUS images to review the detected contours (Fig. 3). Corrections may be performed by "forcing" the contour through a visually identified point (minimum cost), which causes the entire data set to be updated (dynamic programming). This algorithm has been validated with use of a tubular phantom (18) and in histologic studies (19). Furthermore, the intraobserver and interobserver reproducibility of in vivo CSA measurements after nongated acquisition of IVUS images from nonstented atherosclerotic coronary arteries have been reported (18).

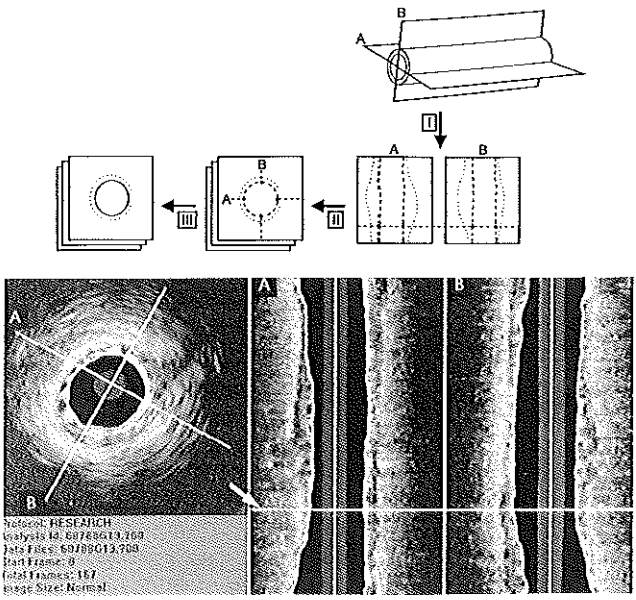

Figure 3. 3D quantitative IVUS analysis. **Upper panel,** Principle of automated lumen contour detection. Two perpendicular longitudinal sections (A, B) were reconstructed from image data of the entire 3D "stack" of images. The lumen contours were detected (I) by use of a minimum cost algorithm. Edge information of these longitudinal contours was represented as points on the planar images (II) and defined regions of interest (center and range of the boundary searching) that guided the final automated contour detection of the lumen boundary on the planar images. **Lower panel,** Clinical example of contour analysis in a stented coronary segment. A horizontal cursor **(arrow)** could be used to scroll through the entire set of planar images **(left).** This cursor indicated on the two perpendicular longitudinal sections (A, B) the site corresponding to the planar image displayed. On the longitudinal sections, note the relative smoothness of both lumen and external vascular boundaries.

Although the algorithm can also be used to detect the external vessel boundary (18,19), only the measurement of the lumen CSA (inside the echo-reflective struts of the metallic stents) and the stent symmetry ratio (i.e., minimal divided by maximal stent diameter) were used in the current study. Reference lumen CSA measurements were obtained at minimally diseased sites 5 mm proximal and distal to the stented segment.

IVUS criteria for optimal stent deployment. Three IVUS criteria, based on the experience of the Milan group (5,6) and our own data (11), were used to define optimal stent deployment: 1) apposition = complete stent apposition to vessel wall along the entire stented segment; 2) symmetry = ratio of minimal/maximal stent diameter (stent symmetry index) ≥0.7; 3) expansion = ratio of minimal stent CSA/mean reference lumen CSA ≥0.8; or, ratio of minimal stent CSA/distal reference lumen CSA ≥0.8 (if the site of the minimal stent CSA was in the distal third of the stent).

Statistical analysis. Quantitative data were given as mean value ± 1 SD; qualitative data were presented as frequencies. Continuous variables were compared by using a two-tailed Student *t* test and linear regression analysis; categoric variables were compared by the chi-square test or Fisher exact test. As proposed by Bland and Altman (25), the agreement of the different approaches was assessed by determining the mean value ± SD of the between-method differences. A p value < 0.05 was considered statistically significant.

Table 1. Comparison of On-Line and Off-Line Intravascular Ultrasound Analyses

	On-Line 2D	On-Line 3D	Off-Line 3D	Δ On-Line 2D vs. On-Line 3D	Δ On-Line 2D vs. Off-Line 3D	Δ On-Line 3D vs. Off-Line 3D
Stent						
Minimal lumen CSA (mm^2)	9.0 ± 2.7	8.6 ± 2.8	8.5 ± 2.8	0.4 ± 0.6*	0.4 ± 0.7†	0.1 ± 0.2
Symmetry index	0.83 ± 0.09	0.81 ± 0.07	0.81 ± 0.08	0.02 ± 0.07	0.02 ± 0.08	0 ± 0.02
Reference						
Proximal lumen CSA (mm^2)	12.7 ± 3.8	12.1 ± 3.8	12.4 ± 4.2	0.6 ± 2.3	0.3 ± 2.2	−0.3 ± 1.3
Distal lumen CSA (mm^2)	10.1 ± 2.8	10.1 ± 3.8	10.1 ± 3.7	0 ± 1.8	0 ± 2.1	0 ± 0.9
Suboptimal stent deployment	7 (21%)	14 (41%)	14 (41%)	−7 (−21%)‡	−7 (−21%)‡	0

*$p < 0.005$; †$p < 0.001$; ‡$p < 0.02$; all other differences were not significant. Values are expressed as mean value ± 1 SD or number (%) of stents. CSA = cross-sectional area; Δ = between-method difference; 3D, 2D = three- and two-dimensional intravascular ultrasound (IVUS) measurements, respectively.

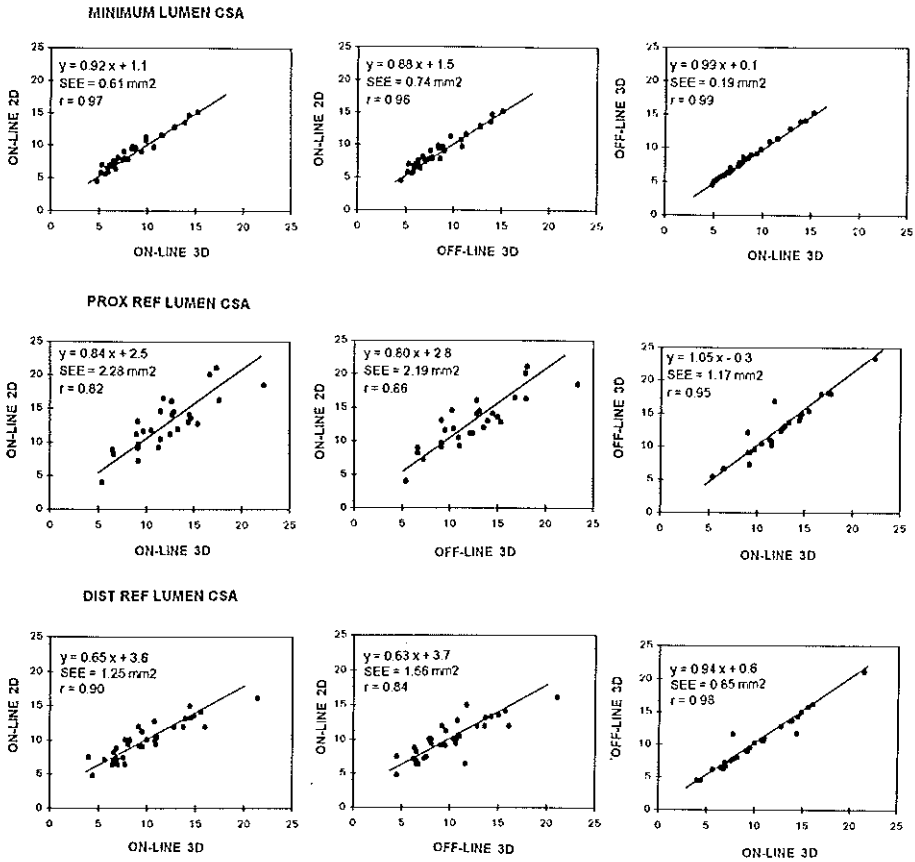

Figure 4. Results of linear regression analyses, comparing the lumen CSA measurements of the minimal stent (upper panels), proximal reference (PROX REF, center panels) and distal reference (DIST REF, lower panels), as obtained from on-line 2D and both on-line and off-line 3D IVUS analyses. Correlations were excellent, especially between on-line and off-line 3D IVUS measurements (the off-line 3D reanalysis represents the maximal confidence approach).

Results

Quantitative angiographic data. Before intervention, the minimal lumen diameter was 0.87 ± 0.42 mm, and the diameter stenosis 70.6 ± 13.7%. After stenting, a smooth angiographic lumen was achieved in all cases, with absence of inflow or outflow obstruction. The final minimal lumen diameter was 3.29 ± 0.41 mm with a corresponding diameter stenosis of 8.4 ± 3.4% (range 1% to 14%). According to the quantitative angiographic criteria, all stents were implanted successfully.

Feasibility of ECG-gated 3D IVUS image acquisition and analysis. After angiographically successful stent deployment, ECG-gated image acquisition was successfully performed in all patients with excellent tolerance. No subjective complaints of the patients were reported, and continuous ECG monitoring showed no evidence of ST segment alteration or increased frequency of arrhythmias during both gated and nongated IVUS imaging runs. The ECG-gated image acquisition required on average 4.6 ± 1.4 min (range 3.6 to 7.8), whereas the image acquisition during conventional continuous pullbacks required 1.7 ± 0.3 min (range 1.5 to 2.4, $p < 0.0001$). The on-line 3D analysis required 8.7 ± 0.6 min (range 7.3 to 10.0),

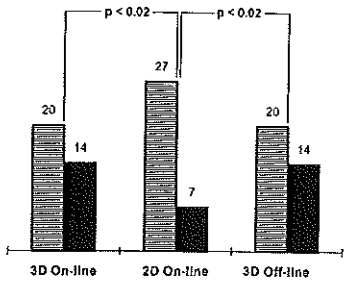

Figure 5. Detection of suboptimal stent deployment based on defined IVUS criteria. After angiography-guided stent implantation, off-line 3D analysis (providing the maximal confidence results) as well as on-line 3D analysis demonstrated that 14 stents (41%) failed to meet the IVUS criteria of optimal stent deployment, but only 7 (21%) of these stents were so classified by the on-line 2D analysis. **Striped** bars = IVUS criteria fulfilled; **solid bars** = IVUS criteria not fulfilled.

whereas reviewing the videotape and manually tracing the 2D IVUS images took 5.8 ± 0.7 min (range 4.8 to 7.4, $p < 0.001$).

IVUS measurements after stent deployment. The results of the different IVUS analyses are given in Table 1. There was a slight but significant overestimation of the minimal stent lumen CSA by the on-line 2D IVUS analysis when results were compared with those of both on-line and off-line 3D analyses ($p < 0.005$ and $p < 0.001$, respectively). The other variables measured (stent symmetry, proximal and distal reference lumen CSA) did not differ among analyses.

The between-method measurement variability, expressed as the standard deviation of the between-methods differences, was consistently higher for the on-line 2D measurement versus both the on-line and the off-line 3D measurements than for the two 3D measurements (Table 1). Nevertheless, the correlations among the CSA measurements obtained from the on-line 2D, on-line 3D and off-line 3D analyses were excellent (Fig. 4). Correlations of the stent symmetry measurements ranged from 0.62 (on-line 2D vs. 3D) to 0.98 (on-line 3D vs. off-line 3D).

IVUS criteria of optimal stent deployment. With the off-line 3D analysis (which provided the maximal confidence results), 14 (41%) of the 34 stents failed to meet the IVUS criteria of optimal stent deployment (Table 1). Only 7 of these stents were so classified by the on-line 2D analysis ($p < 0.02$), whereas all 14 stents were also identified by the on-line 3D analysis ($p < 0.02$ vs. on-line 2D analysis) (Fig. 5). Inadequate stent expansion was the constant reason for the failure to meet the deployment criteria ($n = 14$). There were no instances of incomplete stent apposition; the one case of stent asymmetry (which also had inadequate stent expansion) was revealed by both on-line 3D and off-line 3D analyses, but not by on-line 2D analysis.

Procedural outcome. After completion of the study protocol, any further treatment was left to the discretion of the operator. Additional angiography-guided balloon dilations were performed in six stents that had not met the criteria by both 2D and 3D IVUS ($n = 2$) or by 3D IVUS alone ($n = 4$). Lack of further stent expansion despite high pressure dilation with oversized balloons was the principal reason for omitting further balloon dilations. There were no procedural or post-procedural in-hospital complications.

Reproducibility of on-line 3D IVUS analysis. The intraobserver and interobserver differences of stent CSA measurements were 0.0 ± 0.2 mm^2 and 0.0 ± 0.3 mm^2 (relative SD 2.0% and 3.1%). The correlations were high (Fig. 6).

Discussion

IVUS insights into vessel and stent geometry (5–11) have played a central role in developing the concept of optimized stent deployment using adjunct high pressure balloon inflations (5,6,8,11,26). IVUS-guided stent implantation has reduced the incidence of stent thrombosis and permitted stenting without anticoagulation (5). These studies used planar IVUS analysis; however, changes of the stent dimensions observed during a transducer pullback are frequently smooth and gradual, and thus the minimal lumen area may be difficult to reliably identify visually. Automated 3D reconstruction and

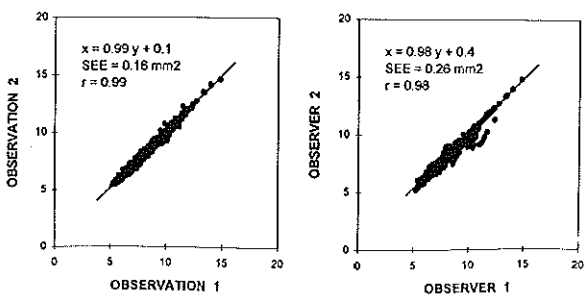

Figure 6. Intraobserver and interobserver measurement variability of on-line 3D IVUS. Correlation between the stent lumen CSA measurements (mm^2), provided by repeated analyses of the same observer (**left panel**, observations 1 and 2) and two independent observers (**right panel**, observers 1 and 2) using the 3D automated analysis method in ECG-gated IVUS image sets. Because actual on-line conditions cannot be reproduced, these data were obtained by using simulated on-line conditions, especially a maximal analysis time of 10 min.

analysis may therefore help to resolve this problem, but it must be both reliable and feasible during on-line application.

Previously, 3D reconstruction performed after stent implantation has been marred by cyclic image artifacts (18) (Fig. 1) that limited on-line application of automated 3D contour detection and analysis systems.

In the present study, to overcome this important limitation, we used ECG-gated IVUS image acquisition (23) and a validated automated 3D analysis system (18,19,27) on-line after angiography-guided stent deployment. The importance of ECG-gated image acquisition for off-line automated 3D IVUS measurements has been demonstrated by other groups (16,21) using alternative 3D contour detection systems. Sonka and colleagues (16) have stated that the correlation between observer-defined and automated lumen contours by their system improved as a result of ECG gating ($r = 0.91$ and 0.98 for nongated and ECG-gated, respectively) (16). We found that ECG-gated image acquisition resulted in much smoother vessel boundaries, readily facilitating the on-line contour detection process.

The main results of this study were that ECG-gated IVUS image acquisition and automated on-line 3D analysis 1) were feasible to evaluate the procedural results after stent deployment, 2) provided reliable and reproducible measurements of the lumen dimensions within the stented segment, and 3) facilitated the detection of the minimal lumen site. Despite the high correlation of the minimal lumen area measurements provided by the on-line 2D and 3D analyses, there was a significant overestimation of minimal lumen area with use of the 2D approach; this was confirmed by the off-line measurement. As a result, there were significant differences between the on-line 2D and 3D analyses in judging the adequacy of stent deployment by using the defined IVUS criteria. The high reliability of the on-line 3D approach in scrutinizing such criteria was confirmed by the off-line measurement. The on-line 3D analysis time (8.7 ± 0.6 min) of the present study is acceptably within the 10-min range set by the board of the Thoraxcenter senior interventional cardiologists. Nevertheless, in parallel with the advances in computer technology and further refinements in the software, further reduction of the analysis time can be expected.

Clinical implications. Although good clinical and angiographic results have been reported for coronary stenting without the use of IVUS (28,29), previous studies using conventional IVUS techniques (5,6,11) have suggested a considerable frequency of suboptimal results, a finding that is again confirmed by our methodology. We also found that conventional 2D IVUS itself underestimated the frequency of suboptimal stenting.

Numerous interventional cardiologists have praised IVUS as helpful in guiding (difficult) stent procedures and in investigating ambiguous angiographic results, but there is no blanket recommendation concerning the use of IVUS in routine stenting (26). However, the indication for stenting is currently broadening to smaller vessels, longer lesions, unfavorable morphology, multivessel disease and unstable syndromes, and the number of different types of stents available is increasing rapidly (30). Considering this increasing complexity of stenting procedures, a feasible and reliable IVUS analysis approach will remain at least extremely valuable, often necessary, and perhaps cost-effective, depending on long-term clinical results; this aspect will undoubtedly be an objective of future trials evaluating the usefulness of IVUS guidance in complex coronary stenting.

Study limitations. Nonuniform transducer rotation of mechanical IVUS catheters, noncoaxial catheter position or vascular curvatures may create image distortion and artifacts in both planar images and 3D reconstructions (17); however, segments are generally relatively straight after stenting. Although coronary angiography itself has several limitations, combined approaches using both angiographic and IVUS data for 3D reconstruction of the vessel may resolve many of the problems mentioned, but these techniques are laborious and still restricted to research (22). As 3D reconstructions of IVUS images generally do not depict the true spatial coronary geometry, careful interpretation by an experienced investigator is required.

Our experience suggests that ECG-gated image acquisition is feasible in 90% to 95% of patients referred for coronary intervention, but it may be difficult in patients with arrhythmias and even impossible in the presence of atrial fibrillation, unless cardiac pacing is performed. ECG-gated image acquisition (23) requires more time than conventional motorized pullbacks at a uniform speed; this longer duration may limit its use before interventions in patients with critical coronary stenoses. Further miniaturization of the IVUS catheters and the use of imaging wires (31,32) may soon help to overcome this limitation.

Conclusions. ECG-gated acquisition of IVUS images during automated transducer pullbacks is feasible after coronary stent deployment. The approach is clinically relevant, as it permits on-line automated 3D reconstruction and analysis, provides reliable and reproducible measurements of lumen dimensions and facilitates the detection of the minimal lumen area, thus guiding optimized stent deployment.

References

1. Fitzgerald PJ, St. Goar FG, Connolly AJ, et al. Intravascular ultrasound imaging of coronary arteries: is three layers the norm? Circulation 1992;86: 154–8.
2. Mintz GS, Painter JA, Pichard AD, et al. Atherosclerosis in angiographically "normal" coronary artery reference segments: an intravascular ultrasound study with clinical correlations. J Am Coll Cardiol 1995;25:1479–85.
3. Erbel R, Ge J, Bockisch A, et al. Value of intracoronary ultrasound and Doppler in the differentiation of angiographically normal coronary arteries: a prospective study in patients with angina pectoris. Eur Heart J 1996;17: 880–9.
4. Pinto FJ, St. Goar FG, Gao SZ, al. Immediate and one-year safety of intracoronary ultrasound imaging: evaluation with serial quantitative angiography. Circulation 1993;88:1709–14.
5. Colombo A, Hall P, Nakamura S, et al. Intravascular stenting without anticoagulation accomplished with intravascular ultrasound guidance. Circulation 1995;91:1676–88.
6. Goldberg SL, Colombo A, Nakamura S, Almagor Y, Maiello L, Tobis JM.

Benefit of intracoronary ultrasound in the deployment of Palmaz-Schatz stents. J Am Coll Cardiol 1994;24:996–1003.
7. Mudra H, Klauss V, Blasini R, et al. Ultrasound guidance of Palmaz-Schatz intracoronary stenting with a combined intravascular ultrasound balloon catheter. Circulation 1994;90:1252–61.
8. Görge G, Haude M, Ge J, et al. Intravascular ultrasound after low and high inflation pressure coronary artery stent implantation. J Am Coll Cardiol 1995;26:725–30.
9. Dussaillant GR, Mintz GS, Pichard AD, et al. Small stent size and intimal hyperplasia contribute to restenosis: a volumetric intravascular ultrasound analysis. J Am Coll Cardiol 1995;26:720–4.
10. von Birgelen C, Kutryk MJB, Gil R, et al. Quantification of the minimal luminal cross-sectional area after coronary stenting by two- and three-dimensional intravascular ultrasound versus edge detection and videodensitometry. Am J Cardiol 1996;78:520–5.
11. von Birgelen C, Gil R, Ruygrok P, et al. Optimized expansion of the Wallstent compared with the Palmaz-Schatz stent: online observations with two- and three-dimensional intracoronary ultrasound after angiographic guidance. Am Heart J 1996;131:1067–75.
12. Rosenfield K, Losordo DW, Ramaswamy K, et al. Three-dimensional reconstruction of human coronary and peripheral arteries from images recorded during two-dimensional intravascular ultrasound examination. Circulation 1991;84:1938–56.
13. Coy KM, Park JC, Fishbein MC, et al. In vitro validation of three-dimensional intravascular ultrasound for the evaluation of arterial injury after balloon angioplasty. J Am Coll Cardiol 1992;20:692–700.
14. Mintz GS, Pichard AD, Satler LF, Popma JJ, Kent KM, Leon MB. Three-dimensional intravascular ultrasonography: reconstruction of endovascular stents in vitro and in vivo. Clin Ultrasound 1993;21:609–15.
15. Matar FA, Mintz GS, Douek P, et al. Coronary artery lumen volume measurement using three-dimensional intravascular ultrasound: validation of a new technique. Cathet Cardiovasc Diagn 1994;33:214–20.
16. Sonka M, Liang W, Zhang X, De Jong S, Collins SM, McKay CR. Three-dimensional automated segmentation of coronary wall and plaque from intravascular ultrasound pullback sequences. In: Computers in Cardiology 1995. Los Alamitos (CA): IEEE Computer Society, 1995:637–40.
17. Roelandt JRTC, Di Mario C, Pandian NG, et al. Three-dimensional reconstruction of intracoronary ultrasound images: rationale, approaches, problems, and directions. Circulation 1994;90:1044–55.
18. von Birgelen C, Di Mario C, Li W, et al. Morphometric analysis in three-dimensional intracoronary ultrasound: an in-vitro and in-vivo study using a novel system for the contour detection of lumen and plaque. Am Heart J 1996;132:516–27.
19. von Birgelen C, van der Lugt A, Nicosia A, et al. Computerized assessment of coronary lumen and atherosclerotic plaque dimensions in three-dimensional intravascular ultrasound correlated with histomorphometry. Am J Cardiol 1996;78:1202–9.
20. Gil R, von Birgelen C, Prati F, Di Mario C, Ligthart J, Serruys PW. Usefulness of three-dimensional reconstruction for interpretation and quantitative analysis of intracoronary ultrasound during stent deployment. Am J Cardiol 1996;77:761–4.
21. Dhawale PJ, Wilson DL, Hodgson J McB. Optimal data acquisition for volumetric intracoronary ultrasound. Cathet Cardiovasc Diagn 1994;32:288–99.
22. von Birgelen C, Slager CJ, Di Mario C, de Feyter PJ, Serruys PW. Volumetric intracoronary ultrasound: a new maximum-confidence approach for the quantitative assessment of progression-regression of atherosclerosis? Atherosclerosis 1996;118 Suppl:S103–13.
23. Bruining N, von Birgelen C, Di Mario C, et al. Dynamic three-dimensional reconstruction of ICUS images based on an ECG-gated pull-back device. In: Computers in Cardiology 1995. Los Alamitos (CA): IEEE Computer Society, 1995:633–6.
24. Hodgson J McB, Graham SP, Savakus AD, et al. Clinical percutaneous imaging of coronary anatomy using an over-the-wire ultrasound catheter system. Int J Cardiac Imaging 1989;4:186–93.
25. Bland JM, Altman DG. Statistical methods for assessing agreement between two methods of clinical measurement. Lancet 1986;2:307–10.
26. Tobis JM, Colombo A. Do you need IVUS guidance for coronary stent deployment? Cathet Cardiovasc Diagn 1996;37:360–1.
27. Li W, von Birgelen C, Di Mario C, et al. Semi-automatic contour detection for volumetric quantification of intracoronary ultrasound. In: Computers in Cardiology 1994. Los Alamitos (CA): IEEE Computer Society, 1994:277–80.
28. Serruys PW, de Jaegere P, Kiemeneij F, et al., for the Benestent Study Group. A comparison of balloon expandable stent implantation with balloon angioplasty in patients with coronary artery disease. N Engl J Med 1994;331:489–95.
29. Fishman DL, Leon MB, Baim DS, et al., for the Stent REStenosis Study (STRESS) Investigators. A randomized comparison of coronary stent placement and balloon angioplasty in the treatment of coronary artery disease. N Engl J Med 1994;331:496–501.
30. Serruys PW, Kutryk MJB. The state of the stent: current practices, controversies, and future trends. Am J Cardiol 1996;78(Suppl 3A):4–7.
31. Di Mario C, Fitzgerald PJ, Colombo A. New developments in intracoronary ultrasound. In: Reiber JHC, van der Wall EE, editors. Cardiovascular Imaging. Dordrecht, The Netherlands: Kluwer Academic, 1996;257–75.
32. von Birgelen C, Mintz GS, de Feyter PJ, et al. Reconstruction and quantification with three-dimensional intracoronary ultrasound: an update on techniques, challenges, and future directions. Eur Heart J 1997;18:1056–67.

CHAPTER 11a

Summary, discussion and conclusions

SUMMARY, DISCUSSION AND CONCLUSIONS

Part I: Three-dimensional reconstruction of the heart and the coronary vessels

Echocardiography has become a commonly used diagnostic modality in the daily practice of cardiology. In this thesis, three-dimensional (3-D) echocardiography of the heart and coronary arteries for imaging and application of quantitative analysis is described. To produce a 3-D reconstruction of any object, a tomographic data set must be acquired. Because of a lack of the method allowing acquisition of tomographic data set of a single heartbeat, a series of 2-D acquired images must be compiled to build up the 3-D data set. Due to heart motion and respiration, the image acquisition must be ECG-triggered, gated and respiratory gated. A system capable of performing acquisition and producing dynamic 3-D volume rendered reconstructions of the heart is described in chapter 2. For such a system to be utilized by practicing cardiologists the provision of additional information over 2-D imaging must be demonstrated. 3-D echocardiography provides computed echocardiographic views unobtainable by other techniques. The assessment of volumes of the left and right ventricles without the need to make geometric assumptions, as is necessary with 2-D imaging is a technique which has been validated by comparison with MRI[1, 2]. 3-D reconstruction is a computative intensive task, for which fast and specialized graphics hardware and large amounts of internal memory and hard disk storage space are necessary. These systems remain expensive but are becoming cheaper. Since the introduction of the 3-D acquisition and reconstruction soft- and hardware (Echoscan system, TomTec GmbH, Munich, Germany, 1993), the calculation times for 3-D reconstructions have been reduced from a half-hour to less than a minute. On newer hard- and software platforms, even multi-processing has become possible (Figure 1). Future software packages will provide specialized programs to calculate valve ste-

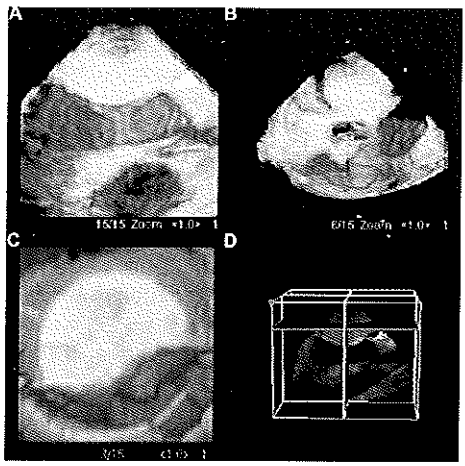

Figure 1
Here an overview of the new 3-D software of TomTec is presented (running on a multi-processing Windows NT™ platform). In panel A-C, 3-D reconstructions can be simultaneously generated. In panel D, the acquired tomographic dataset with different cut-planes is given. In this case a patient with a myxoma in the left atrium is presented. In panel D, a 2-D cut-plane trough the tomographic dataset can be appreciated, in all other panels (A-C) 3-D reconstructions from the same patient are generated.



Figure 2
Here a Hewlett-Packard Sonos 5500-ultrasound scanner is presented. This scanner can be equipped with an optional 3-D package. This makes it possible to acquire a tomographic dataset without the need for an extra acquisition station, and furthermore the image data can be electronically transferred preserving possible loss of image quality or introduction of image artifacts.

noses and septal defect sizes with improved user friendliness, significantly less off-line analysis time and increased accuracy. Data acquisition improvements have also been made. The functionality of the separate acquisition and reconstruction stations (Echoscan) is now integrated as an optional 3-D package in Hewlett-Packard ultrasound scanners Sonos 2500 and 5500 (Figure 2; Hewlett-Packard, Andover, MA, USA). In addition to the improved user friendliness of a single user solitary console, less space is occupied in the echolab, operating theatre or bedside. The advent of digital data transfer has improved the quality of imaging, as the previous technique of video grabbing was prone to image artifacts (all chapters). Hewlett-Packard has also introduced a transthoracic probe (Figure 3), which is able to rotate its imaging array with an integrated micro-motor, instead of the previous method of rotation of the complete probe (chapter 2). This probe is much smaller and lighter and reduces significantly the chance of motion of the observer's hand during acquisition, which may create images/artifacts in the 3-D reconstruction.

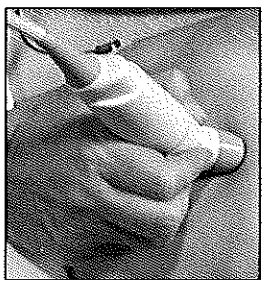

Figure 3
In this image a Hewlett-Packard transthoracic phased array probe with integrated stepping motor can be appreciated. This probe makes it easier to perform a transthoracic 3-D acquisition since the other method, a device rotating the complete probe, uses a larger and heavier device, which can introduce motion of the observer's hand during an

Chapter 3, 4 and 5 describe different aspects of 3-D reconstruction of intracoronary ultrasound (ICUS) images. In chapter 3 the technique of acquiring ECG-triggered and gated tomographic ICUS image data sets together with the exploration of 3-D longitudinal reconstructions is described. Chapter 4 describes an in-vivo study investigating whether implanted intracoronary stent structures can be identified on 3-D reconstructed images and if the stent design influences 3-D reconstruction. We found that stents designed with a predominantly longitudinal strut architecture were able to be reconstructed better than stents with a predominantly transverse strut architecture. In chapter 5 an in-vitro ultrasound examination of 26 intracoronary stents and their 3-D reconstruction is described. The findings of chapter 4 could also be confirmed in a larger group comprising different stent designs in an in-vitro set-up. While the clinical usefulness of the techniques described in chapter 3,4 and 5 seem limited, the ECG-triggered gated ICUS image acquisition provides the ability to produce dynamic reconstructions, and the described techniques results in a smooth appearance of the vessel wall with tiny details visible, evidenced by the recognition of stent struts. The combination of angiography with a pullback ICUS catheter 3-D reconstruction may have clinical application in the future[3-5]. These techniques are able to produce 3-D reconstructions with the true vessel curvature (geometry) preserved and can therefore be used to calculate parameters such as shear stress[4]. The 3-D true curvature technique currently under investigation at the Thoraxcenter employs the described acquisition technique.

The sequence of chapters, whilst alternating between echocardiography of the heart and ICUS, highlights the progressive improvements in 3-D technology. Chapter 6 describes the potential of Virtual Reality (VR) techniques and interactive computer systems for teaching and training in cardiology. 3-D reconstructions makes image interpretation on the one hand easier through being anatomically more realistic, but on the other hand more complex. A viewer can become "lost in space" through having the ability to examine a 3-D data set from an infinite number of viewing positions. Virtual Heart models, coupled to real-time echo images reproducing pathological states, could help to guide the cardiologist through the tomographic

image data sets ("roadmapping"). Furthermore, since most imaging modalities have as an end product a digital format, the patient data can be saved in computer databases (Figure 4). Sample databases with various pathologies could thus be created for teaching and training purposes. This, together with "dummy" equipment could herald a revolution for training and teaching echocardiography.

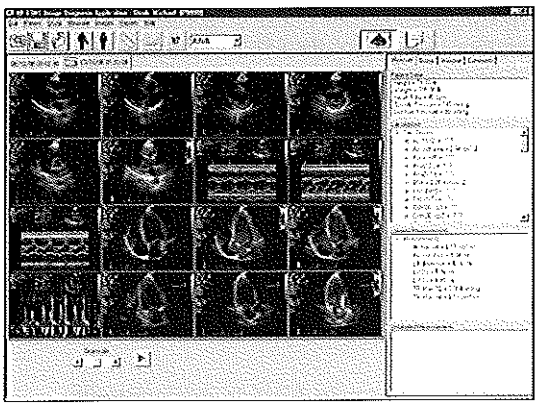

Figure 4
This image shows an example screen of an electronic image database (Enconcert, Hewlett-Packard). Echolab's are now slowly transferring from analog storage of the examinations (videotape), to electronic storage (computer databases). This makes it easier to share the examination results amongst other hospital departments (surgeon's, CCU, outpatient clinic) and to preserve patient data. Furthermore, it makes it easier to produce sample databases incorporating rare pathologies for teaching and training purposes.

Part II: Quantitative analysis of coronary vessel dimensions

The second part of this thesis is focused on the quantitative analysis of coronary vessel dimensions, based on the acquisition technique described in chapters 3-5. In chapter 7 the uniting of two separately developed techniques is described. The ECG-gated pullback device and the 3-D acquisition station (designed for echocardiography of the "whole" heart), was used with a quantitative analysis software package for vessels (designed for analysis of off-line video tape digitized from ICUS catheter pullbacks with a continuous speed of 1 or 0.5mm/s). This formed the basis for measuring vessel dimension changes over the cardiac cycle, with the ability to correct for longitudinal catheter motion which appeared to be present in >90% of the investigated patients. The ICUS catheter moves from distal (end-diastole, peak of the R-wave) to proximal (end-systole) during the heart cycle. If an operator is analyzing vessel dimensions on the ICUS console 2-D images, the catheter motion could influence the results and produce unexpected results, in particular smaller dimensions in diastole and larger dimensions in systole. An ECG-triggered and gated pullback examination can be used to avoid artifacts caused by catheter motion. In chapter 8, a study comparing ECG-gated versus non-gated 3-D intracoronary ultrasound analysis and the implication for volumetric measurements is reported. It appeared that when ICUS images were acquired ECG-gated, the volumetric measurements were significantly smaller than when they were acquired non-gated, but the studied patient population was rather small. Further study of this method is therefore desirable, since many studies incorporating ICUS examinations are performed with non-gated ICUS pullbacks. The drawback of extra equipment costs could be overcome if the ultrasound manufacturers incorporated this technology into their ultrasound scanners, a policy, such as found in the current commercially available Hewlett-Packard echocardiogram machines. The major clinical disadvantage of the ECG-gated method is the longer pullback time needed for a study. This is three times longer than the 0.5 mm/s continuous pullback study, and takes approximately 1 min/cm artery. Currently, the longitudinal step intervals of 0.2mm are applied based on theoretical assumptions with

regard to ICUS catheter resolution. It would be desirable to perform a study to determine which axial step resolution could be used as a practical lower limit. This could result in larger axial steps being found adequate and thus reduced acquisition times.

In chapter 9, the reproducibility and the inter- and intra-observer variability of the ECG-gated ICUS measurements is described. The smooth appearance of the coronary vessel wall in the longitudinal computed sections not only produces a more angiogram-like result, but also results in significantly faster analysis times. This is mainly due to the fact that the software does not have to jump from a small lumen and total vessel contours in image *x*, to a relatively much larger area in image *x+1* (and vice-versa). The catheter motion, earlier described, results in the so-called saw-tooth appearance of the vessel wall. The "hit-ratio" for correct contours is higher in ECG-gated ICUS image data sets, and less operator corrections of the contours are necessary. This is not only of particular interest for core laboratories but also for on-line use in the cathlab. Chapter 10 describes the use of on-line automated analysis of three-dimensional ICUS after coronary stent deployment. The study showed that application of the technique is feasible and that the results are reliable and reproducible, facilitating detection of the minimal lumen site. The setup of the necessary equipment is laborious, and the need for the ICUS scanner and three-dimensional acquisition and analysis station, can be a burden when the space in the cathlab is limited.

Future developments

Three-dimensional echocardiography has been commercially available for 5 years. It has been subject to many research objectives but is still mainly a research tool[1, 2, 6-16]. Rapid developments in the computer technology and in other areas, such as the military and film industries, are bringing new opportunities for further developments in this area. Cardiac 3-D ultrasound is maybe the most challenging area in imaging medicine, since the heart is a dynamic organ. The developments of Virtual Reality (VR) techniques are opening a whole new range of possibilities for medical application, teaching and training. The VR models which now are used in off-line workstations, may come to be incorporated in ultrasound scanners and could help to guide the cardiologists on-line in diagnostic and therapeutic manouvres.

Three-dimensional ICUS is also principally subject to research only. It has however shown great potential in the evaluation of new interventional techniques such as intracoronary stenting[17-19], in determining plaque progression/regression in drug studies or after coronary brachytheraphy[20, 21], and also for calculating radiodensitometry. The new higher frequency catheters (40 MHz, CVIS and 45 MHz, HP) are showing improved imaging capabilities and are offering better imaging resolutions, which could improve 3-D reconstructions of coronary vessels[22] (Figure 5). The new generation of ICUS ultrasound scanners will also offer digital image data transfer and storage capabilities. Workstations capable of performing quantitative coronary angiography (QCA) and quantitative ICUS analysis are under development, combining information of lumen morphology obtained by QCA with information of the whole vessel wall from ICUS. Improved analysis software and 3-D reconstructions combining angio-

graphy and ICUS producing reconstructions with true curvature reproduction could help the interventionalist and diagnostic cardiologist to make even better judgments as to which interventional technique is best for a particular patient.

3-D ICUS appears to have exciting potential for the betterment of diagnostic and therapeutic care of the patient with coronary artery disease.

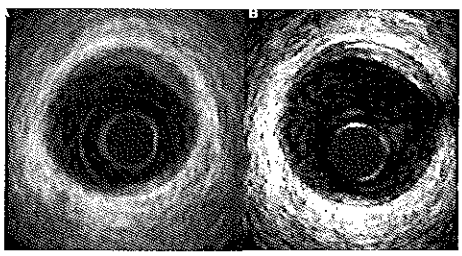

Figure 5
In panel A, an in-vivo image of a 30 MHz ultrasound catheter is presented. In panel B, at almost the same in-vivo site an image of a 40 MHz ultrasound catheter is presented. It can be appreciated that the image in panel B looks sharper. The media behind the plaque is very well defined in panel B.

References

1. Nosir YF, Fioretti PM, Vletter WB, Boersma E, Salustri A, Postma JT, Reijs AE, Ten Cate FJ, Roelandt JR. Accurate measurement of left ventricular ejection fraction by three- dimensional echocardiography. A comparison with radionuclide angiography. Circulation 1996; 94:460-6.

2. Altmann K, Shen Z, Boxt LM, King DL, Gersony WM, Allan LD, Apfel HD. Comparison of three-dimensional echocardiographic assessment of volume, mass, and function in children with functionally single left ventricles with twodimensional echocardiography and magnetic resonance imaging. Am J Cardiol 1997; 80:1060-5.

3. Evans JL, Ng KH, Wiet SG, Vonesh MJ, Bums WB, Radvany MG, Kane BJ, Davidson CJ, Roth SI, Kramer BL, Meyers SN, McPherson DD. Accurate threedimensional reconstruction of intravascular ultrasound data. Spatially correct three-dimensional reconstructions. Circulation 1996; 93:567-76.

4. Slager CJ, Wentzel JJ, Oomen JA, Schuurbiers JC, Krams R, von Birgelen C, Tjon A, Serruys PW, de Feyter PJ. True reconstruction of vessel geometry from combined X-ray angiographic and intracoronary ultrasound data. Semin Interv Cardiol 1997; 2:43-7.

5. Wiet SP, Vonesh MJ, Waligora MJ, Kane BJ, McPherson DD. The effect of vascular curvature on three-dimensional reconstruction of intravascular ultrasound images. Ann Biomed Eng 1996; 24:695-701.

6. Chen Q, Nosir YF, Vletter WB, Kint PP, Salustri A, Roelandt JR. Accurate assessment of mitral valve area in patients with mitral stenosis by threedimensional echocardiography. J Am Soc Echocardiogr 1997; 10:133-40.

7. Dall'Agata A, Taams MA, Fioretti PM, Roelandt JR, Van Herwerden LA. Cosgrove-Edwards mitral ring dynamics measured with transesophageal threedimensional echocardiography. Ann Thorac Surg 1998; 65:485-90.

8. King DL, Harrison MR, King DL, Jr., Gopal AS, Martin RP, DeMaria AN. Improved reproducibility of left atrial and left ventricular measurements by guided three-dimensional echocardiography. J Am Coll Cardiol 1992; 20:1238

9. King DL, Gopal AS, King DL, Jr., Shao MY. Three-dimensional echocardiography: in vitro validation for quantitative measurement of total and "infarct" surface area. J Am Soc Echocardiogr 1993; 6:69-76.

10. King DL, Gopal AS, Keller AM, Sapin PM, Schroder KM. Three-dimensional echocardiography. Advances for measurement of ventricular volume and mass. Hypertension 1994; 23:I172-9.

11. Kupferwasser I, Mohr-Kahaly S, Menzel T, Spiecker M, Dohmen G, Mayer E, Oelert H, Erbel R, Meyer J. Quantification of mitral valve stenosis by threedlmensional transesophageal echocardiography. Int J Card Imaging 1996; 12:241

12. Roelandt JR. Three-dimensional echocardiography: new views from old windows [editorial]. Br Heart J 1995; 74:4-6.

13. Salustri A, Spitaels S, McGhie J, Vletter W, Roelandt JR. Transthoracic threedimensional echocardiography in adult patients with congenital heart disease. J Am Coll Cardiol 1995; 26:759-67.

14. Salustri A, Becker AE, van Herwerden L, Vletter WB, Ten Cate FJ, Roelandt JR. Three-dimensional echocardiography of normal and pathologic mitral valve: a comparison with two-dimensional transesophageal echocardiography. J Am Coll Cardiol 1996; 27:1502-10.

15. Salustri A, Kofflard MJ, Roelandt JR, Nosir Y, Trocino G, Keane D, Vletter WB, Cate FJ. Assessment of left ventricular outflow in hypertrophic cardiomyopathy using anyplane and paraplane analysis of three-dimensional echocardiography. Am J Cardiol 1996; 78:462-8.

16. Sklansky MS, Nelson TR, Pretorius DH. Usefulness of gated three-dimensional fetal echocardiography to reconstruct and display structures not visualized with two-dimensional imaging. Am J Cardiol 1997; 80:665-8.

17. Prati F, Di Mario C, Gil R, von Birgelen C, Camenzind E, Montauban van Swijndregt WJ, de Feyter PJ, Serruys PW, Roelandt JR. Usefulness of on-line three-dimensional reconstruction of intracoronary ultrasound for guidance of stent deployment. Am J Cardiol 1996; 77:455-61.

18. Nakamura S, Colombo A, Gaglione A, Almagor Y, Goldberg SL, Maiello L, Finci L, Tobis JM. Intracoronary ultrasound observations during stent implantation. Circulation 1994; 89:2026-34.

19. Goldberg SL, Colombo A, Nakamura S, Almagor Y, Maiello L, Tobis JM. Benefit of intracoronary ultrasound in the deployment of Palmaz-Schatz stents. J Am Coll Cardiol 1994; 24:996-1003.

20. Wiedermann JG, Leavy JA, Amols H, Schwartz A, Homma S, Marboe C, Weinberger J. Effects of high-dose intracoronary irradiation on vasomotor function and smooth muscle histopathology. Am J Physiol 1994; 267:H125-32.

21. Williams DO. Radiation vascular therapy: a novel approach to preventing restenosis. Am J Cardiol 1998; 81:18E-20E.

22. Foster FS, Knapik DA, Machado JC, Ryan LK, Nissen SE. High-frequency intracoronary ultrasound imaging. Semin Interv Cardiol 1997; 2:33-41.

Samenvatting, discussie en conclusies

SAMENVATTING, DISCUSSIE EN CONCLUSIES

Deel I: Drie-dimensionele reconstructie van het hart en de kransslagvaten

In cardiologie is echografie één van de meest gebruikte diagnostische hulpmiddelen. In dit proefschrift wordt drie-dimensionale (3-D) echocardiografie van het hart en de kransslagvaten voor beeldvorming en quantitatieve analyses (metingen) beschreven. Om een 3-D reconstructie van een "object" te kunnen maken, moet een zg. tomografische data set, een serie van 2-D beelden, verkregen worden. Door het gebrek aan een techniek, hedentendage, om zo'n tomografische data set van het hart binnen één hartslag te verkrijgen (acquisitie), moet een serie van 2-D beelden, verkregen gedurende verschillende hartslagen, bij elkaar gevoegd worden om een 3-D data set op te bouwen. Door het bewegen van het hart en de ademhaling van de patiënt, moet het digitaliseren van de 2-D echobeelden worden gesynchroniseerd met de hartslag en de ademhaling. Een systeem dat deze mogelijkheden biedt en in staat is om 3-D volume gerenderde (renderen is het zichtbaar maken van een 3-D beeld op een 2-D scherm) reconstructies van het hart te maken wordt beschreven in hoofdstuk 2 (Echoscan system, TomTec GmbH, München, Duitsland, 1993). Voor zo'n systeem gebruikt wordt door een praktiserende cardioloog, moet aangetoond worden dat het extra voordelen biedt boven het gebruik van de hun welbekende 2-D echobeelden. 3-D echocardiografie biedt de mogelijkheid om 2-D echocardiografische beelden te reconstrueren, m.b.v. de computer, vanuit perspectieven die niet mogelijk zijn met de normale 2-D echocardiografie te realiseren. Één van de meest klinische toepassingen van de 3-D techniek is het berekenen van de volumina van de linker- en rechterventrikel (kamer) zonder de noodzaak van geometrische aannames, zoals noodzakelijk is met 2-D technieken. Deze nieuwe techniek werd gevalideerd door het te vergelijken met MRI-beelden[1,2]. Het berekenen van 3-D reconstruc-

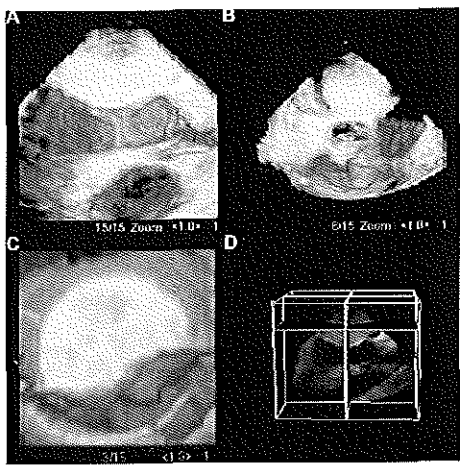

Figuur 1
Hier is een voorbeeld van de nieuwe 3-D software van TomTec afgebeeld, dit kan worden gebruikt op een multi-processor Windows NT™ platform. De panelen A-C, presenteren 3-D reconstructies die i.t.t. vroeger simultaan kunnen worden berekend. In paneel D is te zien hoe de snijlijnen door de tomografische data set gaan en die in de andere panelen zichtbaar gemaakt zijn. De 2-D afbeelding in D is als 3-D, in A, gereconstrueerd. In dit geval betreft het een tumor die zich bevindt in de linkerhartboezem van een patiënt.



Figuur 2
Hier is een Hewlett-Packard Sonos 5500 echo-apparaat gepresenteerd. Dit echo-apparaat kan worden uitgebreid met een optioneel 3-D pakket. Dit maakt het mogelijk om een tomografische data set met één enkel apparaat te verkrijgen, verder kan de data nu geheel digitaal worden verwerkt zonder dat er een analoge conversie slag behoeft plaats te vinden, met evetueel verlies van kwaliteit.

ties maakt het gebruik van krachtige computers, die gespecialiseerd zijn in grafische processen en die beschikken over veel geheugen, noodzakelijk. Deze systemen zijn duur, maar worden op termijn goedkoper. Sinds de introductie van het 3-D werkstation, Echoscan, is de tijd benodigd voor het berekenen van een 3-D reconstructie gedaald van een half uur tot minder dan een minuut. Op nieuwe hard- en software platforms is zelfs het gebruik van meerdere-processoren (parallel processing) mogelijk geworden (Figuur 1). Toekomstige software pakketten voor 3-D echocardiografische beelden zullen de mogelijkheid bieden om gespecialiseerde functies uit te voeren zoals het berekenen van klep vernauwingen en de grootte van gaten in het septum (VSD's en/of ASD's) met verbeterde gebruikersvriendelijkheid, gereduceerde analyse tijden en met verbeterde nauwkeurigheden. Verbeteringen voor het verkrijgen van 3-D echocardiografische beelden zijn reeds gerealiseerd. De functionaliteit van het acquisitie gedeelte van het 3-D werkstation is nu geïntegreerd als een optioneel uitbreidingspakket in de echocardiografische apparatuur van Hewlett-Packard (Sonos 2500 en 5500, Figuur 2; Hewlett-Packard, Andover, MA, USA). Buiten de zo verkregen gebruikersvriendelijkheid om alles binnen één enkel apparaat te hebben (in dit geval het acquisitie gedeelte), is het prettig om minder schaarse ruimte te bezetten in het echolab, operatiekamer of patiëntenkamer. Verder is het nu mogelijk om de beelden geheel digitaal te verwerken. Het 3-D werkstation gebruikt een techniek die de analoge video-beelden van de echocardiografische apparatuur digitaliseert. Deze extra omzetting kan leiden tot fouten in de beelden (alle hoofdstukken). Hewlett-Packard heeft ook een transthoracale probe geïntroduceerd (Figuur 3), welke in staat is door m.b.v. een geïntegreerde micro-motor het beeldvormende segment te roteren, dit i.p.v. het roteren van de gehele probe (hoofdstuk 2). Deze nieuwe probe is veel handzamer en lichter van gewicht, wat de kans op bewegen tijdens een acquisitie reduceert, en welke de kwaliteit van de 3-D reconstructies ten goede zou kunnen komen.

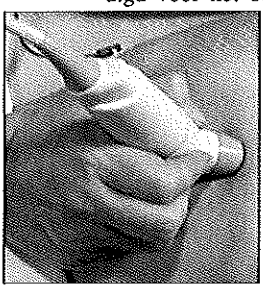

Figuur 3
Hier is een thransthoracele probe, Hewlett-Packard, gepresenteerd. Deze probe, met ingebouwde micro-stappenmotor, is in staat om het beeldvormende element te draaien. Voorheen was het alléén mogelijk om de gehele probe te draaien (hoofdstuk 2) waarvoor een groot apparaat om de probe moest worden geplaatst. Deze kleine probe is handzamer en lichter wat de kans op bewegen tijdens een studie verkleint.

In hoofdstuk 3, 4 en 5 worden verschillende aspecten van 3-D reconstructies met intravasculaire ultrageluidbeelden (ICUS) beschreven. In hoofdstuk 3 wordt de techniek van het verkrijgen van ECG-gesynchroniseerde acquisitie van tomografische ICUS beelden en het produceren van 3-D lengte-doorsneden van de kransslagvaten (coronairen) beschreven. Hoofdstuk 4 beschrijft een in-vivo studie betreffende het produceren van 3-D reconstructies op basis van ICUS beelden, verkregen van geïmplanteerde intracoronaire stents. Hierbij werd tevens onderzocht of de stent architectuur van invloed kon zijn op de 3-D reconstructies en of de architectuur in een 3-D reconstructie kon worden herkend. De bevindingen waren dat stents met draden (struts) die voornamelijk in de lengte richting liepen wel gereconstrueerd konden worden, terwijl stents met draden die voornamelijk in de dwars richting liepen (cirkelvormig) niet zodanig konden worden gereconstrueerd dat de stent kon worden herkend. In hoofdstuk 5 is een in-vitro (in een bak met water) ICUS onderzoek van 26 coronaire stents in combinatie met 3-D reconstructies beschreven. De bevindingen van hoofdstuk 4 konden ook in deze grotere groep, met vele verschillende stent architecturen, worden bevestigd. De klinische applicaties van de technieken beschreven in de

hoofdstukken 3, 4 en 5 lijken gelimiteerd, de ECG-gesynchroniseerde acquisitie van ICUS beelden maakt het echter mogelijk om dynamische 3-D reconstructies van de kransslagvaten te produceren. Het grote voordeel van deze techniek is dat het lumen van het kransslagvat gerepresenteerd wordt zonder artefacten (met een glad oppervlak, i.p.v. met ribbels) waarin zelfs kleine details zoals de draden van een

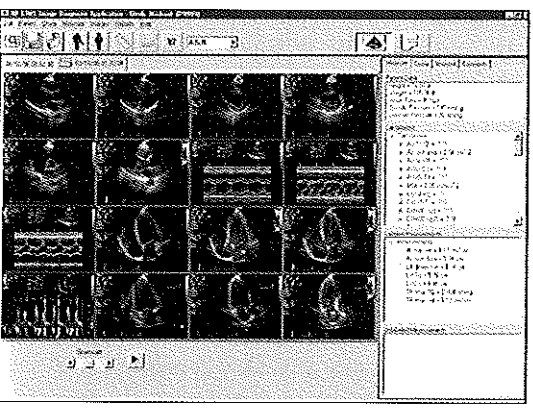

Figuur 4
Dit plaatje laat een voorbeeldscherm zien van een electronische beelden database (Enconcert, Hewlett-Packard). Moderne echo-laboratoria zijn momenteel voorzichtig bezig om over te schakelen van beeldopslag op videobanden naar een electronische beeldopslag. Dit maakt het verspreiden van de informatie, via ziekenhuis netwerken, tussen verschillende departementen (chirurgie, patiënten afdelingen, polikliniek) eenvoudiger en sneller. Het maakt het ook mogelijk om databases aan te leggen van bijzondere afwijkingen voor onderwijs en training.

stent zichtbaar kunnen zijn. De 3-D reconstructies van kransslagvaten van patiënten die een stent geïmplanteerd hebben gekregen en waarin de stent herkenbaar is, bewijzen dat deze acquisitie- en reconstructie-techniek de werkelijkheid dicht benadert in gevallen waarin het stuk kransslagvat dat onderzocht werd redelijk recht was. De combinatie van coronair angiografie met een tomografische ICUS beelden data set, heeft mogelijk meer klinische waarde in de toekomst[3-5]. De techniek van het combineren van de twee verschillende beeld modaliteiten biedt de mogelijkheid om 3-D reconstructies van de kransslagvaten te produceren waarin de oorpronkelijke ruimtelijke geometrie van het vat behouden blijft. Deze reconstructies kunnen bijvoorbeeld gebruikt worden om lokale wandspanningen in het vat te berekenen[4]. Deze nieuwe 3-D techniek is nu in onderzoek in het Thoraxcentrum.

De volgorde van de hoofdstukken lijkt wellicht merkwaardig (van de hak op de tak), 3-D echocardiografie (hele hart) –> 3-D ICUS (kransslagvaten) -> Virtual Reality (hele hart), maar het geeft een goede weergave van de progressie in de ontwikkelingen van 3-D echo technieken (het is eigenlijk meer beschreven in een chronologische volgorde). Hoofdstuk 6 beschrijft de mogelijkheden van het gebruik van Virtual Reality (VR) technieken in combinatie met interactieve computersystemen voor onderwijs en training in cardiologie. Een 3-D reconstructie maakt aan de ene kant de beeld interpretatie eenvoudiger, maar aan de andere kant meer complex. De 3-D data sets kunnen nl. bekeken worden vanuit een oneindig aantal observatie punten, dit werkt het in de hand dat een gebruiker, na verloop van tijd en de nodige veranderingen, niet meer weet wat zijn exacte oriëntatie is. Virtuele hart modellen, gekoppeld aan 3-D data sets kunnen dienen als een 3-D landkaart voor het terug vinden van de juiste oriëntatie. Bovendien, sinds de meeste diagnostische beeldvormende technieken hedentendage de beelden opslaan in een digitaal formaat, is het mogelijk de patiënten data te bewaren in computer databases (Figuur 4). Zo kunnen er, bijvoorbeeld, databases gecreëerd worden met voorbeelden van bijzondere afwijkingen aan het hart welke kunnen dienen als lesmateriaal. Dit in combinatie met een trainingsstation om echocardiogrammen te kunnen simuleren, kan een vernieuwing betekenen in het onderwijs voor echocardiografie.

Deel II: Kwantitatieve analyse van de kransslagvaten

Het tweede deel van dit proefschrift handelt over de kwantitatieve analyse van de kransslagvaten gebaseerd op de acquisitie techniek die in de hoofdstukken 3, 4 en 5 wordt beschreven. In hoofdstuk 7 wordt het combineren van twee verschillende projecten beschreven die beide bedoeld waren voor andere applicaties maar werden gecombineerd t.b.v. 3-D ICUS. Aan de ene kant is er het 3-D acquisitie station waarvoor een speciaal ICUS catheter terugtrekapparaat werd ontwikkeld en aan de andere kant een speciaal software pakket dat was ontwikkeld voor de analyse van niet-ECG-gesynchroniseerde ICUS beelden data sets (de catheter, in dit geval het beeldvormende element, wordt dan teruggetrokken met een constante snelheid van 0.5mm/sec en de beelden worden achteraf gedigitaliseerd vanaf video-tape). Dit was de basis om metingen te verrichten aan de dimensies van de kransslagvaten (doorsnede en oppervlak) in verschillende fases van de hartslag, met de mogelijkheid om te kunnen corrigeren voor bewegingen van de catheter t.o.v. het kransslagvat tijdens de hartslag, welke in meer dan 90% van de patiënten aanwezig bleek. De ICUS catheter beweegt van distaal (eind-diastole, R-top van het ECG) naar proximaal (eind-systole) gedurende de hartslag. Tijdens een analyse van 2-D beelden op het echo-apparaat zelf, zou iemand op deze manier misleid kunnen worden (de beweging van de catheter kan op deze manier niet worden gecorrigeerd) en dit zou tot onverwachte of zelfs foute resultaten kunnen leiden. In hoofdstuk 8 wordt een studie beschreven die het verschil aantoont in meetresulaten tussen ECG-gesynchroniseerde en niet-gesynchroniseerde verkregen 3-D ICUS data sets. Het bleek dat wanneer de ICUS beelden ECG-synchroon werden verkregen, de volume metingen belangrijk kleiner waren dan de metingen op de beelden verkregen met de andere techniek. Grootste nadeel van deze studie was dat de patiënten populatie betrekkelijk klein was (n=15). Verdere studie en validatie van deze techniek is wenselijk, mede door het feit dat de niet-gesynchroniseerde techniek wijdverspreid gebruikt wordt in grote multi-center studies die aan moeten tonen of een nieuwe behandelingsvorm, of medicament, verbetering brengt in het eindresultaat voor de patiënt. Het nadeel van de extra kosten van de ECG-gesynchroniseerde techniek, terugtrekapparaat en extra werkstation, zou overkomelijk kunnen zijn als deze techniek geïntegreerd zou worden in de bestaande intracoronaire echo-apparatuur. Deze politiek wordt momenteel al gevolgd in de echo-apparatuur voor het hele hart (Hewlett-Packard). De grootste klinische belemmering voor het gebruik van deze methodiek is de langere tijd die de ICUS catheter in het kransslagvat verblijft, dit was gemiddeld 1 minuut per "gescande" centimeter (3 maal langer dan de niet gesynchroniseerde techniek). Er werden stappen genomen van 0.2mm tussen twee catheterposities en dit was gebaseerd op de theoretische beeldresoluties van de ICUS catheters. Het zou zo kunnen zijn dat grotere stappen (eerder thuis) toegepast zouden kunnen worden zonder dat dit leidt tot onnauwkeurigheden. Dit dient echter nader onderzocht te worden.

In hoofdstuk 9 wordt de reproduceerbaarheid en de inter- en intra-onderzoeker variabiliteit beschreven van de ECG-gesynchroniseerde techniek. De "gladde" contouren van de kransslagvaten in de gereconstrueerde lengtedoorsneden resulteerden niet alleen in een representatie (plaatje) dat meer leek op een röntgen afbeelding van de kransslagvaten, maar resulteerde ook in een belangrijke reductie van de analyse tijd (met de helft). Dit kwam voornamelijk doordat er minder correcties nodig waren in de contouren zoals die door de software in eerste instantie werden gedetecteerd.

De gladde contouren, verkregen met de ECG-synchronisatie, zorgen er nu voor dat het software algoritme een hogere score behaalt (minder foute contour detecties). Dit is niet alleen van belang in zg. analyse laboratoria maar ook voor direct (on-line) gebruik in het hartcatheterisatielaboratorium tijdens het onderzoek. Hoofdstuk 10 beschrijft het gebruik van de ECG-gesynchroniseerde techniek en 3-D reconstructies voor het on-line bepalen of een geïmplanteerde stent op de juiste manier geplaatst was. Deze studie heeft aangetoond dat dit mogelijk was en dat de resultaten reproduceerbaar waren. De extra apparatuur noodzakelijk voor deze techniek kan echter problemen geven wanneer de ruimte in een hartcatheterisatielaboratorium beperkt is. Tevens dient er personeel aanwezig te zijn dat goed getraind is in het gebruik van zowel de ICUS techniek als in het bedienen van een 3-D werkstation.

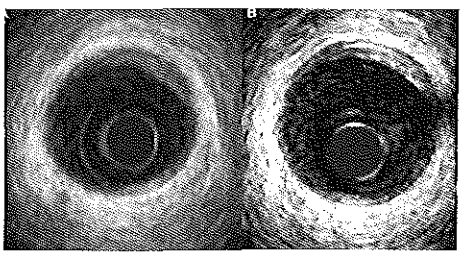

Figuur 5
In paneel A is een ICUS beeld van een kransslagvat gemaakt, met een 30 MHz catheter, te zien. In paneel B is hetzelfde stukje vat te zien bij dezelfde patiënt maar nu gemaakt met een ICUS catheter die werkt met 40 MHz. Het is goed te zien dat het plaatje in paneel B "scherper" is dan in A. De overgang van de plaque naar de buitenwand valt mooi te onderscheiden.

Toekomstige ontwikkelingen

Drie-dimensionele echocardiografie is nu sinds vijf jaar commercieel beschikbaar. Vele onderzoeksprojecten zijn er sindsdien mee uitgevoerd en hebben positieve resultaten gebracht. Het wordt echter nog steeds weinig in de klinische praktijk gebruikt[1, 2, 6-16]. Ontwikkelingen in de computer industrie en op andere gebieden, zoals bijvoorbeeld de film en de militaire industrie, brengen ook nieuwe mogelijkheden op het gebied van 3-D reconstructies voor de gezondheidszorg. 3-D reconstructie van het hart is misschien wel het meest uitdagende gebied, omdat het hart een orgaan is dat veel beweegt. De ontwikkelingen in Virtual Reality (VR) technieken openen nieuwe perspectieven voor medisch onderwijs en training. De VR modellen zoals die nu gebruikt worden in separate werkstations kunnen wellicht in de nabije toekomst worden geïntegreerd in echocardiografische apparatuur om de cardioloog te helpen tijdens het onderzoek van een patiënt.

Drie-dimensionele reconstructies, hier bedoelt voor analyses, van de kransslagvaten zijn momenteel ook voornamelijk alléén onderwerp van onderzoek. Het is aangetoond dat het goed gebruikt kan worden in het evalueren van nieuwe interventie technieken zoals bij de intracoronaire stents[17-19], voor de bepaling van de toe- en/of afname van plaques in de kransslagvaten m.b.v. medicijnen of met straling[20, 21]. Nieuwe hoogfrequente ICUS catheters (40MHz, CVIS and 45 MHz, HP) bieden buiten verbeterde beelden van de kransslagvaten ook een verbeterde resolutie welke van belang kan zijn voor de kwaliteit van 3-D reconstructies[22] (Figuur 5). De nieuwe generatie van ICUS apparatuur biedt ook de mogelijkheid voor een complete digitale verwerking van de ICUS beelden, wat de kwaliteit zeker ten goede zal komen. Werkstations die zowel in staat zijn om kwantitatieve coronaire angiografie (aangeduid

als QCA) en kwantitatieve ICUS (vaak aangeduid als QCU) komen commercieel beschikbaar. Deze stations kunnen de sterke kanten van de twee verschillende technieken combineren, nl. lumen afbeeldingen m.b.v. QCA en de buitenwand van de vaten m.b.v. QCU. Verbeterde analyse software en 3-D reconstructie technieken die de resultaten van QCA en QCU combineren en die in staat zijn om de vaten te presenteren in 3-D met hun werkelijke ruimtelijke geometrie, kunnen de interventie cardioloog helpen in het kiezen van de juiste behandelings strategie voor de patiënt.

3-D reconstructies van het hart en de kransslagvaten gecombineerd met kwantitatieve analyses bieden de potentie voor een verbeterde diagnose stelling en uiteindelijk voor een verbeterde therapie van patiënten die lijden aan problemen met het hart.

Referenties

1. Nosir YF, Fioretti PM, Vletter WB, Boersma E, Salustri A, Postma JT, Reijs AE, Ten Cate FJ, Roelandt JR. Accurate measurement of left ventricular ejection fraction by three-dimensional echocardiography. A comparison with radionuclide angiography. Circulation 1996; 94:460-6.

2. Altmann K, Shen Z, Boxt LM, King DL, Gersony WM, Allan LD, Apfel HD. Comparison of three-dimensional echocardiographic assessment of volume, mass, and function in children with functionally single left ventricles with twodimensional echocardiography and magnetic resonance imaging. Am J Cardiol 1997; 80:1060-5.

3. Evans JL, Ng KH, Wiet SG, Vonesh MJ, Bums WB, Radvany MG, Kane BJ, Davidson CJ, Roth SI, Kramer BL, Meyers SN, McPherson DD. Accurate threedimensional reconstruction of intravascular ultrasound data. Spatially correct three-dimensional reconstructions. Circulation 1996; 93:567-76.

4. Slager CJ, Wentzel JJ, Oomen JA, Schuurbiers JC, Krams R, von Birgelen C, Tjon A, Serruys PW, de Feyter PJ. True reconstruction of vessel geometry from combined X-ray angiographic and intracoronary ultrasound data. Semin Interv Cardiol 1997; 2:43-7.

5. Wiet SP, Vonesh MJ, Waligora MJ, Kane BJ, McPherson DD. The effect of vascular curvature on three-dimensional reconstruction of intravascular ultrasound images. Ann Biomed Eng 1996; 24:695-701.

6. Chen Q, Nosir YF, Vletter WB, Kint PP,

Salustri A, Roelandt JR. Accurate assessment of mitral valve area in patients with mitral stenosis by threedimensional echocardiography. J Am Soc Echocardiogr 1997; 10:133-40.

7. Dall'Agata A, Taams MA, Fioretti PM, Roelandt JR, Van Herwerden LA. Cosgrove-Edwards mitral ring dynamics measured with transesophageal threedimensional echocardiography. Ann Thorac Surg 1998; 65:485-90.

8. King DL, Harrison MR, King DL, Jr., Gopal AS, Martin RP, DeMaria AN. Improved reproducibility of left atrial and left ventricular measurements by guided three-dimensional echocardiography. J Am Coll Cardiol 1992; 20:1238

9. King DL, Gopal AS, King DL, Jr., Shao MY. Three-dimensional echocardiography: in vitro validation for quantitative measurement of total and "infarct" surface area. J Am Soc Echocardiogr 1993; 6:69-76.

10. King DL, Gopal AS, Keller AM, Sapin PM, Schroder KM. Three-dimensional echocardiography. Advances for measurement of ventricular volume and mass. Hypertension 1994; 23:I172-9.

11. Kupferwasser I, Mohr-Kahaly S, Menzel T, Spiecker M, Dohmen G, Mayer E, Oelert H, Erbel R, Meyer J. Quantification of mitral valve stenosis by threedlmensional transesophageal echocardiography. Int J Card Imaging 1996; 12:241

12. Roelandt JR. Three-dimensional echocardiography: new views from old windows [editorial]. Br Heart J 1995; 74:4-6.

13. Salustri A, Spitaels S, McGhie J, Vletter W, Roelandt JR. Transthoracic threedimensional echocardiography in adult patients with congenital heart disease. J Am Coll Cardiol 1995; 26:759-67.

14. Salustri A, Becker AE, van Herwerden L, Vletter WB, Ten Cate FJ, Roelandt JR. Three-dimensional echocardiography of normal and pathologic mitral valve: a comparison with two-dimensional transesophageal echocardiography. J Am Coll Cardiol 1996; 27:1502-10.

15. Salustri A, Kofflard MJ, Roelandt JR, Nosir Y, Trocino G, Keane D, Vletter WB, Cate FJ. Assessment of left ventricular outflow in hypertrophic cardiomyopathy using anyplane and paraplane analysis of three-dimensional echocardiography. Am J Cardiol 1996; 78:462-8.

16. Sklansky MS, Nelson TR, Pretorius DH. Usefulness of gated three-dimensional fetal echocardiography to reconstruct and display structures not visualized with two-dimensional imaging. Am J Cardiol 1997; 80:665-8.

17. Prati F, Di Mario C, Gil R, von Birgelen C, Camenzind E, Montauban van Swijndregt WJ, de Feyter PJ, Serruys PW, Roelandt JR. Usefulness of on-line three-dimensional reconstruction of intracoronary ultrasound for guidance of stent deployment. Am J Cardiol 1996; 77:455-61.

18. Nakamura S, Colombo A, Gaglione A, Almagor Y, Goldberg SL, Maiello L, Finci L, Tobis JM. Intracoronary ultrasound observations during stent implantation. Circulation 1994; 89:2026-34.

19.Goldberg SL, Colombo A, Nakamura S, Almagor Y, Maiello L, Tobis JM. Benefit of intracoronary ultrasound in the deployment of Palmaz-Schatz stents. J Am Coll Cardiol 1994; 24:996-1003.

20.Wiedermann JG, Leavy JA, Amols H, Schwartz A, Homma S, Marboe C, Weinberger J. Effects of high-dose intracoronary irradiation on vasomotor function and smooth muscle histopathology. Am J Physiol 1994; 267:H125-32.

21.Williams DO. Radiation vascular therapy: a novel approach to preventing restenosis. Am J Cardiol 1998; 81:18E-20E.

22.Foster FS, Knapik DA, Machado JC, Ryan LK, Nissen SE. High-frequency intracoronary ultrasound imaging. Semin Interv Cardiol 1997; 2:33-41.

Dankwoord

DANKWOORD

Bij voorbaat wil ik mij verontschuldigen aan een ieder die een bijdrage heeft geleverd tot het tot stand komen van mijn proefschrift en die ik in het vervolg van dit dankwoord ben vergeten te noemen.

Allereerst komt veel dank toe aan mijn promotor Prof. dr J.R.T.C. Roelandt. Beste Jos, jouw gevoel voor nieuwe technologie was de aanleiding om mij in 1993 naar München te sturen om bij een bedrijf, TomTec, te leren werken met 3-D echocardiografie apparatuur en software. De lessen die ik daar heb geleerd, en de ideeën opgedaan, zijn de directe aanleiding voor dit boekje en zonder die reis was ik waarschijnlijk (nog) niet zover gekomen. Jouw enthousiasme om nieuwe technieken verder uit te dragen, zowel intern als extern, zijn een grote stimulans geweest en dragen bij tot een atmosfeer waarin buiten "alléén" maar klinisch onderzoek ook nieuwe technische ontwikkelingen kansen hebben.

Bij deze wil ik ook mijn co-promotor, dr. Niek van der Putten, hartelijk danken voor de gegeven stimulans om te promoveren en het vertrouwen om in "vrijheid" mijn eigen taak in te mogen vullen. Dit zijn voor mij de juiste condities om tot een optimale produktie te kunnen komen.

Drs. C. von Birgelen. Beste Clemens, jouw bijdrage als co-auteur is voor het tot stand komen van vele artikelen en dus indirect tot dit proefschrift van grote betekenis geweest. Jouw vele "herschrijf"-werk, kritische opmerkingen en jouw enthousiasme hiervoor heb ik bijzonder gewaardeerd.

Jan Tuin, Maud van Nierop en Els Toonssen, de Thorax AVC, wil ik graag bedanken voor respectievelijk: de vele video's, foto's (waaronder ook de omslag van dit boekje) en honderden dia's die ik de afgelopen jaren geproduceerd heb. Zij zijn een belangrijke bijdrage geweest aan vele presentaties waarin o.a. ikzelf (maar meer een hele hoop anderen) leuke 3-D beelden konden "showen".

Ik heb een kleine 8 jaar op het cathlab gewerkt en veel geleerd van mijn collega techneuten. Een speciaal woord van dank wil ik richten tot Jurgen Ligthart. Beste Jurg, jouw enthousiasme en je specialisatie in ICUS hebben de laatste jaren een grote bijdrage geleverd tot het vergaren van veel cases waardoor een groot aantal artikelen tot stand kon komen. Ik heb, natuurlijk, ook prettig samengewerkt en veel opgestoken van de vele collega verpleegkundigen waarmee ik door de loop van de jaren heb gewerkt.

Ik heb ook veel geleerd van de op het cathlab werkzame klinici, de "éminences grises": Dr. Marcel van de Brand, Dr. Pim de Feijter en Prof. dr Patrick Serruys. Beste Patrick, jouw gevoel voor nieuwe technische ontwikkelingen en geduld om deze nieuwe technieken in het cathlab te introduceren, wat meestal niet eenvoudig is, zijn een belangrijk aandeel in het produceren van vele artikelen. Pim, jou wil ik hartelijk bedanken voor je aanmoedigende en kritische opmerkingen (al zijn ze soms wat sceptisch). Hierbij wil ik ook dank zeggen aan alle junior-, tussenstaf- en senior-cardiologen van het cathlab, die de afgelopen jaren een bijdrage hebben geleverd aan het tot stand komen van dit boekje.

Dr. Alan Soward. Dear Alan, it is already a long time ago since we worked together at the Thoraxcenter. Through the years, however, we have maintained contact, despite the vast distance between Rotterdam and Mildura (Australia). In recent years we had the opportunity to have even closer contact by email. Through this communication channel it became possible for me to send my poorly written papers to you to be checked for faulty English grammar. I am very grateful for your help in this sense, but I am more grateful for your friendship and that of Bev. I hope we soon can meet again, somewhere around the globe, but more preferable (by me) in Australia.

Dr. Carlo di Mario and Drs. Francesco Prati, the first two inhabitants of the so-called IC-LAB. Your contributions to promote the ECG-gated acquisition technique in the early stages have been very helpful. Furthermore, dear Francesco, I would like to express my gratitude for your friendship and inspiring thoughts and ideas concerning ICUS and

research over the past years. I hope you will find a nice and stimulating environment in Italy.

Binnen de computergroep komt dank toe aan Wim den Hoed en Max Patijn voor het mee helpen ontwikkelen van het allereerste terugtrekapparaat. "Ome" Henk de Graaff was onmisbaar voor het broodnodige ritselwerk en de haastklusjes. Verder wil ik dr. ir Ron van Domburg bedanken voor de adviezen omtrent het juist toepassen van de statistiek, en ir. Simon Meij voor de adviezen omtrent signaalverwerking en als "slapie" tijdens congressen.

De CRW, in deze Joop Bos, Ton Vlasveld, Jack Kamphuis en Bernard Mulder, wil ik bedanken voor het produceren van respectievelijk het tweede en derde terugtrekapparaat.

Ik wil hier ook dank zeggen aan alle medewerkers van TomTec GmbH, en in het bijzonder aan Bernhard Mumm. Dear Bernhard, the cooperation between us, has been very fruitful, at least for me. All chapters are based on and around the technology developed by TomTec. History will judge how far this technology will come. The latest developments with Virtual Reality are promising. I hope that we can extent our cooperation into the future.

Dankzij Marianne Eichholtz loopt de administratieve afhandeling van een promotie "bijna" geautomatiseerd.

Graag wil ik ook alle secretaresses en de fellows bedanken, die mij gedurende vele jaren niet alleen hebben geholpen met het werk op zich, maar ook in sociaal opzicht altijd in waren voor een praatje of een uitje. In het bijzonder wil ik Arita Orgers en Willeke Korpershoek bedanken voor hun vriendschap en hun "*emotionele*" steun.

Niet in de laatste plaats, al staat het hier wel zo, komt veel dank toe aan mijn ouders die gedurende vele jaren mij de mogelijkheden hebben geboden om te kunnen studeren en mij in staat stelden om datgene te doen wat ik leuk vond.

Publications

PUBLICATIONS

1. Bruining N, Krams R, Passchier H, Meij S, de Feijter PJ, Keane D. A modular hard and software system for the analysis of cardiac signals: application to real time pressure-volume loops. Computers In Cardiology, London, IEEE Computer Society Press 1993; 161-64.
2. Bruining N, Ligthart JMR, van der Perk R, de Ruiter R, Serruys PW. Computers in het hartcatheterisatielaboratorium. Tijdschr Cardiol 1994; 6:86-94.
3. Bruining N, Zijlstra A, van der Putten N, Keane D, Lehmann KG, Di Mario C, de Feijter PJ, Serruys PW, Roelandt JRTC. A research-oriented database for integration and comprehensive analysis of intracoronary angioscopic, ultrasonic and angiographic images. The Thoraxcentre J 1994; 6:4-7.
4. Roelandt J, ten Cate FJ, Bruining N, Salustri A, Vletter WB, Mumm B, van der Putten N. Transesophageal rotoplane echo-CT. A novel approach to dynamic three-dimensional echocardiography. The Thoraxcentre J 1994; 6:4-8.
5. Roelandt JRTC, Salustri A, Vletter W, Nosir Y, Bruining N. Precordial multiplane echocardiography for dynamic anayplane, paraplane and three-dimensional imaging of the heart. The Thoraxcentre J 1994; 7:4-13.
6. Bruining N, von Birgelen C, Di Mario C, Prati F, Li W, den Hoed W, Patijn M, de Feyter PJ, Serruys PW, Roelandt JRTC. Dynamic three-dimensional reconstruction of ICUS images based on an ecg-gated pull-back device. Computers In Cardiology, Vienna, IEEE Computer Society Press 1995; 633-36.
7. Di Mario C, von Birgelen C, Prati F, Soni B, Li W, Bruining N, de Jaegere PP, de Feyter PJ, Serruys PW, Roelandt JR. Three dimensional reconstruction of cross sectional intracoronary ultrasound: clinical or research tool? Br Heart J 1995; 73:26-32.
8. Keane D, Schuurbiers J, Slager CJ, Ozaki Y, den Boer A, Bruining N, Serruys PW. Comparitive quantitative mechanical, radiographic, and angiographic analysis of eight coronary stent designs. Cardiology. Rotterdam: Erasmus University, 1995:243-271.
9. von Birgelen C, Di Mario C, Prati F, Bruining N, Li W, de Feyter PJ, Roelandt JRTC. Intracoronary ultrasound: Three-dimensional reconstruction techniques. In:

de Feyter PJ, Di Mario C, Serruys PW, eds. Quantitative coronary imaging. Rotterdam: Barjesteh, Meeuwse & Co., 1995:181-197.

10. von Birgelen C, Erbel R, Di Mario C, Li W, Prati F, Ge J, Bruining N, Gorge G, Slager CJ, Serruys PW, et al. Three-dimensional reconstruction of coronary arteries with intravascular ultrasound. Herz 1995; 20:277-89.
11. Berlage T, Grunst G, Alkar HJ, Mumm B, Angelsen B, Komorowski J, Redel DA, Pinto F, Bruining N, Roelandt JRTC. CardiAssist: Developing a support platform for 3D ultrasound. The Thoraxcentre J 1996; 8:5-8.
12. Bruining N, de Feyter PJ, Roelandt JRTC. Dynamic three-dimensional reconstruction of implanted intracoronary stent structures using ICUS images. The Thoraxcentre J 1996; 8:18-24.
13. Bruining N, von Birgelen C, Mallus MT, de Feyter PJ, de Vrey E, Li W, Prati F, Serruys PW, Roelandt JRTC. ECG-gated ICUS image acquisition combined with a semi-automated contour detection provides accurate analysis of vessel dimensions. Computers In Cardiology, Indianapolis, IEEE Computer Society Press 1996; 53-56.
14. Bruining N, von Birgelen C, Prati F, Mallus MT, Li W, den Hoed W, Patijn M, de Feyter PJ, Serruys PW, Roelandt JRTC. Dynamic three-dimensional reconstruction of ICUS images based on an ECG-gated pull-back device. IEEE Engineering in Medicine & Biology, Amsterdam, IEEE 1996; 43-46.
15. Nicosia A, von Birgelen C, Di Mario C, Prati F, Mallus MT, Bruining N, de Feyter PJ, Serruys PW, Giuffrida G, Roelandt JR. 3-dimensional reconstruction in intracoronary echocardiography: the advantages, limits and future prospects. Cardiologia 1996; 41:1165-74.
16. Von Birgelen C, Di Mario C, Reimers B, Prati F, Bruining N, Gil R, Serruys PW, Roelandt JR. Three-dimensional intracoronary ultrasound imaging. Methodology and clinical relevance for the assessment of coronary arteries and bypass grafts. J Cardiovasc Surg (Torino) 1996; 37:129-39.
17. Bruining N, Berlage T, Grunst G, Alkar HJ, Mumm B, Angelsen B, Komorowski J, Redel DA, Pinto F, Roelandt JRTC. CardiAssist: Developing a support

platform for 3D ultrasound. Computers In Cardiology, Indianapolis, IEEE Computer Society Press 1997; 557-60.

18. Prati F, Di Mario C, Gil R, Bruining N, Camenzind E, von Birgelen C, Serruys PW, Roelandt JR. On-line three-dimensional intracoronary ultrasound for guidance of catheter based interventions. G Ital Cardiol 1997; 27:123-32.

19. Prati F, Gil R, Di Mario C, Ozaki Y, Bruining N, Camenzind E, de Feyter PJ, Roelandt JR, Serruys PW. Is quantitative angiography sufficient to guide stent implantation? A comparison with three-dimensional reconstruction of intracoronary ultrasound images. G Ital Cardiol 1997; 27:328-36.

20. von Birgelen C, de Feyter PJ, de Vrey EA, Li W, Bruining N, Nicosia A, Roelandt JR, Serruys PW. Simpson's rule for the volumetric ultrasound assessment of atherosclerotic coronary arteries: a study with ECG-gated three-dimensional intravascular ultrasound. Coron Artery Dis 1997; 8:363-9.

21. von Birgelen C, de Vrey EA, Mintz GS, Nicosia A, Bruining N, Li W, Slager CJ, Roelandt JR, Serruys PW, de Feyter PJ. ECG-gated three-dimensional intravascular ultrasound: feasibility and reproducibility of the automated analysis of coronary lumen and atherosclerotic plaque dimensions in humans. Circulation 1997; 96:2944-52.

22. von Birgelen C, Mintz GS, de Feyter PJ, Bruining N, Nicosia A, Di Mario C, Serruys PW, Roelandt JR. Reconstruction and quantification with three-dimensional intracoronary ultrasound. An update on techniques, challenges, and future directions. Eur Heart J 1997; 18:1056-67.

23. von Birgelen C, Mintz GS, Nicosia A, Foley DP, van der Giessen WJ, Bruining N, Airiian SG, Roelandt JRTC, de Feyter PJ, Serruys PW. Electrocardiogram-gated intravascular ultrasound image acquisition after coronary stent deployment facilitates on-line three-dimensional reconstruction and automated lumen quantification. J Am Coll Cardiol 1997; 30:436-443.

24. Bruining N, de Feyter PJ, Ligthart J, Roelandt JRTC, Serruys PW. 3 D reconstruction and volumetric measurements of ECG-gated acquired intracoronary ultrasound images. J Cardiovascular Interv 1998; 1:10-12.

25. Bruining N, Roelandt JRTC, Janssen M, Grunst G, Berlage T, Waldinger J, Mumm B. Virtual Reality: a teaching and training tool or just a computer game? The Thoraxcentre J 1998; 10:17-20.

26. Bruining N, Sabate M, Serruys PW. Clinical implications of intravascular ultrasound imaging for stenting procedures. Am Heart J 1998:in press.

27. Bruining N, Tuin J. ICUS appearences of the stent. In: Serruys PW, Kutryk MJB, eds. Handbook of coronary stents (second edition). London: Martin Dunitz, 1998:289-316.

28. Bruining N, von Birgelen C, de Feyter PJ, Ligthart J, Li W, Serruys PW, Roelandt JR. ECG-gated versus nongated three-dimensional intracoronary ultrasound analysis: implications for volumetric measurements. Cathet Cardiovasc Diagn 1998; 43:254-60.

29. Bruining N, Von Birgelen C, De Feyter PJ, Ligthart J, Serruys PW, Roelandt JR. Dynamic imaging of coronary stent structures: an ECG-gated three- dimensional intracoronary ultrasound study in humans. Ultrasound Med Biol 1998; 24:631-7.

30. Bruining N, von Birgelen C, de Feyter PJ, Roelandt JRTC, Serruys PW. Ultrasound appearances of coronary stents as obtained by three-dimensional intracoronary ultrasound imaging in-vitro. J Invasive Cardiol 1998; 10:332-38.

31. Prati F, Di Mario C, Gil R, von Birgelen C, Bruining N, Serruys PW, Roelandt JRTC. Three-dimensional intravascular ultrasound for stenting. In: Erbel R, Roelandt JRTC, Ge J, Gorge G, eds. Intravascular Ultrasound. London: Martin Dunitz, 1998:239-247.

Curriculum Vitae

Nico Bruining werd geboren op 23 februari 1963 te Rotterdam.

Hij behaalde in 1980 het MAVO-diploma aan de Hugo de Groot scholengemeenschap in Rotterdam. In 1985 behaalde hij het MTS-Electonica diploma aan de Christiaan Huygens-MTS. Zijn stage werd geheel vervuld op het hartcatheterisatielaboratorium van het Thoraxcentrum alwaar hij gedurende die periode in dienst trad.

In 1988 behaalde hij, wederom op de Christiaan Huygens-MTS, het getuigschrift van de tweejarige deeltijdopleiding MTS-Computertechniek.

In 1991 werd het getuigschrift verkregen voor de opleiding hogere compterkunde aan de Hogeschool Rotterdam & Omstreken. In 1993 werd het diploma van de HTS-Elektrotechniek afstudeerrichting technische computerkunde (TCK) behaald. Het afstudeerproject was het construeren van druk-volume curves bij hartpatiënten. Hiermee werd de eerste steen gelegd voor het intensief werken met ultrageluid beelden, wat de aanleiding was voor dit proefschrift.

In 1993 verruilde hij zijn baan als technicus op het hartcatheterisatielaboratorium en werd technisch automatiseerder bij de computergroep van het Thoraxcentrum.

In 1994 werd aan de Haagse Hogeschool het getuigschrift behaald van de post-HBO opleiding systeemontwerpen.

Financial contributions of:



TomTec Imaging Systems GmbH, Hewlett-Packard, Schwarz Pharma AG, Boston Scientific International, Cardialysis BV, Schneider, Pfizer BV, Spectranetics International BV, Parke-Davis BV, Bayer BV, Medtronic BV, Lorex Synthélabo BV, Medicor Nederland BV and Boehringer Ingelheim are gratefully acknowledged.